THE STABILITY OF DETONATION

HENRY EYRING,[1] RICHARD E. POWELL, GEORGE H. DUFFEY,
AND RANSOM B. PARLIN

Princeton University, Princeton, New Jersey

CONTENTS

[1] Present address: Department of Chemistry, University of Utah, Salt Lake City, Utah.

FOREWORD

At the high temperature inside a detonating explosive the chemical reaction is much too fast to be studied directly (it is complete in perhaps one-millionth of a second). For a large class of phenomena this does not matter; all that needs to be known is the composition of the detonation products. With only this knowledge—and the aid of thermodynamic and hydrodynamic theory—we can find the detonation velocity itself, the pressure shock set up in air (or water, or earth), and the fragment velocities of a shell case.

But for another class of phenomena the chemical reaction is all-important: the conditions under which a high explosive may be detonated by a hammer blow or by another detonating explosive; the conditions under which a detonation will fail, and those under which it will build up to its full value; the comparison of unconfined with confined charges. All these involve the reaction rate.

The present paper is concerned with the theory of phenomena of this second class. It is in considerable measure a summary of theoretical studies by this research group, undertaken under the auspices of the Office of Scientific Research and Development and (in part) of the Bureau of Ordnance of the Navy Department.

In writing this paper, the authors have attempted:

(1) To simplify the mathematical derivations. With this in mind, every section of their earlier reports (OSRD 2026 and OSRD 3796) has been completely rewritten. Mathematical details which are off the main channel of the discussion have been relegated to appendices.

(2) To present the results in a form usable even without detailed study of the theory. To this end worked-out examples using representative data have been included regularly. No attempt has been made, however, to give encyclopedic coverage of all the experimental data on every topic.

(3) To make this as complete a manual in its part of the field of explosives as possible, by inclusion of theoretical treatments by various investigators and of many pertinent experimental results. In this connection it should be recognized that a considerable body of experimental fact and theoretical interpretation is as yet not available to the general public. Some other important work has not been published, although available in the form of unclassified reports.

Section I is a critical résumé of the classical theory of the detonation wave. In particular, the classical theory gives temperatures, pressures, and velocities within a detonating explosive.

Sections II B, II C, and II D contain the theories developed for detonation in finite charges, time-dependent detonation, and failure of detonation. These theories lead to the conclusions (Section II E) that the chemical reaction in a detonation starts at load-bearing contact points, proceeds only at the surfaces of grains, and is possibly diffusion-controlled.

Section III is a study of initiation by impact. A model is proposed whereby mechanical impact leads to internal burning, which goes over into detonation.

It is difficult under the present circumstances to give proper acknowledgment in every case for the benefits derived from discussion and conference with the many workers in this field, and for the considerable quantity of unpublished work which has contributed in large measure to the conclusions presented here. The authors are particularly indebted to Professor George B. Kistiakowsky for his discussions at the time this work was initiated and subsequently with him and Drs. Kirkwood, MacDougall, Messerly, and Boggs. These workers and others at the Explosives Research Laboratory at Bruceton made major contributions, both in experimental work and in the interpretation of the nature of explosives. Dr. Kistiakowsky asked the authors to explore the effects of charge diameter and finite reaction rates on the velocity of the explosion process. The prevailing opinion among the investigators in the field of explosives at that time was that kinetically the reaction in the detonation wave was identical with the process of deflagration of explosives and that the reaction was a heterogeneous one, starting at the surface of grains and extending into the gas phase. The development of this general idea and of the more specific arguments that arose from it proceeded in a coöperative manner among a large number of individuals and groups; under such circumstances any effort to establish priority is difficult, if not impossible, to achieve.

I. THE IDEAL DETONATION WAVE

A. FUNDAMENTAL THEORY

The discovery of detonation waves was made in 1881, independently by Berthelot and Vieille (8, 9) and by Mallard and Le Chatelier (52). Within twenty-five years of the discovery the fundamental theory of the detonation velocity in terms of thermodynamic and hydrodynamic properties had been correctly developed. Subsequent papers on the theory of detonation have chiefly been summaries of the results of the early writers (5, 7, 10, 41, 47, 51, 67, 75), detailed justifications of some of their assumptions, or numerical refinements in the application of their theory to actual explosives.

The development of the theory of the detonation velocity breaks naturally into two parts. The first part gives the relation between pressure and volume in a wave which propagates unchanged in type. In 1859 Earnshaw (25) obtained this relation correctly, but by a somewhat circuitous method. The still classic

researches of Riemann on sound waves (1860) went astray on this point, for he wrongly assumed the adiabatic relation $PV^\gamma = $ constant (61). Rankine (59) in 1870 gave a clear and correct derivation of the relation, but his work was overlooked by later workers. Hugoniot (39) independently (for he refers to no previous workers) rediscovered the relation (1887), and it was his presentation which was later utilized. The pressure–volume relation is now commonly linked with the names of both the latter men, and is called the Rankine–Hugoniot relation.

The second part of the theory of detonation velocity to be developed relates the detonation velocity to the sonic velocity behind the detonation wave. The earliest investigators give tentative explanations of the detonation velocity— thus Berthelot (8) (1881) thought that it was the mean kinetic velocity of the hot molecules, and Dixon (21) (1893) thought that it was the velocity of sound in the hot gases—but did not hit upon the correct explanation. Chapman (15) (1899) was the first to make the assumption now generally accepted, but his final results are somewhat in error since he followed Riemann's belief that the pressure–volume relation is adiabatic. Finally Jouguet (42) in 1905 independently made the same assumption, which is now generally called the Chapman–Jouguet condition. Jouguet made use of the Hugoniot relation, and with his investigation the fundamental hydrodynamic-thermodynamic theory reached its completion.

Both because the results of the hydrodynamic-thermodynamic theory are themselves interesting in giving a description of the structure of the detonation wave, and because the intermediate equations will be needed in later sections of this report, we shall here repeat the derivation of the fundamental theory.

As an idealization, consider a plane detonation wave propagating through a semi-infinite block of explosive. In front of the wave is the intact explosive (subscript zero); behind the wave are the products of explosion (subscript one). Separating these two regions is a "reaction zone" whose length we shall discuss presently. Now the explosive at the end of the reaction zone is described by these properties: the pressure P, specific volume (reciprocal density) V, the temperature T, the material velocity or velocity of flow W, and the detonation velocity D. To solve for all these properties, we use the following conditions:

(1) The equation of continuity or conservation of mass.[2]

$$\frac{dV}{dt} = V \frac{\partial W}{\partial x} \qquad\qquad \text{Mass} \quad \text{(1a)}$$

(2) The equation of motion or conservation of momentum.[2] Here the effects of viscosity are neglected.[3]

_____

[2] For three dimensions the equations of continuity and of motion are in the vector notation

$$\frac{dV}{dt} = V \operatorname{div} \vec{W}$$

$$\frac{\mathrm{d}W}{\mathrm{d}t} = -V\frac{\partial P}{\partial x} \qquad \text{Momentum} \quad \text{(1b)}$$

(3) The first law of thermodynamics, or law of conservation of energy. Any contribution of heat by thermal conduction is neglected,[3] although contribution of heat by chemical reaction is of course considered.

$$C_v\mathrm{d}T = \mathrm{d}E = \mathrm{d}Q - P\mathrm{d}V \qquad \text{Energy} \quad \text{(1c)}$$

(4) The assumption that the velocity and shape of the detonation wave do not change with time, whereupon we may choose a coördinate system in which the detonation wave is at rest in space and constant in time. In default of a rigorous *a priori* proof that such a steady detonation wave can exist, we shall use the fact that steady detonation waves are experimentally found.

If $y = Dt - x$ and $\tau = t$, then

$$\frac{\partial}{\partial \tau} = 0 \qquad \text{Steady state} \quad \text{(1d)}$$

(5) The Chapman–Jouguet condition, which says that the detonation velocity is the sum of the material velocity and the velocity of sound, both evaluated at the end of the reaction zone.[4]

$$D = W_1 + C_1$$

where

$$C_1 = V_0 \sqrt{-\left(\frac{\partial P}{\partial V}\right)_s} = V_0 \sqrt{-\gamma\left(\frac{\partial P}{\partial V}\right)_T} \qquad \text{Chapman–Jouguet} \quad \text{(1e)}$$

(6) The equation of state of the products of explosion. The one used here will be the simple Abel equation of state, with the covolume α assumed constant. The theory can be extended to more complicated equations of state without particular difficulty.[5]

and

$$\frac{\mathrm{d}\vec{W}}{\mathrm{d}t} = -V \operatorname{grad} P$$

[3] See appendix A for a detailed discussion of the validity of neglecting viscosity and thermal conductivity.

[4] See appendix B for a detailed discussion of the validity of the Chapman–Jouguet condition.

[5] Cook, for example, uses the equation of state

$$P\{V - \alpha(V)\} = RT$$

while Halford, Kistiakowsky, and Wilson use an equation of the form

$$P(V - V_{\text{solids}}) = RT(1 + xe^{0.3x})$$

where

$$x = \frac{k}{T^{0.25}(V - V_{\text{solids}})}$$

$$P(V - \alpha) = RT \qquad \text{State} \quad (1f)$$

Making use of the transformation of coördinates (equation 1d) and defining the material velocity in the new coördinate system as $U = D - W$, the three conservation equations take the following forms:

$$\frac{dV}{V} = \frac{dU}{U} \qquad \text{Mass} \quad (2a)$$

$$UdU = -VdP \qquad \text{Momentum} \quad (2b)$$

$$dE + PdV = dQ \qquad \text{Energy} \quad (2c)$$

and these combinations of the above:

$$\frac{D}{V_0} dU + dP = 0 \qquad \text{Mass + Momentum} \quad (2d)$$

$$dE + UdU + d(PV) = dQ \qquad \text{Energy + Momentum} \quad (2e)$$

Of these differential equations, equations 2a, 2d, and 2e can be integrated upon inspection, yielding:

$$\frac{V}{V_0} = \frac{U}{D} \qquad (3a)$$

$$P + \frac{U^2}{V} = P_0 + \frac{D^2}{V_0} \qquad (3b)$$

$$\Delta E + \tfrac{1}{2}U^2 + PV = \Delta Q + \tfrac{1}{2}D^2 + P_0 V_0 \qquad (3c)$$

and these combinations of the above

$$U^2 = V^2 \frac{P - P_0}{V_0 - V} \qquad (4a)$$

$$D^2 = V_0^2 \frac{P - P_0}{V_0 - V} \qquad (4b)$$

$$\Delta E = \Delta Q + \tfrac{1}{2}(P + P_0)(V_0 - V) \qquad (4c)$$

Also

$$\frac{P - P_0}{D^2} V_0 = \frac{W}{D} = 1 - \frac{V}{V_0} \qquad (4d)$$

and

$$(P - P_0)V_0 = WD \qquad (4e)$$

Either of the sets of equations 3 or 4 gives the results first obtained by Rankine and Hugoniot. Equation 4b gives the relation between P and V in all parts of a wave propagating at constant velocity D or, as the original investigators called it, "the condition for constancy of type." This is then the Rankine–Hugoniot adiabatic or "dynamic adiabatic" condition, and it will be seen that it makes P a linear function of V.

Some of the early investigators were troubled because the Rankine–Hugoniot adiabatic relation is not consistent with the ordinary adiabatic (i.e., isentropic) relation PV^γ = constant. Thus Rankine states: "No substance yet known fulfils the condition ... at a constant temperature, nor in a state of non-conduction of heat (called the adiabatic state)." Lamb (49), in his *Hydrodynamics*, repeats this statement and also remarks, "but no physical evidence is adduced in support of the proposed law." The explanation of this apparent difficulty is simple; the entropy is *not* constant in a shock or detonation wave, and there is accordingly no reason to expect the isentropic law to be followed. (In fact, the entropy exhibits a sharp increase at the front of detonation wave, and an additional increase throughout the reaction zone.)

Now equations 4 cannot be solved simultaneously to yield a unique value of D; an additional condition is needed, and this is the Chapman–Jouguet condition (equation 1e). When the sonic velocity is explicitly evaluated for equation of state (equation 1f),

$$U_1^2 = V_1^2 \gamma \frac{P_1}{V_1 - \alpha} \tag{5}$$

which when inserted into equations 4 gives at once the following results:[6]

$$\frac{V_1}{V_0} = \frac{\gamma + \alpha/V_0}{\gamma + 1} \tag{6a}$$

$$P_1(V_0 - \alpha) = 2R \frac{\Delta Q + \bar{C}_v T_0}{\bar{C}_v} \tag{6b}$$

$$T_1 = \frac{\Delta Q + \bar{C}_v T_0}{\bar{C}_v} \frac{2\gamma}{\gamma + 1} \tag{6c}$$

$$D^2 = (\Delta Q + \bar{C}_v T_0) \frac{2(\gamma^2 - 1)}{(1 + \alpha/V_0)^2} \tag{6d}$$

$$\frac{W_1}{D} = \frac{1 - \alpha/V_0}{\gamma + 1} \tag{6e}$$

B. APPLICATION OF FUNDAMENTAL THEORY TO ACTUAL EXPLOSIVES

Equations 6a to 6e furnish the detonation velocity and all properties of the explosion products with only four data: (*i*) the mean heat capacity of the products, (*ii*) the heat of explosion, (*iii*) the covolume, and (*iv*) the gas constant per gram. It is noteworthy that the *rate of chemical reaction* does not affect the detonation velocity or any of the properties of the products. (The properties at the shock front are likewise independent of the reaction rate; indeed, the properties at any point within the reaction zone are determined only by the extent of completion of the chemical reaction at that point, and not by the rate of chemical reaction.)

[6] These results are obtained by neglecting P_0, which is very small compared to P, in most problems of practical interest. However, the exact equations are assembled in appendix C.

Numerical refinement in the application of the fundamental theory has correspondingly taken three directions: (*i*) Accurate computation of the heat capacity at high temperatures and pressures, by the methods of statistical mechanics. (*ii*) Accurate evaluation of the heat of explosion, which requires first good calorimetric measurement of the heat of combustion, and secondly a calculation of the heat of explosion based on the composition of the explosion products, which supposes knowledge of chemical equilibria at high temperatures and pressures. A knowledge of the product composition also gives the mean molecular weight of the products, and thence the gas constant per gram. (*iii*) Theoretical prediction of the covolume to be used. Generally the fundamental theory is used in an inverted sense, to determine covolumes from the measured detonation velocities. But after enough explosives have been examined, it becomes possible to predict the covolume approximately from the final volume (Cook) or from the final volume, temperature, and composition (Halford, Kistiakowsky, and Wilson).

Summaries of the results of these numerical refinements will be found elsewhere.[7] For purposes of this report, high precision in these numbers is not essential, so we shall use the heats of explosion and heat capacities as tabulated by others, and find the covolume in the Abel equation of state by use of the known detonation velocities.

A single worked-out example will serve to illustrate the calculation. For TNT of density 1.57 we assume the data

$$V_0 = 0.6360 \text{ cm.}^3 \text{ g.}^{-1}$$

$$\bar{C}_v = 0.326 \text{ cal. deg.}^{-1} \text{ g.}^{-1}$$

$$\gamma = 1.240$$

$$D = 6.85 \times 10^5 \text{ cm. sec.}^{-1}$$

$$\Delta Q = 1080 \text{ cal. g.}^{-1}$$

$$R = \frac{82.07}{25.9} = 3.17 \text{ cm.}^3 \text{ atm. deg.}^{-1} \text{ g.}^{-1}$$

and find

$$\alpha = 0.4225 \text{ cm.}^3 \text{ g.}^{-1}$$

$$V_1 = 0.54 \text{ cm.}^3 \text{ g.}^{-1}$$

$$P_1 = 109,000 \text{ atm.}$$

$$T_1 = 3870°\text{K.}$$

$$W_1/D = 0.15$$

A word as to the probable accuracy of the properties predicted by the thermodynamic-hydrodynamic theory: (*1*) The temperature T_1 depends only on the

[7] A series of papers by A. Schmidt (33). Also unpublished work of Cook, Kistiakowsky, Brinkley, Wilcox, and others.

heat ΔQ and the heat capacity $\bar{C}_v$, and in particular is independent of the co-volume or the initial density (except insofar as changes in final pressure may have a small effect on ΔQ and $\bar{C}_v$); the temperature should thus be the most accurately known property. (2) The ratios V_1/V_0 and W_1/D depend chiefly on the covolume α, which is not known with great certainty, so these are less accurate. (3) The velocity D involves all three data ΔQ, $\bar{C}_v$, and α, and so would be less certain than the preceding properties. (4) The pressure P_1 involves all three data and also the gas constant R per gram, which requires knowledge of the molecular weight of the products; this added uncertainty makes the pressure the least reliable of the predictable properties.
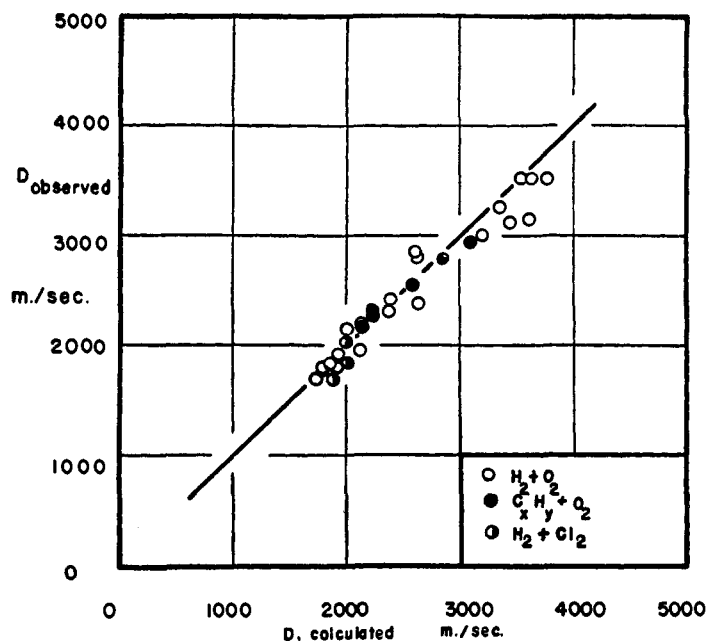
FIG. 1. Theoretical and calculated detonation velocities

Inspection of equations 6b and 6c shows that the temperature T_1 is only about 10 per cent higher than it would be if the reaction occurred at rest and at constant volume, while the pressure P_1 is precisely twice what it would be if the reaction occurred at rest and at constant volume.

C. DIRECT EXPERIMENTAL VERIFICATION OF THE FUNDAMENTAL THEORY

One test of the correctness of the hydrodynamic-thermodynamic theory lies in its ability to predict correctly the detonation velocities for gaseous explosives, since for these the covolumes are unimportant. The velocities for a number of gaseous explosives (chiefly hydrogen–oxygen or hydrocarbon–oxygen mixtures) were calculated by early investigators of the theory (43, 50) and found to be in good agreement with experimental velocities (8, 9, 21, 43, 50, 57). Their results are assembled in figure 1. Although these results were for many

years the sole verification of the hydrodynamic-thermodynamic theory, they are an altogether compelling verification of it.

The application of the hydrodynamic-thermodynamic theory to liquid and solid explosives does not provide a very stringent test of the theory, for it only shows that it is possible to predict detonation velocities if *reasonable* covolumes are assumed.

Recently the theory has been checked in three further ways: (*1*) Fox and Cairns have found the temperature T_1 spectroscopically, by assuming the radiation to be black-body and measuring its intensity at two or more wave lengths. (*2*) The velocity W_1 has been measured by x-ray photography (Clark) of charges containing alternate layers of explosive with and without lead ("zebra charges"). (*3*) The pressure P_1 can be computed from the initial velocity of the shock wave set up in a medium adjoining the explosive (e.g., lead, water, air).

The first of these methods measures only the heat/heat capacity ratio, not the covolume; the second and third methods measure only the covolume, not the heat or (appreciably) the heat capacity.[8]

Complete reports on these experiments are available elsewhere. The results of the experiments are found to be consistent with the hydrodynamic-thermodynamic theory.

D. PROPERTIES WITHIN THE REACTION ZONE

The pressure, temperature, and other properties appropriate to the partly decomposed explosive within the reaction zone can be found merely by inserting in equations 6 the value $N \cdot Q$ for the heat of reaction, where N is the fraction of the reaction completed.

For pressure, the result is:

$$P = \frac{D^2}{V_0} \cdot \frac{1 + \alpha/V_0}{1 + \gamma} \left\{ 1 + \sqrt{1 - \frac{N\Delta Q + \bar{C}_v T_0}{\Delta Q + \bar{C}_v T_0}} \right\} \qquad (7a)$$

or since the first factor is merely P_1 and since ΔQ is much larger than $\bar{C}_v T_0$,

$$\frac{P}{P_1} \cong 1 + \sqrt{1 - N} \qquad (7b)[9]$$

For temperature, the result is given by equation 8a below if the medium is supposed to be at constant temperature; even if the medium is heterogeneous, equation 8a gives the average temperature. If the partly decomposed explosive is (as we shall later offer evidence to indicate) composed in part of completely reacted material whose temperature rise is the sum of that due to chemical

[8] For

$$\frac{W_1}{D} = \frac{1 - \dfrac{\alpha}{V_0}}{1 + \alpha} \quad \text{and} \quad \frac{P_1 V_0}{D^2} = \frac{1 - \dfrac{\alpha}{V_0}}{1 + \alpha}$$

[9] Another possible solution would be equation 7b, but with a negative sign; this, however, is a spurious solution. See appendix D.

reaction and to compression, and in part of the unreacted residues of grains whose temperature rise is due only to compression, these two temperatures are given by equations 8b and 8c.

$$T_{\text{ave}} = (1 - N)T_0 + NT_1 + \frac{\gamma - 1}{2\gamma} T_1 \frac{P^2}{P_1^2} - NT_1 \frac{\gamma - 1}{2\gamma} \qquad (8a)$$

$$T_{\text{ext}} = T_1 \left[1 + \frac{\gamma - 1}{2\gamma} \left(\frac{P^2}{P_1^2} - 1 \right) \right] \qquad (8b)$$

$$T_{\text{int}} = T_0 + T_1 \frac{\gamma - 1}{2\gamma} \frac{P^2}{P_1^2} \qquad (8c)$$

The weighted mean of the external temperature T_{ext} and the internal temperature T_{int} is equal to the average temperature T_{ave} (as of course it must be physically).

The result for material velocity W is

$$\frac{W}{W_1} = \frac{P}{P_1} \qquad (9)$$

and the result for specific volume V is

$$\frac{1 - \dfrac{V}{V_0}}{1 - \dfrac{V_1}{V_0}} = \frac{P}{P_1} \qquad (10)$$

The result for the ratio $(C + W)/D$ is

$$\frac{C + W}{D} = 1 - \left[1 - \frac{P}{P_1} \frac{1 + \dfrac{\alpha}{V_0}}{1 + \gamma} \right] \cdot \left[\sqrt{\frac{\gamma \dfrac{P}{P_1}}{\gamma + 1 - \dfrac{P}{P_1}}} - 1 \right] \qquad (11)$$

Finally, the result for the entropy increase is

$$\Delta S = \Delta S_{v.T} + \bar{C}_v \ln \frac{T}{T_0} - R \ln \frac{V_0 - \alpha}{V - \alpha} \qquad (12)$$

where $\Delta S_{v.T}$ is the entropy increase of the chemical reaction if it be assumed to take place at constant temperature and constant volume.[10] (If the explosive is supposed to be heterogeneous, the entropy rise must be computed by equation 10 for the exterior of the grains and the interior of the grains separately, and the two contributions added.)

All of the results given by equations 7 to 12 have been assembled and plotted in figure 2, which represents a detonation wave moving toward the reader's left. The computation has been made for TNT of density 1.57, but the results will be approximately the same for any other high explosive. Each property is plotted in figure 2 as a percentage of its final value.

[10] For details of the method of calculating $\Delta S_{V,T}$, see appendix E.

The properties immediately behind the front of the detonation zone, where the extent of reaction is still zero (subscript $0'$), have a particular interest,

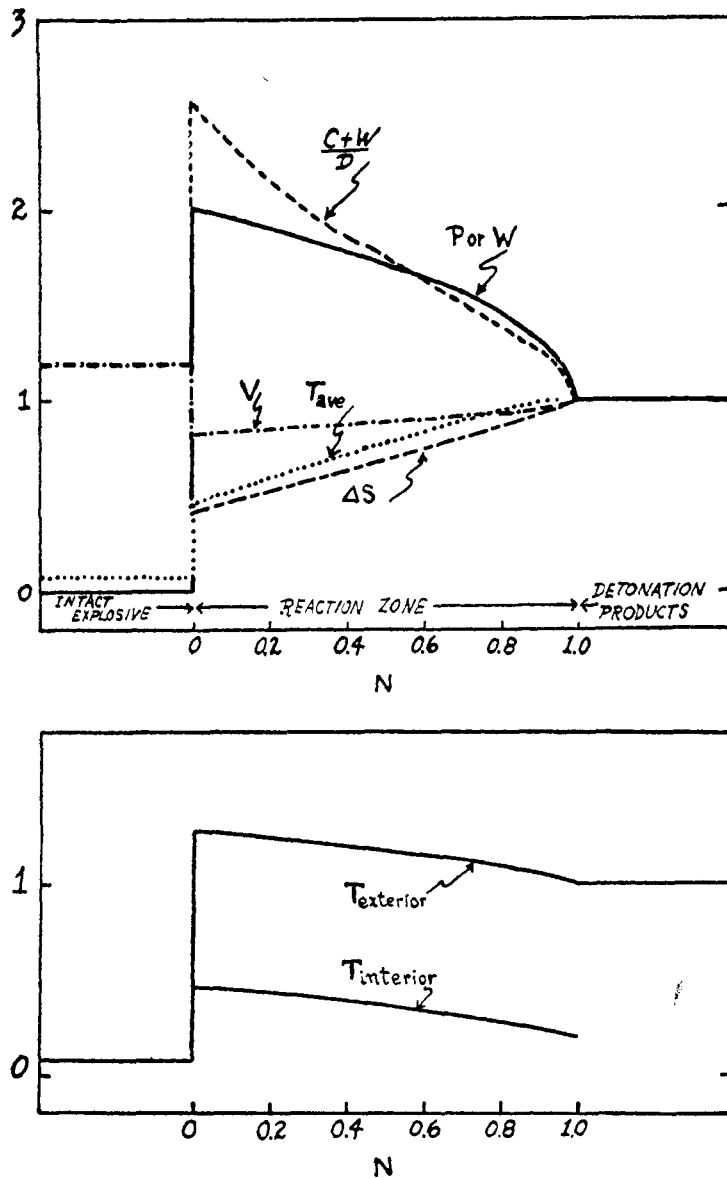FIG. 2. Upper: Distribution of wave properties through the reaction zone. Lower: Temperature distribution for heterogeneous case.

since they are the properties behind a pure shock wave traveling with the velocity D in the intact explosive.

(a) The *pressure* at the shock front is precisely twice the pressure P_1, and is accordingly four times the pressure that would be found if the reaction oc-

curred at rest and at constant volume. This statement would of course be somewhat changed if a more elaborate equation of state for the unreacted material were employed. The *volume* and the *material velocity* show changes which would be expected from the corresponding pressure change.

(b) The *temperature* at the shock front is raised, but to a value considerably less than the final detonation temperature; the temperature here estimated is about 1500°C., but this estimate is closely bound up with the equation of state of the intact explosive and may be considerably in error. Moreover, in an explosive composed of grains the initial compression can hardly be uniform; a greater stress (and higher temperature) would exist near the points of contact and a smaller stress (and lower temperature) within the interior of grains. This conclusion is in accord with the evidence we shall present later, that the grains do not in fact become hot enough for reaction to proceed in their interior.

The temperature exterior to the grains is chiefly due to the heat of reaction, so it immediately reaches (or slightly exceeds) its final value T_1.

(c) The *entropy* shows a sharp increase at the shock front, followed by a gradual increase within the reaction zone as the reaction proceeds.

(d) The *ratio* $(C + W)/D$ is about 2.5 at the shock front, and does not reach unity until the end of the reaction zone. This means that in a pure shock wave the velocity of a rarefaction wave (which is $C + W$) is greater than the detonation velocity D, so that the rarefaction wave will continually eat away the shock wave; it is for this physical reason that no *steady* pure shock wave is possible. Further, those "microshocks" which are produced within the reaction zone by chemical reactions will at first travel with the local $C + W$, and therefore at a velocity higher than D; but they will attenuate as they travel, so they do not in the long run send any signal in advance of the detonation wave.

In the study of chemical decomposition which will take up much of the remainder of this paper, we shall then suppose the reaction to take place at temperatures and pressures in the reaction zone as given by figure 2.

The question arises: How is the reaction initiated? The reaction is surely initiated at the shock front, but theories differ as to the manner of the initiation there. The theory to which the authors subscribe is that the *temperature* is sufficient at the shock front—at least, in local regions as discussed above—to initiate chemical reaction in the ordinary way. This brings the initiation, as well as the subsequent reaction, into the province of ordinary chemical-kinetic theory. We know of no evidence inconsistent with this assumption.

Another theory (F. Eirich) holds that the *pressure* in a detonation wave is sufficient to bring about decomposition; the process is visualized as a sort of bending of one molecular grouping until it is in proximity to another grouping, whereupon the groups interact to yield decomposition products. Now in the first place Bridgman (14) has shown by direct experiment that high hydrostatic pressure has in itself no effect on explosives. In the second place, even if the entire differential detonation pressure could be applied across a single primary bond (which is highly unlikely), it would not present nearly enough force to break the bond and could at most stretch it a few hundredths of an Ångström or bend it a few tenths of an Ångström. In the third place, even granting that

one could by pressure move one grouping into proximity with another, still no reaction would occur unless it could occur spontaneously (i.e., exothermically) under those conditions; but practically every conceivable first step in the decomposition of organic nitro or nitroxy explosives, however juxtaposed or distorted the molecules be assumed, is *endothermic;* thus the theory is untenable from the point of view of detailed chemical mechanism. And in the fourth place, the decomposition rate predicted by this theory would be much too high (see below).

Yet another theory, proposed from time to time both in and out of print, is that the *material velocity* is responsible for initiation (for example, reference 72). This theory ascribes a special importance to the high translational velocity in the forward direction within the detonation wave. Impact of fast-moving molecules is visualized as tearing off fragments from intact molecules, thus initiating the reaction. The effect may properly be described as a "one-dimensional temperature," which would then amount to more than a thousand degrees. It is not easy to disprove the "one-dimensional temperature" hypothesis completely, but two arguments make a strong case against it. In the first place, let us assume that the kinetic energy of a fast molecule is delivered to a particular bond or grouping; then if dissociation takes place *before* the energy has time to become redistributed among the various vibrational degrees of freedom of the molecule, the dissociation can really be said to be caused by the impact; but if the dissociation does not take place until *after* the redistribution, the dissociation is merely due to the high temperature in the ordinary sense. We wish to know the rates of the competing processes,—dissociation and redistribution. Redistribution requires a small or zero activation energy, while dissociation requires a high activation energy (about equal to the strength of the bond broken); thus it is probable that redistribution will outrun dissociation, and the molecule will have reached a uniform temperature long before dissociation occurs.

The second argument against the material velocity theory is also an argument against the pressure theory of initiation, and appeals to the experimental observation (see Section II) that the reaction time is about 1 microsec. for typical explosives. According to either of the latter theories, the influence leading to initiation should affect all of the explosive material alike (since pressure and velocity are substantially homogeneous in the reaction zone); thus all the explosive in a cross-section would be simultaneously initiated. But any reasonable treatment of reaction rate indicates that then the reaction should be over in about one vibration period, or about h/kT seconds, which amounts to about 10^{-14} sec., or somewhat more than this when the effects of activation energy and activation entropy are included. The proponents of the latter theories are thus left with the problem of explaining, not why the decomposition in a detonation is so fast, but *why it is as slow as it is*—a discrepancy of about 8 powers of 10.

APPENDIX A: JUSTIFICATION FOR NEGLECT OF VISCOSITY AND THERMAL CONDUCTIVITY

Rigorously speaking, there is not at the shock front a discontinuity in pressure, temperature, velocity, and entropy. Rather, the transition takes place over a

narrow region whose length is determined by the viscosity and the thermal conductivity. If the length of this "shock zone" is very small in comparison with other lengths under consideration (e.g., the reaction zone length or the length of the rarefaction zone), the shock may without error be treated as a discontinuity. The length of the shock zone may be investigated for any particular case, by the inclusion of viscosity and thermal conductivity in the hydrodynamic equations.

For three-dimensional motion, the equations of motion[11] and of energy (74) are in vector notation:

$$\frac{d\vec{W}}{dt} = -V \text{ grad } P + \frac{1}{3}\eta V \text{ grad div } \vec{W} + \eta V \nabla^2 \vec{W} \tag{A1}$$

$$\frac{dE}{dt} = \frac{dQ}{dt} - P\frac{dV}{dt} - 2\eta V \text{ div } (\vec{W} \text{ grad})\vec{W} - \frac{2}{3}\eta V(\text{div } \vec{W})^2 + \kappa V \nabla^2 T \tag{A2}$$

where η is the viscosity and κ is the thermal conductivity. For one-dimensional motion these simplify to

$$\frac{dW}{dt} = -V\frac{\partial P}{\partial x} + \frac{4}{3}\eta V \frac{\partial^2 W}{\partial x^2} \tag{A3}$$

$$\frac{dE}{dt} = \frac{dQ}{dt} - P\frac{dV}{dt} + \frac{4}{3}\eta V \left(\frac{\partial W}{\partial x}\right)^2 + \kappa V \frac{\partial^2 T}{\partial x^2} \tag{A4}$$

and for a steady state, upon transformation to the coördinate system in which the shock wave is at rest:

$$P - P_0 + \frac{U^2}{V} - \frac{D^2}{V_0} = \frac{4}{3}\eta \frac{dU}{dy} \tag{A5}$$

$$\Delta E - \Delta Q - \frac{1}{2}(D - U)^2 - P_0(V_0 - V) = \frac{\kappa V_0}{D}\frac{dT}{dy} \tag{A6}$$

The pair of differential equations A5 and A6 has never been solved in closed form for general values of the parameters. For the case of a pure shock wave (ΔQ identically zero) R. Becker (6) expressed the temperature as a power series in the velocity, the series fortuitously terminating for the value $\kappa/\eta = C_p/3$. As an example of the calculation of shock zone length by Becker's method, we list the recent calculations by Thomas (69) for a shock wave in air. These calculations have taken into consideration the change of viscosity and conductivity with pressure and temperature.

Calculations for a shock wave in air

SHOCK PRESSURE	SHOCK ZONE LENGTH FREE PATHS
atm.	
4.5	3.98
9.8	3.08
19.7	2.25
43.4	1.98
	1.74

[11] The famous Navier–Stokes equation. See references 35, 49, 53, 58.

Similar calculations by Becker for a shock wave in liquid diethyl ether give the following results:

Calculations for a shock wave in ethyl ether

SHOCK PRESSURE	SHOCK ZONE LENGTH
atm.	*Å.*
100	520
1,000	53
10,000	6.5
100,000	1.4

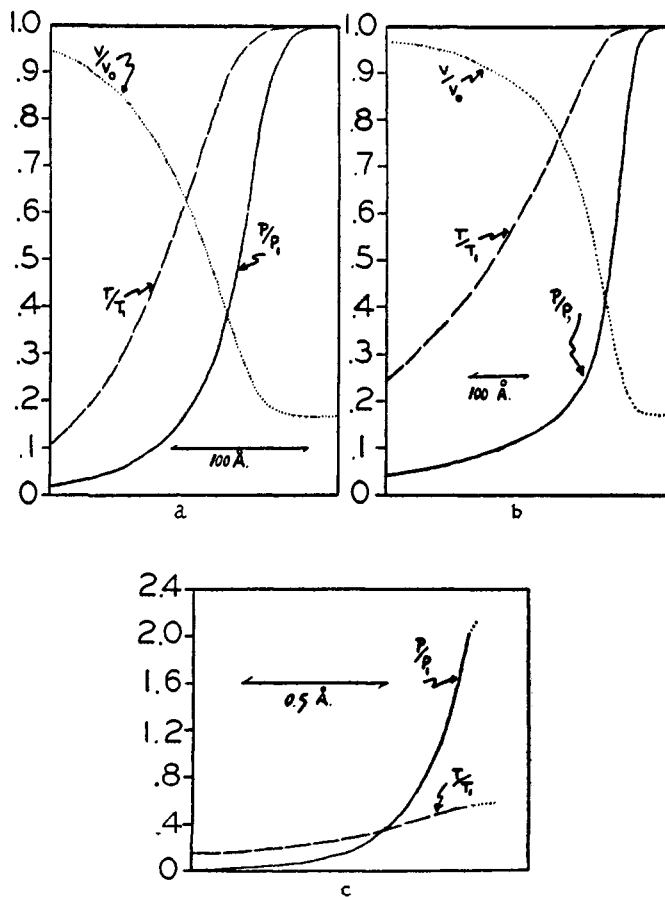
FIG. 3. Pressure, volume, and temperature distribution with η and κ

The structure of the shock zone is shown graphically in figures 3a, 3b, and 3c. Figure 3a is Becker's solution for a gas. Figure 3b is for a gas with a thermal conductivity four times as great as in Becker's solution (27). Figure 3c is for a solid explosive with an assumed viscosity of 0.2 centipoise and a thermal

conductivity of 10^4 ergs cm.$^{-2}$ sec.$^{-1}$ (28). The computation of figures 3b and 3c was carried through by a somewhat tedious step-by-step simultaneous numerical integration of the differential equations A5 and A6. Similar step-by-step computations have been carried through for a shock wave in which chemical reaction is occurring (27); not only are these calculations tedious and excessively sensitive to assumed boundary conditions, but for known explosives the reaction zone is so long in comparison with the shock zone (e.g., millimeters against Ångström units) that the shock zone may be analyzed on the assumption that no reaction has occurred.

The important qualitative result of all these computations is that the *shock zone is exceedingly narrow, amounting to a few free paths for a gas or a few molecules thickness for a solid.* One is thus justified in neglecting viscosity and conductivity when he is interested in the general structure of a detonation wave.

Rather than solve equations A5 and A6 rigorously, we may attack the problem by an alternative method which requires less mathematical labor and is more easily grasped intuitively.

First we consider viscous forces alone and set up a simplified model of the conditions behind and before the shock front. Suppose a number of molecules of very high average velocity to be brought adjacent to a number of molecules of very low average velocity. Then the initial velocity distribution at the interface is highly non-Maxwellian, and we wish to find the rate at which Maxwellian distribution is approached. Note that this is not a mere analogy, but a close description of what happens in a shock zone, where a portion of the directed energy (non-Maxwellian velocity distribution) is converted by viscous dissipation into temperature energy (Maxwellian velocity distribution) with an accompanying increase in entropy.

Now the problem of the "relaxation time of velocity distribution" has been solved in detail for gases (16, 44). Briefly, when a very fast-moving molecule collides with a slow-moving molecule, the fast molecule loses half its velocity. We see that any fluctuation in velocity will die out exponentially, roughly half of it disappearing in the time taken for each molecule to make one collision. We thus obtain a qualitative idea of the great rapidity of the process by which departures from Maxwellian velocity distribution are smoothed out. The corresponding problem for condensed phases has not been studied in detail, but here also there is little doubt that velocity differences will be smoothed out by a few collisions.[12] We may summarize by saying: So far as velocity (or pressure) is concerned, a shock zone thickness will be that within which a few molecular collisions have occurred.

Secondly, we consider the spread of temperature, and again set up a simplified model of the shock front. Suppose one stationary body at the shock temperature instantaneously to be brought adjacent to another stationary body at room temperature. Then we wish to find the rate at which temperature spreads from

---

[12] In the theory of viscous flow, it has been assumed that the excess energy of a moving molecule is completely dissipated between one transport process of "jump" and the next (26). However, such a molecule undergoes some thousands of collisions between jumps.

the hot to the cold body, and to compare this with the rate at which the wave itself would travel.

This is a familiar problem in heat conduction, whose solution is

$$T/T_1 = 1 - 2Erf\left[x/\sqrt{2Vt/C_v}\right] \tag{A7}$$

and this solution is presented graphically in figure 4 for three different time intervals, along with the distance traveled by the shock wave in those same times. In this calculation the parameter $\kappa V/C_v$, which is roughly equal to velocity of sound $\times$ interatomic distance, was taken to be 0.018 cm.^{2} sec.$^{-1}$, a value appropriate for a solid explosive.

It will be observed that the spread of heat can keep pace with the travel of the shock wave for a distance of a few Ångström units, but not more. We may summarize: The temperature rise in a shock wave will run in advance of the pressure rise, but only for a distance amounting to a few interatomic distances.
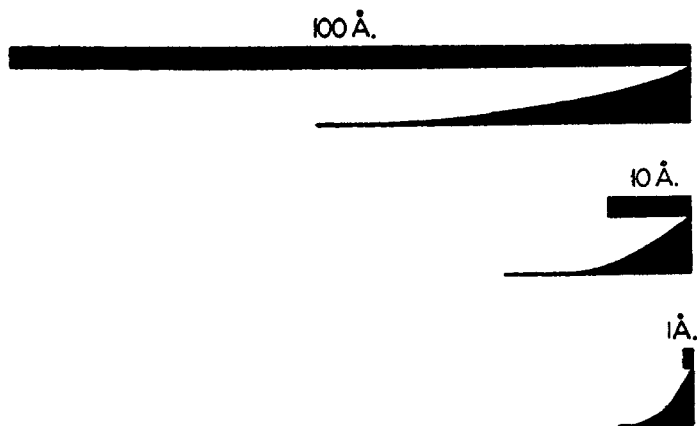

FIG. 4. Conduction range vs. velocity range

It is gratifying that both the rigorous numerical analysis and the simpler analysis lead to the same result, giving shock zones of molecular dimensions and thus justifying the neglect of viscosity and conductivity.

APPENDIX B: THE CHAPMAN–JOUGUET CONDITION

The equations of hydrodynamics do not suffice to determine the detonation velocity D uniquely. The additional assumption made by Chapman and by Jouguet, that the detonation is sonic with respect to the products at the end of the reaction zone,

$$D = W_1 + C_1 \tag{1e}$$

does permit an unique choice of the velocity. We proceed to examine the arguments offered to justify this Chapman–Jouguet condition.

To help visualize the problem, we plot equations 4b and 4c on a P,V diagram. Such a diagram, drawn approximately to scale for TNT, is figure 5. Equation

4b is a straight line

$$\frac{P - P_0}{V_0 - V} = \frac{D^2}{V_0^2} \tag{4b}$$

whose slope is D^2/V_0^2. Equation 4c gives a graph which is hyperbolic in shape: thus for the Abel equation of state, equation 4c becomes, for small P_0:

$$P\left[V - V_0 \frac{2\alpha/V_0 + \gamma - 1}{2 + \gamma - 1}\right] = \frac{2R}{\gamma + 1}[T_0 + \Delta Q/\bar{C}_v]$$
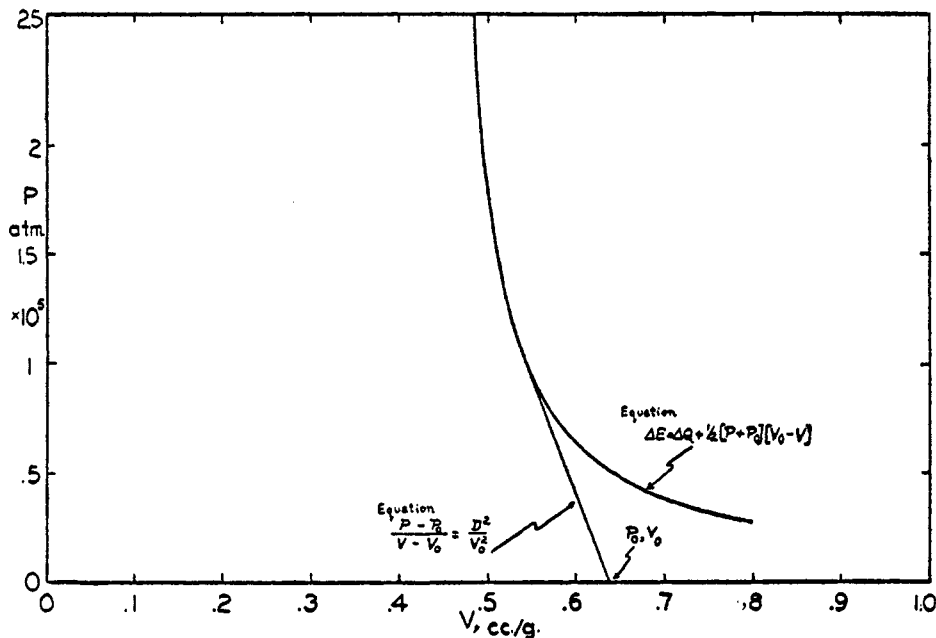

FIG. 5. Rankine–Hugoniot diagram for TNT of density 1.6 g./cc.

which resembles closely the Abel equation of state, but with special parameters replacing the covolume and the gas constant.

To determine the detonation velocity D, we wish to find the point of intersection of these two lines in the P,V diagram. The Chapman–Jouguet condition says that the desired intersection is the point of tangency of one line to the other, as the lines are drawn in figure 5. That this condition is identical with the condition $D = W_1 + C_1$ can be proved by algebraic manipulation of the equations of the two curves; or more elegantly by a geometrical method due to von Neumann. If we draw a straight line joining any two points of the hyperbola representing complete reaction, that straight line will represent a shock wave in the completely reacted material. If we let the two points approach one another, the straight line becomes tangent to the curve and represents a sonic wave in the reacted material.

Inspection of figure 5 shows that the Chapman–Jouguet condition can be

stated in several other ways which are geometrically equivalent. Thus (*i*) the Chapman–Jouguet velocity is the only detonation velocity which is uniquely specified; also (*ii*) the Chapman–Jouguet velocity is the minimum detonation velocity compatible with the hydrodynamic equations. (It was in this latter form that Chapman assumed the condition.)

Discussion according to von Neumann

von Neumann (73) has pointed out that if the reaction zone in a detonation wave is finite, the hydrodynamic and thermodynamic equations must be valid at all points within the wave, so that one can draw a family of Hugoniot curves corresponding to successive amounts of chemical reaction, from $N = 0$ to $N = 1$. Now the straight line which represents conditions within the shock wave must begin somewhere on the curve $N = 0$, must intersect the curves for increasing N in order, and must end somewhere on the curve $N = 1$. In order that there
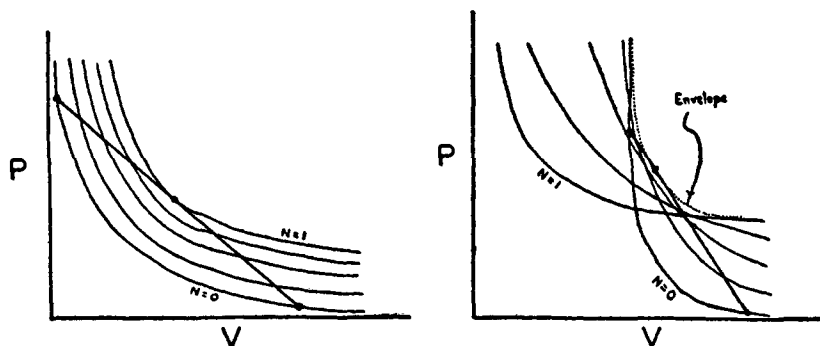

FIG. 6. von Neumann's curves

exist a discontinuity in pressure and temperature at the shock front so as to initiate the reaction, the intersection of the straight line with the curve $N = 0$ must be the *upper* intersection. If the straight line intersects the curve $N = 1$ at an upper intersection point, the tangent to the curve at that point would be steeper, so the velocity of sound in the products would exceed the detonation velocity and a rarefaction wave would engulf the detonation wave; thus the intersection with the curve $N = 1$ must be the *lower* intersection.

In order to proceed continuously from an upper intersection at $N = 0$ to a lower intersection at $N = 1$, either (*i*) the upper intersection and the lower intersection coincide at $N = 1$, giving a point of *tangency* (this is the usual Chapman–Jouguet result), or (*ii*) if the curves cross one another so that an envelope exists, the straight line may be tangent to the envelope. These two possibilities are given graphically in figure 6, taken from von Neumann's paper. The latter possibility, which was first proposed in the paper by von Neumann. does not correspond to any known physical situation.

Discussion according to Scorah

Scorah (65) has shown by straightforward thermodynamics that at the Chapman–Jouguet velocity the entropy increase is a minimum; also that the ratio

entropy increase/available energy fed into the wave front is a maximum. Scorah states: "The normal detonation wave proceeds at that speed which allows the greatest degradation of each unit of energy supplied to the wave. This result is in accord with the fundamental principle of degradation of energy in all natural processes—a principle that is so universally verified that when the extent of degradation brought about by a natural process is discovered to vary with the speed of the process, it would seem only consistent that the stable speed would be that which allowed the greatest degradation." Since this principle is not derivable from the second law of thermodynamics, nor is it generally valid for chemical kinetics, the argument must be regarded as one of plausibility rather than of strict proof. The result is nevertheless an interesting one.

Discussion according to Devonshire

Jouguet originally justified his assumption by appealing to considerations of stability of the wave. Devonshire (20) and also Eyring et al. (29) have extended the method to include waves other than ideal steady waves, thus obtaining a generalized Chapman–Jouguet condition.

The derivation has been carried through for three cases: (i) the wave is non-planar; (ii) the wave is not in its steady state; (iii) the wave is both non-planar and non-steady.

Case (i): Non-planar wave

Suppose the propagating wave to be symmetric about an axis (plane), and represent the wave front in a small region by a spherically (cylindrically) curved surface. Denote the radius of curvature of the wave front by r_0, and the angle between the radius vector and the axis (plane) of symmetry by ϕ. If the components of particle velocity in a fixed coördinate system are W_r in the radial direction and W_ϕ in the direction of increasing ϕ, in a coördinate system moving with velocity D these are

$$U_r = W_r - D \cos \phi \qquad (B2)$$

$$U_\phi = W_\phi + D \sin \phi \qquad (B3)$$

A steady state is assumed, so that at the axis (plane) of symmetry

$$\frac{\mathrm{d}}{\mathrm{d}t} = -(D - W_r)\frac{\mathrm{d}}{\mathrm{d}r}$$

whereupon the equations of continuity and of motion become, near the wave front

$$(D - W_r)\frac{\mathrm{d}V}{\mathrm{d}r} = -V\frac{\mathrm{d}W_r}{\mathrm{d}r} - \frac{kV}{r}\left[W_r + \left(\frac{\partial W_\phi}{\partial \phi}\right)_{\phi=0}\right] \qquad (B4)$$

$$(D - W_r)\frac{\mathrm{d}W_r}{\mathrm{d}r} = V\frac{\mathrm{d}P}{\mathrm{d}r} \qquad (B5)$$

where k is 2 for spherical waves and 1 for cylindrical waves.

By the equation of state, the pressure is a function of the three variables T,

V, and N. But the first law of thermodynamics gives us another relation between T, V, and N, so that any one of these variables may be eliminated from the equation for pressure. (It is not necessary to write explicitly the first law relation between T, V, and N; the mere fact that such a relation exists is sufficient.) Then

$$P = P(V, N)$$

$$\frac{dP}{dr} = \left(\frac{\partial P}{\partial V}\right)_N \frac{dV}{dr} + \left(\frac{\partial P}{\partial N}\right)_V \frac{dN}{dr} \tag{B6}$$

Of these derivatives, one is determined by the velocity of sound C:

$$\left(\frac{\partial P}{\partial V}\right)_N = \left(\frac{\partial P}{\partial V}\right)_{N,S} = -\frac{C^2}{V^2} \tag{B7}$$

We define a new quantity χ such that

$$\chi = \left(\frac{\partial P}{\partial N}\right)_V \frac{dN}{dt} = -(D - W_r)\left(\frac{\partial P}{\partial N}\right)_V \frac{dN}{dr} \tag{B8}$$

so that with the two substitutions B7 and B8, equation B6 becomes

$$\frac{dP}{dr} = -\frac{C^2}{V^2}\frac{dV}{dr} - \frac{\chi}{D - W_r} \tag{B9}$$

With this substitution into the equations of continuity and of motion, we obtain:

$$-\frac{(D - W_r)}{V}[(D - W_r)^2 - C^2]\frac{dV}{dr}$$

$$= (D - W_r)^2 \frac{k}{r}\left[W_r + \left(\frac{\partial W_\phi}{\partial \phi}\right)_{\phi=0}\right] - \chi V \tag{B10}$$

$$[(D - W_r)^2 - C^2]\frac{dW_r}{dr} = \frac{C^2 k}{r}\left[W_r + \left(\frac{\partial W_\phi}{\partial \phi}\right)_{\phi=0}\right] - \chi V \tag{B11}$$

As one proceeds through the wave three possibilities may occur:

(I) $D < W_r + C$ throughout. Any rarefaction wave arising in the products will travel at a sonic velocity with respect to the products, or $W_r + C$. Such a wave would move faster than the detonation, and hence engulf and destroy it.

(II) $D = W_r + C$ at a point where the right sides of equations B10 and B11 are (positive or negative) finite. In this situation the derivatives dV/dr and dW_r/dr become (positively or negatively) infinite, so that a shock discontinuity is occurring within the detonation wave. It may be assumed that any such discontinuity would be only a transient, would rapidly propagate to the front or rear of the detonation wave, and would there be destroyed.

(III) $D = W_r + C$ at a point where the right sides of equations B10 and B11 vanish; thus where

$$\chi = \frac{kC^2}{Vr}\left[W_r + \left(\frac{\partial W_\phi}{\partial \phi}\right)_{\phi=0}\right] \tag{B12}$$

This is the desired solution for the generalized Chapman–Jouguet condition for a non-planar wave.

Note that for the special case treated by von Neumann, that with no radial loss, this becomes $\chi = 0$, therefore

$$\left(\frac{\partial P}{\partial N}\right)_v \frac{dN}{dr} = 0$$

The vanishing of dN/dt means that the Chapman–Jouguet point is at the end of the chemical reaction; or the vanishing of $\left(\frac{\partial P}{\partial N}\right)_v$ is the condition for the Chapman–Jouguet point to lie on the envelope of Hugoniot curves. The present result thus includes von Neumann's result.

In order to assess this result, we examine again the continuity equation B4 with the substitution B9:

$$\frac{dP}{dr} = \frac{C^2/V}{D - W_r} \frac{dW_r}{dr} - \frac{kC^2/V}{(D - W_r)r}\left[W_r + \left(\frac{\partial W_\phi}{\partial \phi}\right)_{\phi=0}\right] - \frac{\chi}{D - W_r} \quad \text{(B13)}$$

Clearly the first term on the right is the rate of pressure change due to the change in particle velocity, which would be found even in passing through an ideal wave. The second term is the rate of pressure change due to curvature of the wave front and the interaction between adjacent elements of fluid. The third term is the rate of pressure change due to chemical reaction. When the condition B12 holds, the last two terms drop out. We may now summarize by saying: The detonation velocity for a wave with a curved front is given by $D = C_{CJ} + W_{CJ}$, where C_{CJ} and W_{CJ} are evaluated at that point where the rate of pressure rise due to reaction is just equal to the rate of pressure fall due to the curvature of the front and the interaction of neighboring elements of the fluid. For a convex wave of high curvature, the effective reaction zone will be shortened.

Case (ii): Time-dependent planar wave

If a plane wave is propagating with the instantaneous (but not steady) velocity D, we write the equations of continuity and motion in a coördinate system moving with this velocity so that $y = Dt - x$:

$$(D - W)\frac{\partial V}{\partial y} = -V\frac{\partial W}{\partial y} + \frac{\partial V}{\partial t} \quad \text{(B14)}$$

$$(D - W)\frac{\partial W}{\partial y} = V\frac{\partial P}{\partial y} - \frac{\partial W}{\partial t} \quad \text{(B15)}$$

As before, the equation of state furnishes the relation

$$\frac{\partial P}{\partial y} = \left(\frac{\partial P}{\partial V}\right)_{N,S}\frac{\partial V}{\partial y} + \left(\frac{\partial P}{\partial N}\right)_{V,S}\frac{\partial N}{\partial y} + \left(\frac{\partial P}{\partial S}\right)_{V,N}\frac{\partial S}{\partial y} \quad \text{(B16)}$$

or

$$\frac{\partial P}{\partial y} = -\frac{C^2}{V^2}\frac{\partial V}{\partial y} + \frac{\chi}{D - W} \quad \text{(B17)}$$

where C is the velocity of sound and χ is defined as

$$\chi = (D - W)\left\{\left(\frac{\partial P}{\partial N}\right)_{v,s}\frac{\partial N}{\partial y} - \left(\frac{\partial P}{\partial S}\right)_{N,V}\frac{\partial S}{\partial y}\right\}$$

$$= \left(\frac{\partial P}{\partial N}\right)_{v,s}\left(\frac{dN}{dt} - \frac{\partial N}{\partial t}\right) + \left(\frac{\partial P}{\partial S}\right)_{v,N}\left(\frac{dS}{dt} - \frac{\partial S}{\partial t}\right) \qquad (B18)$$

As before, the substitution of B17 into the equation of continuity and motion gives two new equations

$$-\frac{D - W}{V}[(D - W)^2 - C^2]\frac{\partial V}{\partial y} = V\chi - (D - W)\frac{\partial W}{\partial t} + \frac{(D - W)^2}{V}\frac{\partial V}{\partial t} \quad (B19)$$

$$[(D - W)^2 - C^2]\frac{\partial W}{\partial y} = V\chi - (D - W)\frac{\partial W}{\partial t} + \frac{C^2}{V}\frac{\partial V}{\partial t} \qquad (B20)$$

and again there are three possibilities, of which two are ruled out by instability. Then the instantaneous detonation velocity will be given by $D = C + W$ at the point where

$$\chi = \frac{C}{V}\frac{\partial W}{\partial t} - \frac{C^2}{V^2}\frac{\partial V}{\partial t} \qquad (B21)$$

To interpret this result, we write

$$\frac{\partial P}{\partial y} = \frac{C^2/V}{(D - W)^2}\frac{\partial W}{\partial t} - \frac{1}{D - W}\left\{\frac{C^2/V}{D - W}\frac{\partial W}{\partial t} - \frac{C^2}{V}\frac{\partial V}{\partial t}\right\} + \frac{\chi}{D - W} \quad (B22)$$

in which it is evident that the second term on the right gives the space rate of decrease of pressure due to the time rate of change of velocity and volume, while the third term is the space rate of increase of pressure due to the space rate of change of chemical composition and entropy. These two rates are equal at the Chapman–Jouguet point, where $D = W + C$.

For a rapidly accelerating wave, the effective reaction zone will be shortened.

Case (iii): Time-dependent non-planar wave

Finally, if a detonation wave is propagating both with a curved front and at a velocity different from its equilibrium velocity, we write the equations of continuity and motion near the wave front as:

$$\frac{dV}{dt} = V\frac{\partial W}{\partial r} + \frac{kW}{Vr} \qquad (B23)$$

$$\frac{dW}{dt} = -V\frac{\partial P}{\partial r} \qquad (B24)$$

Proceeding with the analysis as before, we find that $D = W + C$ at the point where

$$\chi = \frac{D - W}{V}\frac{\partial W}{\partial t} - \frac{C^2}{V^2}\frac{\partial V}{\partial t} + \frac{kC^2W}{Vr} \qquad (B25)$$

We may now state a generalized version of the Chapman–Jouguet condition for a wave both non-planar and non-steady:

> The detonation velocity is given by $D = C_{CJ} + W_{CJ}$, where C_{CJ} and W_{CJ} are evaluated at that point where the space rate of increase of pressure due to the space rate of change of chemical composition and entropy is just equal to the sum of the space rate of decrease of pressure due to the time rate of change of velocity and volume and that due to the curvature of the wave-front.
>
> (B26)

For any detonation wave whose deviation from planarity and from its equilibrium velocity is not large, the Chapman–Jouguet point will be very near to the point where the chemical reaction becomes complete. We shall always assume this to hold in subsequent sections of the present study, with the exception of the investigation of highly curved waves where the effect of curvature will be explicitly included.

APPENDIX C: EXACT DETONATION PROPERTIES

The exact equations for a detonation wave in which the initial pressure P_0 is too large to be neglected are the following:

$$\frac{V_1}{V_0} = \frac{\gamma + \dfrac{\alpha}{V_0} - \dfrac{\alpha}{V_0} \cdot \dfrac{P_0}{P_1}}{\gamma + 1 - \dfrac{P_0}{P_1}}$$

$$P_1 = \frac{2R}{V_0 - \alpha} \frac{\Delta Q + \bar{C}_v T_0}{\bar{C}_v} \frac{1 + \dfrac{\gamma - 1}{\gamma + 1} \cdot \dfrac{P_0}{P_1}}{1 + \dfrac{1}{\gamma + 1} \cdot \dfrac{P_0}{P_1}}$$

$$T_1 = \frac{\Delta Q + \bar{C}_v T_0}{\bar{C}_v} \cdot \frac{2\gamma}{\gamma + 1 - \dfrac{P_0}{P_1}}$$

$$D^2 = (\Delta Q + \bar{C}_v T_0) \frac{2(\gamma^2 - 1)}{\left(1 - \dfrac{\alpha}{V_0}\right)^2} \frac{1 + \dfrac{\gamma - 1}{\gamma + 1} \dfrac{P_0}{P_1}}{1 - \dfrac{P_0}{P_1}}$$

$$\frac{W_1}{D} = \frac{\left(1 - \dfrac{\alpha}{V_0}\right)\left(1 - \dfrac{P_0}{P_1}\right)}{1 + \gamma - \dfrac{P_0}{P_1}}$$

APPENDIX D: SPURIOUS SOLUTION FOR THE PROPERTIES WITHIN THE REACTION ZONE

If the negative sign is taken in equation 7b, the properties within the reaction zone would be those plotted in figure 7. It will be noticed that at the wave front

there is no change in pressure, temperature, particle velocity, or entropy. From a chemical point of view, there is nothing at such a front to initiate reaction. This solution therefore represents no known physical situation, and must be treated as spurious.
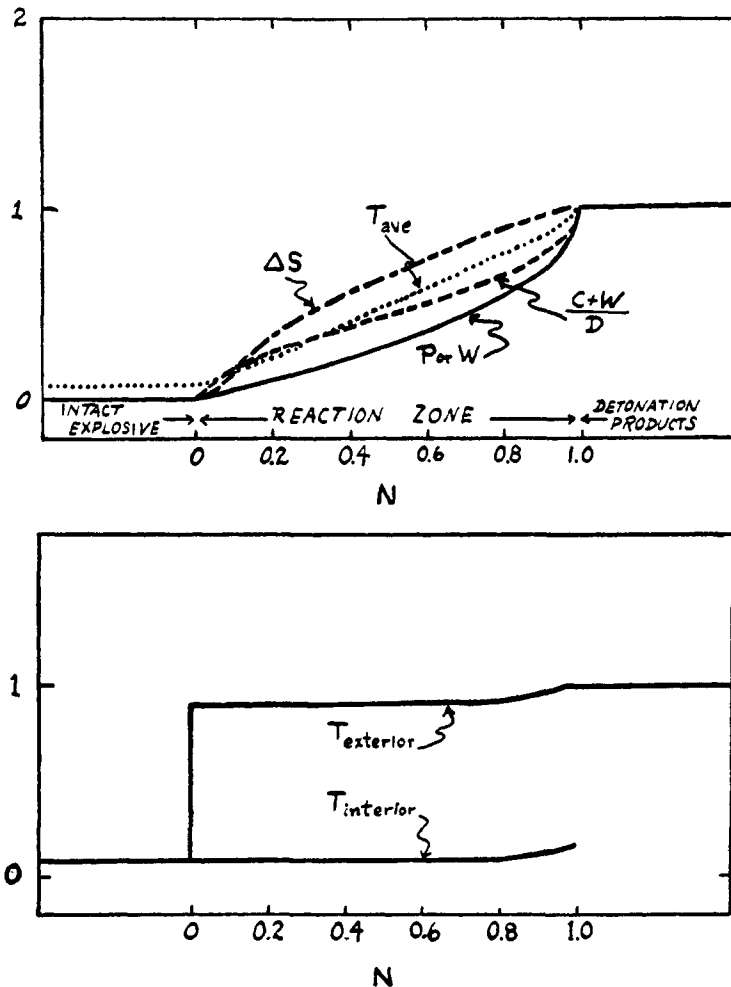

FIG. 7. Upper: Distribution of wave properties through the reaction zone; spurious solution. Lower: Temperature distribution for the heterogeneous case; spurious solution.

APPENDIX E: ENTROPY CHANGE OF EXPLOSION AT
CONSTANT VOLUME AND TEMPERATURE

The entropy increase across a shock front can be calculated at once from the temperature and the volume before and behind the wave front when the equation of state is known. In a detonation wave there is an additional contribution to the entropy increase, because the detonation products are chemically different from the intact explosive. We calculate this entropy change of chemical decom-

position at constant temperature and volume, by carrying out the change in two hypothetical steps.

Step 1: The explosive at room temperature decomposes to form its products of detonation also at room temperature, but at the volume they would occupy each at a partial pressure of 1 atm. This is the usual standard state for entropies which are tabulated for the products and can be estimated rather closely for the intact explosives.

Step 2: The products, at the volume they would occupy each at a partial pressure of 1 atm., are compressed to a volume equal to the original volume. The products will be supposed to obey the Abel equation of state.

The entropy change is for this sequence of processes

$$\Delta S = S^0_{products} - S^0_{explosive} - R \ln \frac{V_{atm} + \alpha}{V_0 - \alpha} \tag{E1}$$

The calculation may be clarified by two examples:

Example 1: TNT of density 1.6. Reaction assumed to be:

$$\underset{\substack{O_2N \quad NO_2 \\ \\ NO_2}}{CH_3} \rightarrow \tfrac{3}{2}N_2 + \tfrac{5}{2}H_2O + CO + 6C$$
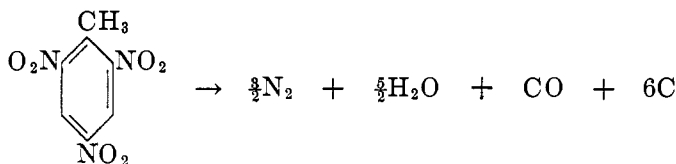
Step 1: S^0 of 3/2 mole gaseous N_2 .... 1.5×45.79
S^0 of 5/2 mole gaseous H_2O .... 2.5×45.13
S^0 of 1 mole gaseous CO 47.32
S^0 of 6 moles solid C .... 6×1.36
$-S^0$ of 1 mole solid TNT .... -65

Entropy change per mole TNT .... 172 E.U.
Entropy change per gram TNT .... 172/239 = 0.720 E.U.

Step 2: $R = \dfrac{1.986}{\text{Mean mol. wt. gaseous products}} = \dfrac{1.986}{23} = 0.0864$ cal. deg.$^{-1}$ g.$^{-1}$

$V_0 = 0.636$ cm.^{3} g.$^{-1}$

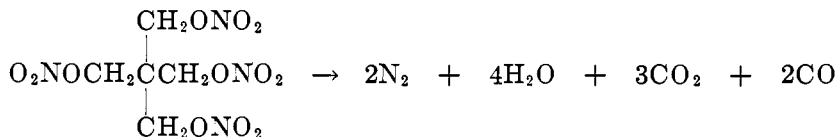$\alpha = 0.4225$ cm.^{3} g.$^{-1}$ assumed

$V_{atm} = \dfrac{24,500 \times (3/2 + 5/2 + 1)}{239} = 512$ cm.^{3} g.$^{-1}$

Entropy change per gram $= -0.0864 \ln \dfrac{512}{0.2135} = -0.680$

$$\Delta S_{T,V} = +0.040$$

Example 2: PETN of density 1.6. Reaction assumed to be:

$$\underset{\underset{\displaystyle CH_2ONO_2}{|}}{\overset{\displaystyle CH_2ONO_2}{\overset{|}{O_2NOCH_2CCH_2ONO_2}}} \rightarrow 2N_2 + 4H_2O + 3CO_2 + 2CO$$

Step 1: S^0 of 2 moles gaseous N_2 .... 2×45.79

S^0 of 4 moles gaseous H_2O .... 4×45.13

S^0 of 3 moles gaseous CO_2 .... 3×51.07

S^0 of 2 moles gaseous CO .... 2×47.32

$-S^0$ of 1 mole solid PETN .... -2×55

Entropy change per mole PETN .... 465 E.U.

Entropy change per gram PETN .... $465/316 = 1.47$ E.U.

Step 2: $R = \dfrac{1.986}{28.7} = 0.0691$ cal. deg.$^{-1}$ g.$^{-1}$

$V_0 = 0.625$ cm.^{3} g.$^{-1}$

$\alpha = 0.41$ cm.^{3} g.$^{-1}$ assumed

$V_{atm} = \dfrac{24,500 \times (2 + 4 + 3 + 2)}{316} = 852$ cm.^{3}. g.$^{-1}$

Entropy change per gram $= -0.0691 \ln \dfrac{852}{0.215} = -0.573$

$$\Delta S_{T,V} = +0.897$$

II. THE NON-IDEAL DETONATION WAVE

A. INTRODUCTION

Even the earliest investigators of detonation (*viz.*, Berthelot and Vieille) noticed that if the detonation were sent through a tube of too small a diameter, it traveled with less than its full velocity. With the more recent extension of detonation velocity measurements over a wide variety of liquid and solid explosives, it has become a commonplace observation that the detonation velocity in a narrow stick is below its ideal value. Thus in any program of measurement of a detonation velocity, one is careful to repeat the measurement using explosive charges of greater and greater diameter until he is sure he has eliminated the effect of charge diameter on the detonation velocity.

Although this phenomenon has been known for many years, a good theory of its cause was not until recently to be found in the literature.[13] One formulation of the now generally accepted explanation was put forward by Jones (40) in

[13] Thus, as recently as 1938, Parisot and Laffitte (56) ascribed the effect to chain breaking by the walls. While this would produce a longer reaction zone, that does not of itself lead to a lower detonation velocity, since the hydrodynamic-thermodynamic ideal velocity does not depend on reaction zone length.

1942. If the reaction occurs over a finite zone, the high pressure within that zone will have led to an appreciable lateral expansion before the reaction becomes complete; the consequent drop in pressure and temperature will lead to a decrease in detonation velocity. Otherwise stated, not all of the energy of the explosive is available to maintain the full detonation velocity, because a portion of the energy is dissipated out the sides of the explosive charge. The theory may be briefly described as the *lateral-loss theory*. It can be seen intuitively—and will also be shown by detailed mathematical analysis—that the effect of lateral loss on the detonation velocity becomes significant when the radius of the explosives charge is of the same order of magnitude as the reaction zone length. Another phenomenon which was observed first for gaseous explosives and later for solid explosives is that an explosive charge initiated at a velocity below its ideal velocity (as by a weak priming charge) does not immediately attain its ideal velocity. Rather, the velocity builds up gradually and approaches its ideal value asymptotically.

A theory of the building-up rate as a function of the reaction zone length has been developed by the authors (29), who find that the detonation velocity covers half the difference between its initial value and its ideal value in a distance of a few reaction zone lengths. The details of the theory will be given below.

Finally, the detonation wave may experience such severe losses that the wave can no longer propagate stably, so that failure of the detonation occurs. This failure phenomenon has been found in experimental detonation velocity measurements—the trace of the detonation on the photographic plate ends abruptly, and the undamaged remainder of the charge can be recovered later. The same phenomenon, also called "fading," has been encountered in the service use of high explosives.

One theory of the failure process says first, that any lateral losses will lead both to a lower detonation velocity and a lower temperature; the lower temperature will lead to a slower reaction and a longer reaction zone; this in its turn will lead to additional losses. When the cumulative effect becomes sufficiently great, failure will occur. The details of the theory will be given below.

It will be noticed that in the theories of all three non-ideal waves—the wave in a finite charge, the transient building-up wave, the failing wave—the reaction zone length plays a leading role. If one understands the chemical reaction kinetics in a detonation explosive well enough, he can predict the reaction zone length under any desired conditions, and so the stability of the propagating wave. In this way, it should be possible to develop a rational approach to such technical problems as, say, boostering of explosive charges. However, not enough facts are now known concerning the chemical kinetics of detonation to make such a program feasible.

Another approach, and a more fruitful one from the point of view of fundamental investigation, will be followed here. That is *to use the theories in an inverted sense, in order to determine by measurements on non-ideal waves the reaction zone lengths in detonating explosives*. By suitable variation of the external conditions, it is possible to study in this way the kinetics of the chemical reaction in a

detonation—even though such a chemical reaction is complete in less than one millionth of a second!

1. *Introduction*

Two theoretical treatments of the non-ideal detonation velocity in a cylindrical stick of explosive of finite radius have appeared. One treatment is by H. Jones (40) and the other is by the present authors (29). The two theories have in common their basic assumption: Of the hydrodynamic equations, only the equation of continuity is perturbed by the expansion in the reaction zone. The two theories, after all the mathematical details have been worked out, also yield numerically similar results.
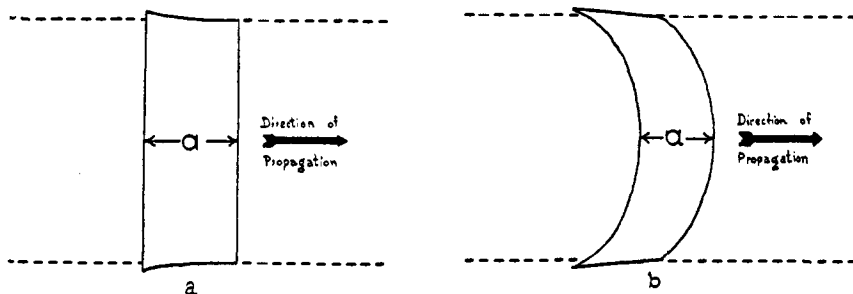

FIG. 8. Models for nozzle theory and curved-front theory. (a) Reaction zone in a detonation, as visualized in the theoretical treatment by H. Jones. (b) Reaction zone in a detonation, as visualized in the theoretical treatment by H. Eyring and coworkers. The two figures are drawn approximately to the correct proportions for a detonation wave in a stick of solid explosive propagating at a velocity 75 per cent of the total velocity, as calculated according to the respective theories.

But the methods of working out the two theories are quite different. Figure 8 represents (approximately to scale) the reaction zone in a detonation, as visualized in the respective theories.

Jones pictures the reaction as beginning at a plane shock front, and becoming complete at another plane the reaction zone length a distant. As seen by an observer moving with the detonation velocity, the detonating stick of explosive looks like a material issuing from a nozzle, the mouth of the nozzle being situated at the wave front. The first step in Jones's theory is to solve the hydrodynamic equations to find the relationship between the expansion of the stream tube and the velocity of propagation. The second step in Jones's theory is to find the amount of expansion for various types of confinement, thus: (*i*) for unconfined or lightly confined charges, the outer layers of explosive are assumed to follow the flow lines given by Meyer's solution for flow around a corner, while the inner part of the explosive expands at constant pressure in a cross-section; (*ii*) for moderately heavily cased charges, the expansion is determined by the motion of the case, which is being accelerated outward because of the pressure in the explosive; and (*iii*) for extremely heavily cased charges, the expansion of the case

is brought about by a shock wave sent into the case. The theory developed by Jones will hereinafter be referred to as the "nozzle" theory.

Alternatively, one may suppose that the reaction zone is curved into a lens-shaped figure convex at the front, the argument running as follows: At the edge of the charge a rarefaction wave will be sent into the reaction zone. Since the local velocity of sound is greater than the detonation velocity, such a rarefaction wave will overtake the front of the wave and slow down the edge of the wave front, thereby giving rise to a curved front. This process will continue until the angle of intersection of the wave front with the edge of the charge is small enough so that the rarefaction wave is no longer reflected. The steady-state velocity will now be below that of a plane wave because of the curvature of the front.

Accordingly, the first step in this theory is to solve the hydrodynamic equations to find the relationship between curvature of the wave front and the velocity of propagation. The second step is then to find, by a graphical construction, the actual shape of the wave for any desired degree of confinement, thus: (*i*) for unconfined charges, the angle of intersection of the edge of the shock wave with the case is 90°; (*ii*) for moderately cased charges, the angle is determined by the expansion of the case; and (*iii*) for heavily cased charges, the angle is determined by the velocity of the shock wave sent into the case. This theory will hereinafter be referred to as the "curved-front" theory.

We now proceed to the mathematical details of the two theories.

2. *Nozzle theory*

(a) The effect of expansion[14]

If the streamlines within the reaction zone are nearly parallel to the charge axis (as they would be for small expansions), the approximate equation of continuity is

$$\frac{V}{V_0} = \frac{U}{D} r^2 \tag{1}$$

where r is the relative expansion of the stream tube. For small expansions, no considerable amount of momentum or energy is lost by lateral motion, and the Chapman–Jouguet condition is also identical with that for a plane wave. Thus we may at once write down the three equations (motion, energy, and Chapman–Jouguet) which are, for an intense wave in a perfect gas:

$$P + \frac{U^2}{V} = \frac{D^2}{V_0} \tag{2}$$

$$\frac{\gamma}{\gamma - 1} PV + \tfrac{1}{2} U^2 - \tfrac{1}{2} D^2 = \Delta Q + \bar{C}_v T_0 \tag{3}$$

$$U_1^2 = P_1 V_1 \gamma \tag{4}$$

[14] For the sake of uniformity we have here changed Jones's notation into that used throughout this paper. We have also slightly simplified Jones's original derivation at a few minor points.

We also recall that the detonation velocity D_i of an ideal plane wave in the gaseous explosive here described is (see Section I):

$$D^2 = 2(\Delta Q + \bar{C}_v T_0)(\gamma^2 - 1) \tag{5}$$

Upon combining these five equations, we obtain without difficulty the final equation

$$\frac{D_i^2}{D^2} = 1 + \gamma^2(r_1^4 - 1) \tag{6}$$

or numerically
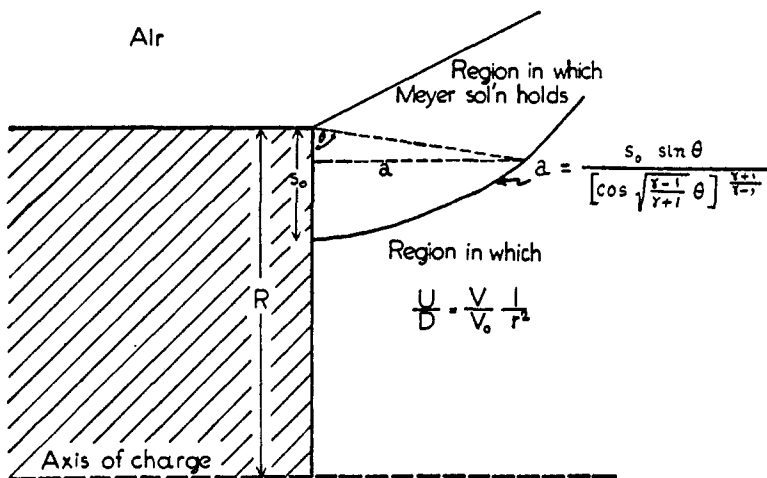
$$\frac{D_i^2}{D^2} \cong 1 + 2.25(r_1^4 - 1)$$

FIG. 9. Jones's construction for nozzle theory

This equation relating the detonation velocity to the relative expansion of a central stream tube at the end of the reaction zone is the foundation upon which all the further nozzle theory of finite charges is built.

(b) The uncased charge

Instead of actually finding the expansion at the end of the reaction zone length a of reacting explosive, which would be very difficult, Jones finds the corresponding radial expansion in the same distance of reaction product gases assumed to be expanding adiabatically. The one process should bear a satisfactorily close resemblance to the other.

Figure 9 represents gas issuing from a nozzle at a velocity equal to the local velocity of sound, it being desired to find the expansion at a distance a from the nozzle. This itself is a problem in hydrodynamics which had not been previously solved, but for which Jones succeeded in obtaining a good approximate solution.

The flow from the nozzle is considered to be separable into two regions. In

the outer region, the stream lines will be those of Meyer's solution for the flow around an edge, the equation for which is:

$$a = s_0 \frac{\sin \theta}{\left[\cos \sqrt{\dfrac{\gamma - 1}{\gamma + 1}} \theta\right]^{(\gamma+1)/(\gamma-1)}} \tag{7a}$$

where the gaseous products are assumed to obey the polytropic equation

$$PV^\gamma = \text{const.} \tag{8}$$

With the exponent $\gamma = 3$, the Meyer streamlines are

$$a = s_0 \frac{\sin \theta}{\cos^2 \dfrac{\theta}{\sqrt{2}}} = s_0 \frac{2 \sin \theta}{1 + \cos \sqrt{2}\theta} \tag{7b}$$

The relative expansion along any Meyer streamline is easily found, for from the evident geometry of the system

$$r = \frac{R - a \operatorname{ctn} \theta}{R - s_0} = \frac{R}{R - s_0}\left[1 - \frac{a}{R} \operatorname{ctn} \theta\right] \tag{9a}$$

In the inner region the streamlines are assumed to be sufficiently nearly parallel to the axis, so that the equation of continuity is

$$\frac{U}{D} = \frac{V}{V_0} \frac{1}{r^2} \tag{10}$$

the relative expansion and the pressure remaining constant across this internal stream tube. It is the relative expansion in this region we desire to find. Since the relative expansion can readily be found along any Meyer streamline from equations 7b and 9, it only remains to choose a value of s_0 such that the Meyer streamline is most nearly representative of the interior streamlines.

The choice of the best Meyer streamline is made in the following manner: The pressure along a Meyer streamline is calculated according to the equation

$$\frac{P_{\text{Meyer}}}{P_1}\left(\cos \sqrt{\frac{\gamma - 1}{\gamma + 1}} \cdot \theta\right)^{2\gamma/(\gamma-1)} \tag{11}$$

The pressure along this same streamline is calculated according to the equation holding for the interior region, which with the Bernoulli equation

$$\tfrac{1}{2}U^2 + \frac{D^2}{\gamma - 1}\left[\left(\frac{P}{P_1}\right)^{(\gamma-1)/\gamma} - 1\right] = \tfrac{1}{2}D^2 \tag{12}$$

is for pressure

$$r^4 = \frac{\left(\dfrac{P_1}{P}\right)^{2/\gamma}}{\dfrac{\gamma + 1}{\gamma - 1} - \dfrac{2}{\gamma - 1}\left(\dfrac{P}{P_1}\right)^{(\gamma-1)/\gamma}} \tag{13}$$

The two pressures so calculated are in general different. Then s_0 is so chosen that the closest agreement is obtained between the two pressures, over a distance along the axis of about one charge radius. The value so found turns out to be $s_0/R = 0.46$, so that the dividing streamline begins 46 per cent of the distance from the surface toward the axis. Figure 10 shows the kind of agreement obtained with this choice of s_0.

With the above choice of streamline, the equations for determining the expansion as a function of reaction zone length become numerically

$$r = 1.85 \left(1 - \frac{a}{R} \, \text{ctn} \, \theta \right) \tag{9b}$$

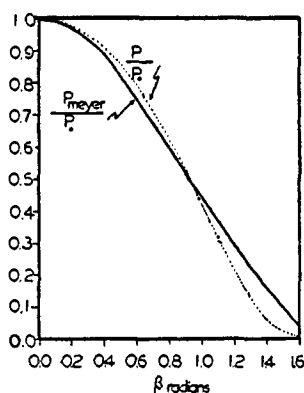$$\frac{a}{R} = 0.92 \, \frac{\sin \theta}{1 + \cos \sqrt{2} \theta} \tag{7c}$$

FIG. 10. Match to Meyer solution

Equations 6, 7c, and 9b now determine completely D/D_i as a function of a/R, and the results are given in table 1. The application of this theory to experimental data will be postponed to a later section.

Wilkinson has applied this same method to a lightly cased charge. The only difference is that the solution in the outer region is the Meyer solution for flow around a curved surface, the shape of the surface being calculated and depending on the mass of the casing.

Wilkinson's calculations are given in table 2, for two different values of the ratio weight of case/weight of explosive. The application of these results will likewise be postponed to a later section.

(c) The cased charge

In order to find the radial expansion for a cased charge, consider an idealized casing of negligible strength which is a thin (but possibly heavy) sheath. The equation of motion of the casing under the pressure P is

$$\sigma R \, \frac{d^2 r}{dt^2} = Pr \tag{14}$$

where σ is the mass per unit area of casing. Upon changing the time derivative to a space derivative, and introducing the ratio W_c/W_e, defined by

$$\frac{W_c}{W_e} = \frac{2\pi R\sigma}{\pi R^2/V_0}$$

the equation of motion of the case becomes

$$\frac{d^2 r}{dx^2} = 2\frac{PV_0}{D^2}\frac{1/R^2}{W_c/W_e}r \tag{15}$$

Of the quantities on the right of equation 15, both P and r are variable along the reaction zone, other quantities being constant. Jones first proposed to solve

TABLE 1

a/R	r	D/D_i
0.3	1.0044	0.9806
0.4	1.0120	0.9491
0.5	1.0245	0.9022
0.6	1.0418	0.8451
0.7	1.0626	0.7863
0.8	1.0869	0.7270
0.9	1.1192	0.6621

TABLE 2

$W_c/W_e = 2/3$			$W_c/W_e = 4/3$		
a/R	r	D/D_i	a/R	r	D/D_i
0.3	1.0044	0.9806	0.3	1.0044	0.9806
0.4	1.0109	0.9535	0.4	1.0099	0.9578
0.5	1.0194	0.9206	0.5	1.0194	0.9206
0.6	1.0318	0.8770	0.6	1.0277	0.8909
0.7	1.0466	0.8305	0.7	1.0408	0.8482
0.8	1.0627	0.7857	0.8	1.0562	0.8032
0.9	1.0869	0.7274	0.9	1.0728	0.7603

this general problem by numerical integration. Later he integrated the equation directly for P constant and r variable, but this solution would not seem to correspond closely to the physical situation, for P falls to one-half its initial value while r is changing by only a few per cent. The simplest solution is to consider *all* quantities on the right to be constant (or to have their average values) upon which the solution is:

$$r = 1 + \frac{\overline{P}V_0}{D^2}\frac{(a/R)^2}{W_c/W_e} \tag{16}$$

With this expression for the expansion, the detonation velocity according to equation 6 is approximately

$$\frac{D_i^2}{D^2} = 1 + 9\frac{\overline{P}V_0}{D^2}\cdot\frac{(a/R)^2}{W_c/W_e}$$

or

$$\frac{D_i^2}{D^2} = 1 + 2.5 \frac{(a/R)^2}{W_c/W_e} \tag{17}$$

which is a result obtained by Jones.

The application of this result to experimental data will be postponed to a later section.

(d) The charge with very thick casing

When the casing surrounding an explosive charge is too thick (as when the casing is an extended block of metal), the simple lamina theory does not apply
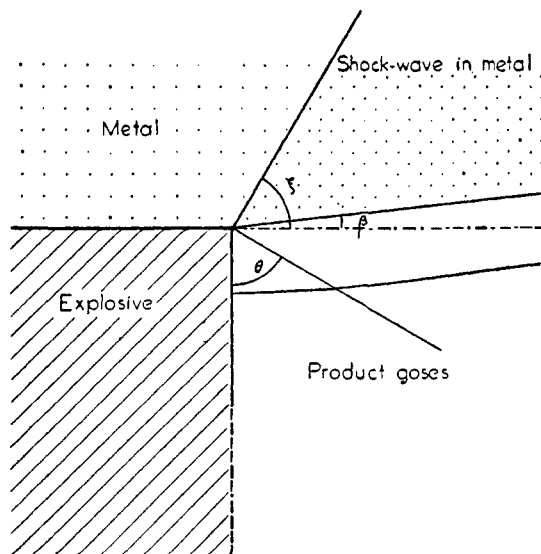

FIG. 11. Jones's construction for metal-sheathed charges

Jones and Strickland have developed a theory which finds the expansion by considering the propagation of a shock wave into the metal surrounding the charge.

Figure 11 presents the geometry of the cylindrical charge expanding as it sets up a shock wave in the surrounding metal. The conditions we seek to satisfy are that (*i*) the component of material velocity be normal to the shock front and (*ii*) the pressure match both at the boundary of the expanding charge and at the metal. When by the use of these matching conditions, we have found the angle of expansion β, then the relative expansion at the end of the reaction zone a is given at once by

$$r = 1 + \frac{a}{R} \tan \beta \tag{18}$$

In order to accomplish the matching, first consider the relation between the pressure in the case P_c (all quantities pertaining to the case will be denoted by the subscript c) and the expansion angle β. The angle at which the shock wave

in the metal is propagated is given by

$$\sin \xi = \frac{D_c}{D} \tag{19a}$$

This may also be written in the form

$$\sin^2 \xi = \left(\frac{P_1 V_0}{D^2}\right)\left(\frac{D_c^2}{P_c V_{0c}}\right)\left(\frac{V_{0c}}{V_0}\right)\frac{P_c}{P_1} \tag{19b}$$

in which the first factor in brackets is a property of the explosive and is equal to

$$\frac{P_1 V_0}{D^2} = \frac{1 - \alpha/V_0}{\gamma + 1}$$

The second quantity in brackets is a property of the metal, depending on the pressure:

$$\frac{P_c V_{0c}}{D_c^2} = 1 - \frac{V_c}{V_{0c}}$$

where

$$\frac{V_c}{V_{0c}} = 1 - A^2/2B \cdot \ln\left[1 + \frac{2B}{A} P_c\right]$$

is used as the equation of state of the metal.

The third quantity in brackets is the initial density ratio. Thus equation 19b determines the angle ξ as a function of P_c/P_1.

The matching of the normal component of material velocity requires that

$$D \sin \beta = W \cos (\xi - \beta) \tag{20a}$$

which with the aid of the shock relation

$$\frac{W_c}{D_c} = 1 - \frac{V_c}{V_{0c}}$$

is trigonometrically equivalent to

$$\frac{\tan (\xi - \beta)}{\tan \xi} = \frac{V_c}{V_{0c}} \tag{20b}$$

Thus the pair of equations (19b and 20b) gives the relation between P_c/P_1 and expansion angle β for any particular casing substance, and several such curves are given in figure 12 (from Jones and Strickland's paper).

Next it is necessary to consider the relation between pressure and expansion within the product gases. The products are once more supposed to obey the polytrope $PV^3 = $ const. and to expand according to the Meyer streamlines up to a region within the angle θ, at which point the pressure is constant; thereafter the streamlines are straight lines at the angle β to the axis. The pressure along this Meyer streamline is

$$\frac{P_{\text{Meyer}}}{P_1} = \cos^3 \frac{\theta}{\sqrt{2}} \tag{21}$$

and the angle of expansion β of the Meyer streamline is given by

$$\tan (\theta - \beta) = \sqrt{2} \cdot \tan \frac{\theta}{\sqrt{2}} \tag{22}$$

The pair of equations (21 and 22) gives the relation between P_{Meyer}/P_1 and expansion angle β for any explosive with the polytropic exponent 3, suitably TNT. This curve is also drawn in figure 12. Since the required matching condition is that $P_c = P_{\text{Meyer}}$, the intersections of these lines give the desired expansion angles β. The results obtained by Jones and Strickland are listed in table 3. These results, together with equations 18 and 6, determine the detonation
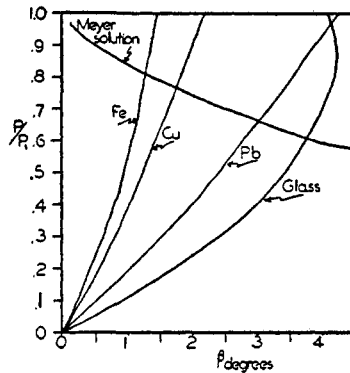

FIG. 12. Shock pressures for various sheaths

TABLE 3

SUBSTANCE	β
TNT in copper	1° 46'
TNT in iron	1° 18'
TNT in lead	3° 3'
TNT in glass	3° 48'
TNT in bakelite	10° 40'

velocity as a function of a/R for a heavy-cased charge of any particular explosive and casing material.

(e) Assembled results

Since each of the studies of the expansion of a finite charge leads to a relation between the ratio D/D_i and the ratio a/R, the results may all be presented on a single graph, and this has been done in figure 13.

This figure may in fact be used as a convenient working diagram for the application of the nozzle theory to experimental data, in lieu of using the algebraic expressions in equations 6, 7c, 9b, 17, and 18. It is only necessary to enter the diagram at the appropriate values of D/D_i and W_c/W_e, and to read the corresponding value of a/R. The actual application of this theory to experimental

data will be postponed until after the presentation of the curved-front theory
of the detonation velocity of finite charges.

3. The curved-front theory

(a) The effect of curvature

The alternative theory of the finite charge begins with the assumption that
any small portion of the actual detonation wave can be approximated by a
spherical detonation wave. It is therefore necessary to find the effect of curvature
of a detonation front upon its velocity.

We first write the four hydrodynamic-thermodynamic equations: continuity,
motion, energy, and Chapman–Jouguet. If the detonation front be a sphere of
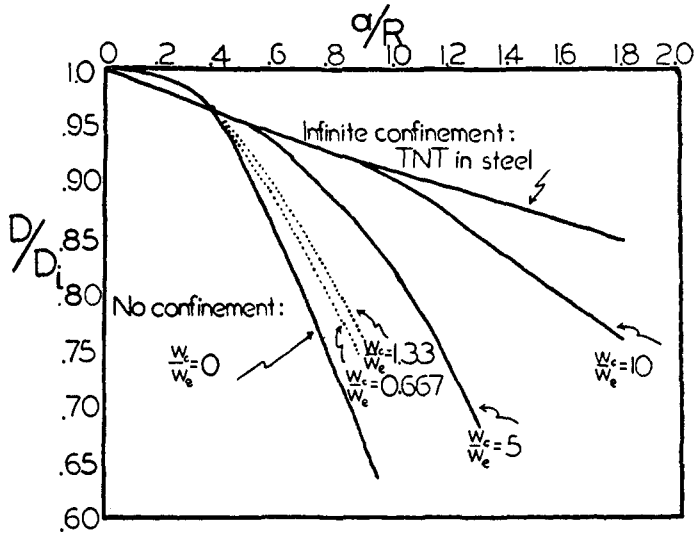radius of curvature r_0, the differential equation of continuity is, if a steady state

FIG. 13. Characterizing chart for nozzle theory

be assumed:

$$(D - W)\frac{dV}{dr} = -\frac{2VW}{r} - V\frac{dW}{dr} \tag{23a}$$

This is also equation B5 of appendix B. Upon integration, this becomes

$$\frac{D - W}{V} = \frac{D}{V_0} - 2\int_{r_0}^{r_0 - a}\frac{W}{Vr}\,dr \tag{23b}$$

or with the notation $U \equiv D - W$ and the notation

$$\vartheta \equiv 1 + \frac{2V_0}{D}\int_{r_0}^{r_0 - a}\frac{W}{Vr}\,dr \tag{24a}$$

the equation of continuity may be written

$$\frac{U}{D} = \frac{V}{V_0}\vartheta \tag{23c}$$

The defining equation for ϑ now becomes

$$\vartheta = 1 - 2 \int_{r_0}^{r_0-a} \frac{\dfrac{V_0}{V} - \vartheta}{r} \, dr \tag{24b}$$

or making the approximation of taking the integrand outside the sign of integration

$$\vartheta = 1 - 2 \left(\frac{V_0}{V_1} - 1 \right) \frac{a}{r_0} \tag{24c}$$

If V_1/V_0 has the numerical value 0.8 appropriate to solid explosives,

$$\vartheta = 1 - 0.5 \, \frac{a}{r_0} \tag{24d}$$

In the practical evaluation of ϑ, equation 24d will be used.

The differential equation of motion is

$$V dP + U dU = 0 \tag{25}$$

just as for the plane detonation. Although this equation cannot be integrated exactly, it can be integrated approximately by substituting for U and dU their values obtained from the continuity equation 23c:

$$dP + \frac{D^2}{V_0^2} V\vartheta d\vartheta + \frac{D^2}{V_0^2} \vartheta^2 dV = 0 \tag{26a}$$

which upon integration becomes

$$P + \frac{1}{2} \frac{D^2}{V_0^2} \vartheta^2 V + \frac{1}{2} \frac{D^2}{V_0^2} \int \vartheta^2 dV = \text{const.} \tag{26b}$$

Since most of the contribution to the integral in equation 26b will be near $\vartheta = 1$, we make the approximation of assigning it that value, whereupon the equation of motion becomes

$$P + \frac{U^2}{V} \frac{1 + \vartheta^2}{2\vartheta^2} = \frac{D^2}{V_0} \tag{26c}$$

The differential equation of energy is

$$dE + d(PV) + U dU = dQ \tag{27a}$$

just as for the plane wave, and its integrated form can be written down at once

$$\Delta E + PV + \tfrac{1}{2} U^2 = \Delta Q + \tfrac{1}{2} D^2 \tag{27b}$$

or for an imperfect gas such that $P(V - \alpha) = RT$,

$$\frac{1}{\gamma - 1} P(V - \alpha) + PV + \tfrac{1}{2} U^2 = \Delta Q + \tfrac{1}{2} D^2 \tag{27c}$$

The Chapman–Jouguet condition is, if the wave front is not too strongly curved,

identical with that for the plane wave:

$$U_1^2 = \frac{P_1 V_1^2 \gamma}{V_1 - \alpha} \tag{28}$$

We return later to the situation which will hold for waves of small radii of curvature: namely, that the simple Chapman–Jouguet condition does not hold.

Upon combining the four hydrodynamic-thermodynamic equations (23c, 26c, 27c, and 28), and recalling that the detonation velocity D_i of an ideal plane wave in an imperfect gas is

$$D_i^2 = 2(\Delta Q + \bar{C}_v T_0) \frac{(\gamma^2 - 1)}{\left(1 - \dfrac{\alpha}{V_0}\right)^2} \tag{I:6d}$$

we obtain without approximations the final relation between detonation velocity and the parameter ϑ:

$$\frac{D_i^2}{D^2} = \left[\frac{\gamma + 1}{1 + \gamma \dfrac{1 + \vartheta^2}{2\vartheta^2}}\right]$$

$$\cdot \left[1 + \frac{1 - \vartheta^2}{\vartheta^2}\left\{\frac{\gamma^2\left(1 - \dfrac{\alpha}{V_0}\right) + \dfrac{\gamma}{2}\left(1 - \dfrac{\alpha\vartheta^2}{V_0^2}\right) - \dfrac{\gamma^2}{4}(\gamma - 1)\left(\dfrac{1 - \vartheta^2}{\vartheta^2}\right)}{\left(1 - \dfrac{\alpha}{V_0}\right)^2\left(1 + \gamma \dfrac{1 + \vartheta^2}{2\vartheta^2}\right)}\right\}\right] \tag{29}$$

The volume at the end of the reaction zone is also found to be:

$$\frac{V_1}{V_0} = \frac{\dfrac{\gamma}{\vartheta^2} + \dfrac{\alpha}{V_0}}{1 + \gamma \dfrac{1 + \vartheta^2}{2\vartheta^2}} \tag{30}$$

Values computed from equation 29 with equation 24d are listed in table 4.

When the radius of the spherical wave is of the order of one reaction zone length, and a fortiori for smaller radii, it is necessary to make use of the generalized Chapman–Jouguet condition as discussed in appendix B. We first determine the Chapman–Jouguet point for a wave whose radius of curvature is r_0. The Chapman–Jouguet point is where the rate of pressure increase due to reaction is exactly equal to the rate of pressure loss due to curvature; thus where

$$\left(\frac{\partial P}{\partial N}\right)_v \frac{dN}{dt} = \frac{2s^2 W}{V r_0} \tag{31}$$

We now approximate the derivatives in equation 31:

$$\left(\frac{\partial P}{\partial N}\right)_v \approx P_1 \tag{32}$$

$$\frac{dN}{dt} \approx \frac{1}{\tau} \tag{33}$$

Here τ is the time spent by the particle in the reaction zone, and is related to the reaction zone length a by

$$\tau = \int \frac{dr}{U} \approx \frac{V_0}{V_{1r}} \frac{a}{D} \tag{34}$$

(Note that the reaction time τ is greater (by about 25 per cent) than the time required for the reaction zone to pass a stationary observer. This is because the reacting particle has a velocity in the same direction as the velocity of propagation.)

With these substitutions, together with the continuity equation and the definition of sound velocity, equation 31 gives:

$$\frac{a}{r_0} = \frac{V_{1r}(V_1 - \alpha)}{2V_1(V_0 - \vartheta V_1)} \tag{35a}$$

TABLE 4

r_0/a	D_{r_0}/D_i	r_0/a	D_{r_0}/D_i
1	0.638 (?)	7.5	0.874
1.25	0.625	10	0.902
1.75	0.662	15	0.932
2.5	0.721	20	0.948
5	0.826	40	0.974

TABLE 4A

r_0/a_i	D_{r_0}/D_i	r_0/a_i	D_{r_0}/D_i
1.5	0.627	0.50	0.362
1.25	0.573	0.25	0.256
1.0	0.512	0	0
0.75	0.444		

For numerical solution, it is necessary to solve this equation simultaneously with equations 30 for V_1 and 24d for ϑ. The result is

$$\frac{a}{r_0} = 0.616 \tag{35b}$$

It is now possible to extend table 4 to smaller radii, if it be assumed that the detonation velocity is approximately proportional to the square root of the fraction of material reacting in the "reaction zone". Thus,

$$\frac{D}{D_i} \approx \frac{D_{r_0=a_i/0.616}}{D_i} \sqrt{\frac{a}{a_i}} = 0.652 \sqrt{\frac{0.616 r_0}{a_i}} \tag{36}$$

The results of tables 4 and 4a are plotted in figure 14; the curve is composed of two portions, the reaction being progressively less complete in the region of small radii (represented by a dashed line on the figure). The relation between

detonation velocity and curvature expressed in figure 14 is the foundation for the remainder of the curved-front theory of finite charges.

(b) The uncased charge

It will be assumed that the wave front in a detonation propagating along a charge of finite radius is meniscus-shaped; and further, that any small portion of this meniscus can be satisfactorily approximated by a segment of a steady spherical wave. This means that if the forward velocity of the detonation wave is
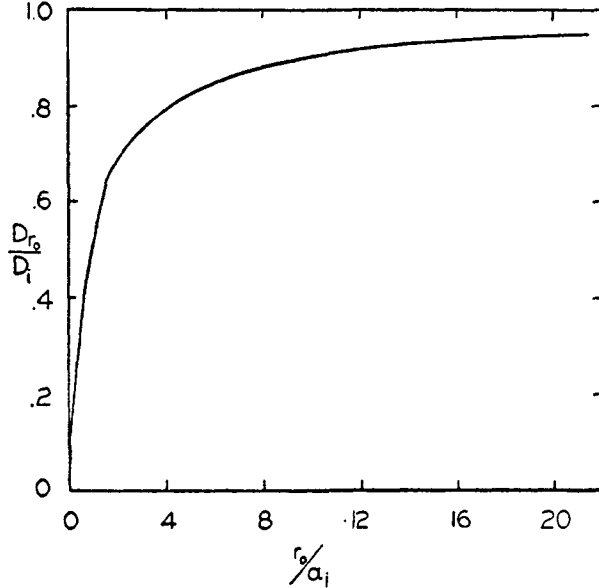

FIG. 14. Detonation velocity *vs.* curvature of wave front

D and the angle between the axis and the normal to a point on the wave front is ϕ, the radial velocity of the wave front at that point is

$$D_{r_0} = D \cos \phi \tag{37}$$

and the curvature of the wave front at that point is read (in units of a_i) from figure 14.

It is now possible by a step-by-step graphical construction to find the shape of a detonation front for any desired value of D/D_i. Thus for the first 10° of arc the front is constructed with a radius read from figure 14, with D_{r_0}/D_i taken to be $D/D_i \cos 5°$; for the second 10° of arc, the corresponding velocity is $D/D_i \cos 15°$; and so on until an angle of 90° has been reached, it being assumed that for an uncased charge the wave front will reach the surface at this angle. The ratio reaction zone length a/radius of charge R is now measured on the drawing. An example of the method of construction is given in figure 15.

In the region of high curvature which should exist near the surface of the

charge, the reaction will be progressively less complete. However, it is just in this region that the interactions of neighboring elements of fluid become important, so that the assumptions of the treatment are no longer valid. Therefore the position of this zone of incomplete reaction cannot be specified with any real precision.

This graphical construction has been carried through for a series of values of D/D_i, and the corresponding values of a/R are given in table 5 and in figure 16. Since the curves constructed to compute table 5 are of some interest in themselves, as giving the shape of wave fronts calculated by this theory, they are reproduced in figure 16.
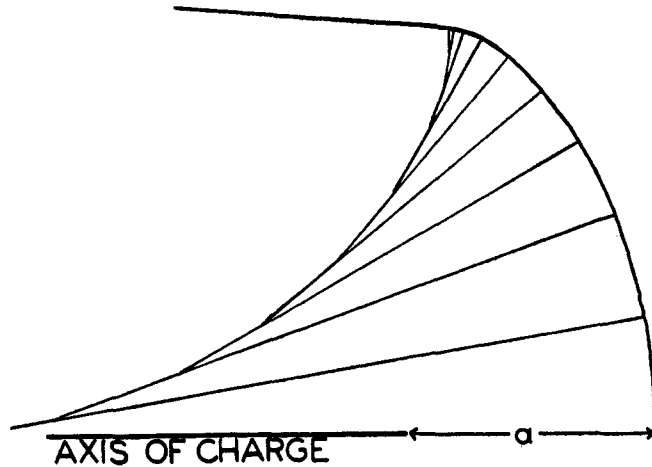

AXIS OF CHARGE

FIG. 15. Construction of wave front

TABLE 5

a/R	D/D_i	a/R	D/D_i
0	1	0.40	0.80
0.11	0.95	0.52	0.70
0.20	0.90	0.68	0.70
0.29	0.85	0.82	0.65

The data of figure 17 are represented with considerable faithfulness by the empirical equation:

$$\frac{D}{D_i} = 1 - 0.5 \frac{a}{R} \tag{38}$$

Equation 38 will be used for the application of the theory to experimental data, which will be postponed to a later section.

(c) The cased charge

Consider a cased charge and assume that the confining action is due to the inertia of the case. It can now be assumed that the meniscus-shaped detonation

front adjusts itself to such an angle ϕ of intersection with the case that the elements of the case move away neither faster nor slower than the elements of fluid in contact with it, both moving in the direction normal to the wave front at the
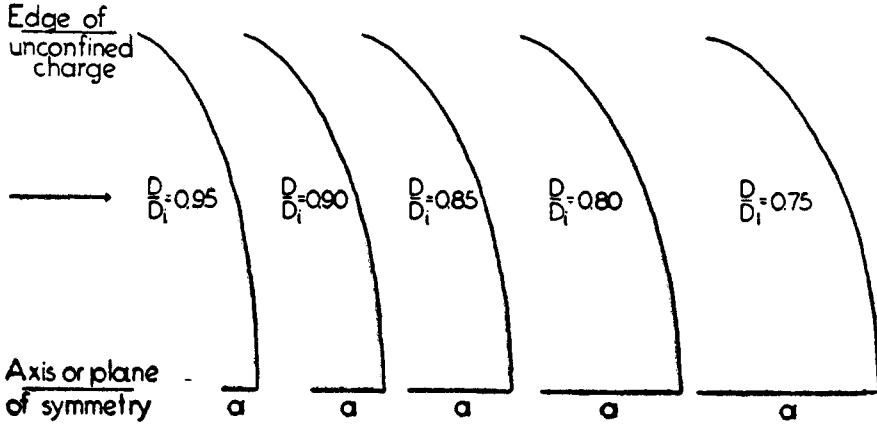

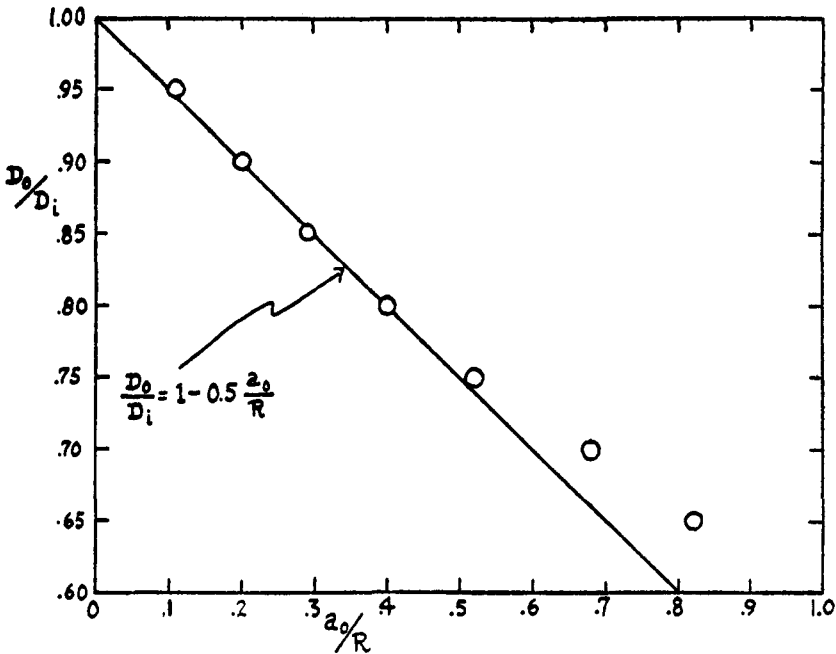FIG. 16. Wave fronts for various reaction zone lengths

FIG. 17. Justification curve for approximation: infinitely thick casing

point of intersection. Then the momentum delivered to unit area of the case is approximately $\sigma W_1 \sin \phi$, and this is produced by a pressure of approximately P_1 acting for a time τ. Thus

$$P_1\tau = \sigma W_1 \sin \phi \tag{39a}$$

Upon substituting for P_1 and W_1 their values for the ideal wave, for τ in terms of a, and for σ in terms of W_c/W_e, this becomes

$$\sin \phi = 2 \, \frac{V_0}{V_1} \, \frac{a/R}{W_c/W_e} \tag{39b}$$

or numerically

$$\sin \phi \approx 2.5 \, \frac{a/R}{W_c/W_e} \tag{39c}$$

Now it is only necessary to use the curves constructed in figure 16, but considering the surface of the charge to be at the point where ϕ is given by equation 39c. Numerical values so computed are given in table 6 and in figure 18.

<div align="center">TABLE 6</div>

SIN ϕ	$(a/R)^2/(W_c/W_e)$		
	$D/D_i = 0.95$	$D/D_i = 0.90$	$D/D_i = 0.85$
0.065	0.017		
0.075	0.017		
0.10	0.020	0.044	
0.15	0.020	0.042	0.066
0.20	0.020	0.043	0.066
0.25	0.020	0.044	0.068
0.30	0.021	0.045	0.071
0.35	0.022	0.045	0.070
0.40	0.024	0.047	0.073
0.45	0.024	0.050	0.076

The data of figure 18 are represented with reasonable fidelity by the empirical equation

$$\frac{D}{D_i} = 1 - 2.17 \, \frac{(a/R)^2}{W_c/W_e} \tag{40}$$

Equation 40 will be used later for the application of the theory to experimental data.

<div align="center">(d) The charge with very thick casing</div>

Consider a cased charge and assume that the confining action is due to the setting up of a shock wave in the case, and that the meniscus-shaped detonation front adjusts itself so that the pressure and the particle velocity match at the boundary of the charge.

If the detonation front at the boundary is moving with the local velocity D_r at an angle ϕ with the axis, and the shock wave in the case has the velocity D_c at the angle ϕ_c, these are given by

$$D_r = D \cdot \cos \phi \tag{41}$$

$$D_c = D \cdot \cos \phi_c \tag{42}$$

The requirements that the pressures must match at the boundary and that the particle velocities must match at the boundary are written

$$P_{1c} = P_{1r} \tag{43}$$

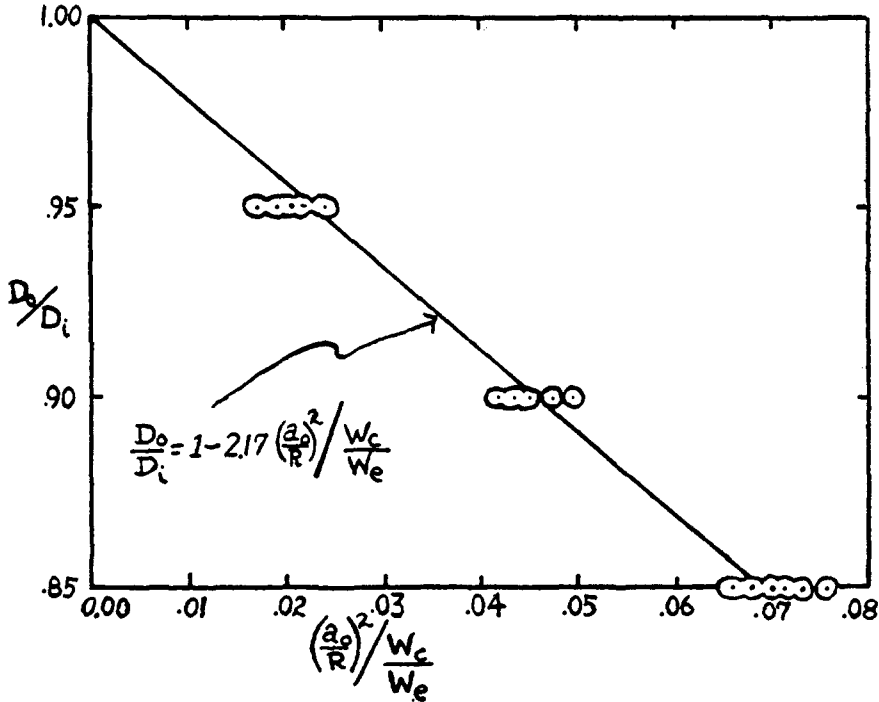$$W_{1c} \sin \phi_c = W_{1r} \sin \phi \tag{44}$$

FIG. 18. Justification curve for approximation: heavily cased charges

The shock conditions in the explosive and in the case respectively are

$$P_{1r}V_0 = W_{1r}D_r \tag{45}$$

$$P_{1c}V_{0c} = W_{1c}D_c \tag{46}$$

When the preceding six equations are combined, they yield

$$\tan \phi = \frac{V_{0c}}{V_0} \sqrt{\frac{D^2}{D_c^2} - 1} \tag{47}$$

If the velocity D_c of the shock wave in the case has been measured, equation 47 gives at once the angle at which the wave front intersects the case.

If, as is more usual, the shock wave velocity has not been measured, it must be calculated from the sonic velocity C in the case and the equation of state of the case material.

For velocities not far above sonic, the velocity of a shock wave in a solid is given approximately by

$$\frac{D_c}{C} = 1 + AP \tag{48}$$

where A is the compressibility of the solid. With the pressure given by

$$P = \frac{D^2 \cos^2 \phi}{V_0} \cdot \frac{1 - \alpha/V_0}{1 + \gamma} \tag{49}$$

a few iterations of equations 49, 48, and 47 will easily give the value of D_c and so of the angle ϕ.

When the angle ϕ is known, it is only necessary to use the curves constructed in figure 16 to determine a/R. Numerical values so computed are given in table 7 and in figure 19.

TABLE 7

SIN ϕ	$\frac{a}{R}$ SIN ϕ		
	$D/D_i = 0.95$	$D/D_i = 0.90$	$D/D_i = 0.85$
0.04	0.053		
0.05	0.045		
0.065	0.042		
0.075	0.043		
0.10	0.050	0.109	
0.15	0.050	0.104	0.165
0.20	0.048	0.107	0.164
0.25	0.051	0.111	0.171
0.30	0.052	0.112	0.178
0.35	0.054	0.112	0.175
0.40	0.059	0.118	0.183
0.45	0.061	0.124	0.190

The data of figure 19 are represented with reasonable fidelity by the empirical equation

$$\frac{D}{D_i} = 1 - 0.88 \frac{a}{R} \sin \phi \tag{50}$$

Equation 50 will be used later in the application of the theory to experimental data.

(e) Assembled results

The relations between D/D_i and a/R for uncased, cased, and heavily cased charges may all be presented on a single graph, and this has been done in figure 20. This figure may in fact be used as a convenient working diagram for the application of the curved-front theory to experimental data, in lieu of using the algebraic expressions in equations 38, 40, and 50. It is only necessary to enter
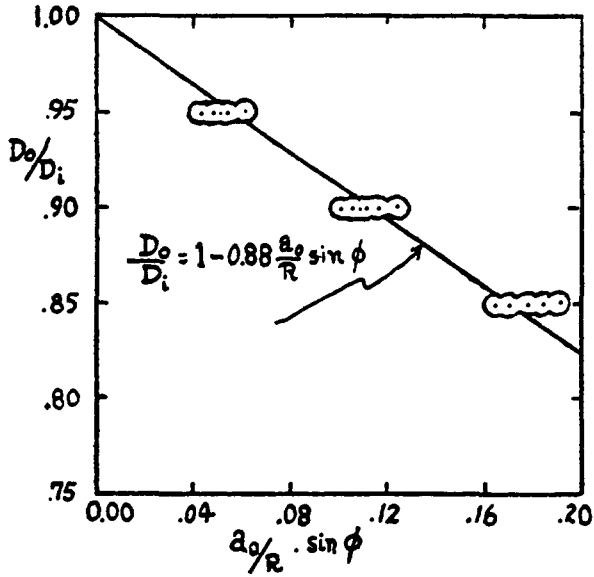
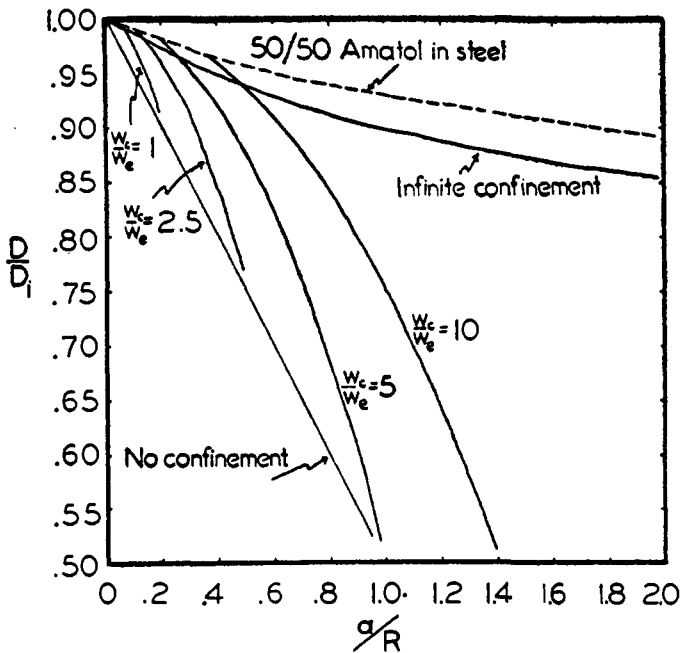FIG. 19. Justification curve for approximation: lightly cased or unconfined charges

$$\frac{D_o}{D_i} = 1 - 0.88 \frac{a_o}{R} \sin \phi$$

FIG. 20. Characterizing chart for cased charges

the diagram at the appropriate values of D/D_i and W_c/W_e, and to read the corresponding value of a/R.

The reader will notice the similarity of the final results of this theory to those of the nozzle theory (figure 13).

4. Critique of the theories

Hydrodynamic assumptions common to both theories: In the development of both theories it is assumed that the only perturbation on the hydrodynamic equations is on the continuity equation; this means in particular that no transport of momentum or of energy out the edges of the charge is considered. This simplification makes the hydrodynamic equations tractable enough to permit
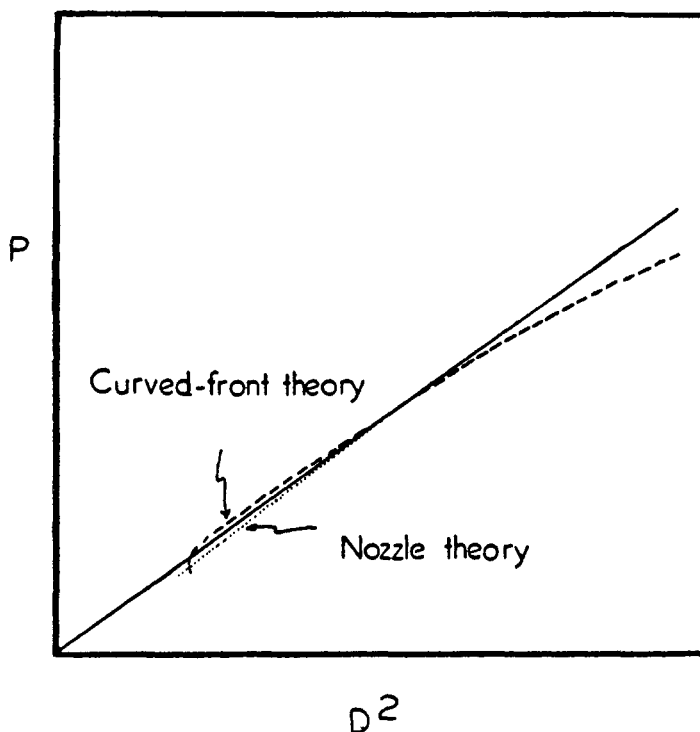

FIG. 21. Comparison between nozzle and curved-front theories

their solution; and in view of the comparatively low lateral velocities, the simplification seems to be an acceptable one. Nevertheless, it would be desirable in a further theoretical treatment to make some explicit allowance for the loss of momentum and energy (as well as material) laterally.

There is a possibility of attacking the problem by a direct experimental method; this is to measure the material velocity W for various finite sticks by the x-ray "zebra-charge" method, and then to compare the measured ratio W/D with that predicted by the theories. However, the effect of the perturbation is in any event small, and may well be undetectable within the accuracy of the x-ray method.

As a result of the initial assumption that only the continuity equation is perturbed, it turns out that in the final results of both theories, the relation of P to D (and to W) is very close to that for the ideal plane wave. This is demonstrated in figure 21, which presents the P,D relation according to the respective theories, together with the P,D relation for an ideal plane wave in the same explosive, corresponding to various heats of reaction. (Actually, because of loss of momentum laterally, the points in the P,D plane for $D < D_i$ must lie somewhere *below* the ideal pressure line.)

Because of the neglect of the lateral loss of momentum and energy, it must be remembered that the velocity loss caused by a given expansion (or curvature) will be somewhat underestimated by the present theories. *This is to say that any reaction zone lengths computed by the present theories are to be viewed as possibly high estimates.* There is in fact some evidence obtained by Herzberg and Walker which indicates that the reaction zones may be shorter by a factor of several-fold than would be estimated by the present theories. Thus they obtain from photo-

TABLE 8

EXPLOSIVE	LUMINOUS ZONE
	cm.
RDX-BWX, density 1.56	0.03
Tetryl, density 1.52	0.07
NENO, density 1.53	0.07
NENO + 1% graphite, density 1.6	0.08
TNT, density 1.52	0.06
TNT + 5% Al, density 1.6	0.09
Amatol 55/45, density 1.5	0.09

graphs lengths of the luminous zones as given in table 8, which may be contrasted with the longer zones given in a later section of this report.

It may be well to mention in passing that the expansions (and consequent lowerings of velocity) calculated by the nozzle and by the curved-front theory are alternative, not supplementary to one another. The two treatments adopt different means of attaining the same result: namely, finding the flow lines in the reaction zone. It would be quite erroneous to superimpose on the losses computed from the nozzle theory additional losses according to the curved-front theory, or *vice versa*.

Experimental detection of the meniscus-shaped front: One notable result of the theory of finite charges as developed by the present writers is the prediction[15] that the detonation front will be meniscus-shaped.

The shape of the wave front has been investigated by means of high-speed rotating-mirror cameras by two research groups. Herzberg and Walker took

[15] Actually, it had been shown earlier by means of rotating-drum camera pictures of low-density nitroguanidine charges that the wave was indeed meniscus-shaped. However, this experimental observation was not known to Eyring *et al.* at the time the theory was being developed.

photographs of a 16-mm. diameter charge of RDX-BWX, a 16-mm. diameter charge of TNT of density 1.55, and a 55/45 Amatol charge of 31 mm. diameter. They found that for the RDX-BWX the deviation from the plane wave front was less than 0.3 mm.; in the TNT, the bending back near the edge of the detonation front was 0.4 ± 0.2 mm.; and in the Amatol the deviation of the actual wave front from the "geometrical" wave front near the edge of the charge was 3.7 mm.
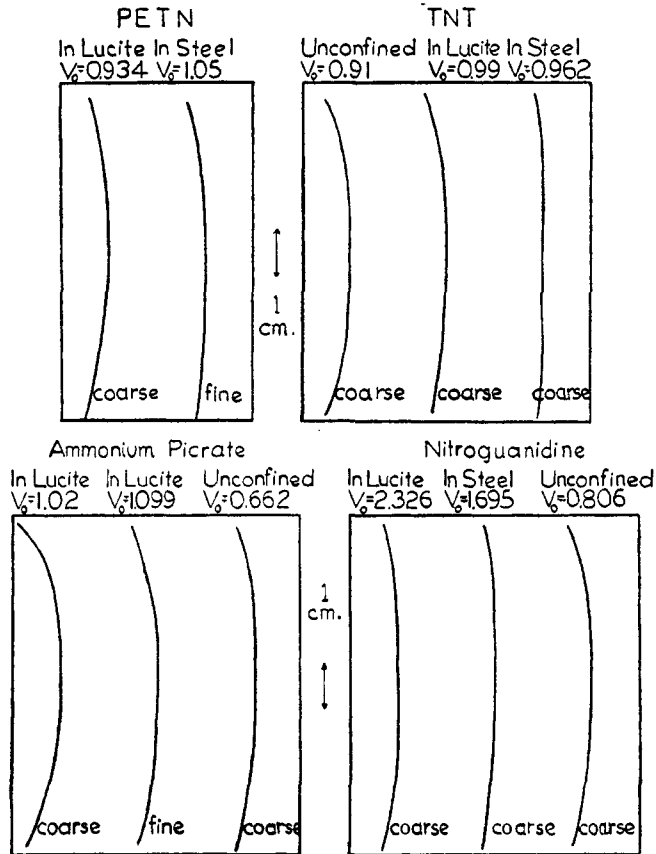

Fig. 22. Experimental wave shapes

Hurwitz and Strecker took head-on rotating-mirror photographs of a number of explosive charges of 65-mm. diameter, and succeeded in finding curved fronts in most instances. The effect is particularly marked with the low-density explosives. Figure 22 reproduces the wave shapes as determined by Hurwitz and Strecker.

This direct experimental evidence for the curvature of the wave front is supporting evidence for the curved-front theory for the velocity in finite charges.

Extrapolated ideal detonation velocities: Inspection of figures 13 and 20 shows

that the chief difference between the final results of the nozzle theory and the curved-front theory lies in that the former obtains a graph for D/D_i *vs.* a/R which is almost horizontal for small a/R, sloping sharply downward at a/R near unity, while the latter obtains a graph which slopes downward over its whole length. If then a sufficient number of measurements were made over a range of R, it should be possible to choose between the two treatments.

Actually, the experimental data for any one explosive are not sufficient in number or precision to force a decision on this basis. The ideal detonation velocity obtained by extrapolation of data for finite charges according to the curved-front treatment is usually slightly higher than the value measured for very large sticks; while the ideal velocity by extrapolation according to the nozzle treatment is usually lower than the measured value. Of the two, the curved-front treatment gives somewhat more consistent results.

In the analysis of experimental data which will be presented in the next section, the curved-front treatment will be followed.

5. *Applications to experimental data*

We may now proceed to an analysis of the available data on detonation velocities of finite charges, with the intention of using the theories just developed to find from the measured velocities the corresponding reaction zone lengths.

The data of Parisot and Laffitte (56) and a considerable number of experiments by British and American investigators[16] can be drawn upon. This material has been presented graphically in figures 23–31.

In the instance of cased charges, it is necessary to know whether the casing is to be treated as thin or thick ("characterizing" the charge). To do this one merely plots the experimental data upon the assembled-results diagram of figure 20, entering the diagram with the appropriate D/D_i and W_c/W_e. It then becomes obvious at once whether the experiments fall in the region of thin casing or of infinitely thick casing. Figures 26, 27, and 28 are such "characterizing" plots. Most of the data plotted for Amatol will be seen to fall in the region of moderate confinement, while the data for TNT in steel and Minol 2 in lead clearly fall in the region of infinitely thick confinement.

The reaction zone length a is computed from the slopes of the lines in figures 23–56, according to the equation developed earlier:

$$\frac{D}{D_i} = 1 - \frac{1}{2}\frac{a}{R} \qquad\qquad \text{Uncased} \quad (38)$$

$$\frac{D}{D_i} = 1 - 2.17\,\frac{a/R}{W_c/W_e} \qquad\qquad \text{Cased} \quad (40)$$

$$\frac{D}{D_i} = 1 - 0.88\,\frac{a}{R}\sin\phi \qquad \text{Infinitely cased} \quad (50)$$

[16] Among the workers who made important experimental and theoretical contributions in this field are D. P. MacDougall, G. H. Messerly, M. D. Hurwitz, H. A. Strecker, R. W. Cairns, and R. W. Lawrence; also the British workers A. R. Ubbelohde, W. B. Cybulski, J. L. Copp, and others.

In each instance the ideal velocity D_i was included on the figure if known by direct measurement; otherwise the extrapolated value was used. For the infinitely cased charges, the angle ϕ of intersection was for TNT in steel 8°10′ (from the velocity of sound in steel, 5130 m./sec.) and for Minol 2 in lead 20° (from the velocity in lead of a shock produced by Pentolite, 2745 m./sec.).

Figures 23–25 give the experimental vs. theoretical relation for uncased charges, and figures 26–31 that for cased charges.

C. THE TIME-DEPENDENT WAVE

Although every explosive possesses an unique steady-state velocity D_i, it is quite easy to impose upon an explosive charge a velocity either higher than D_i or
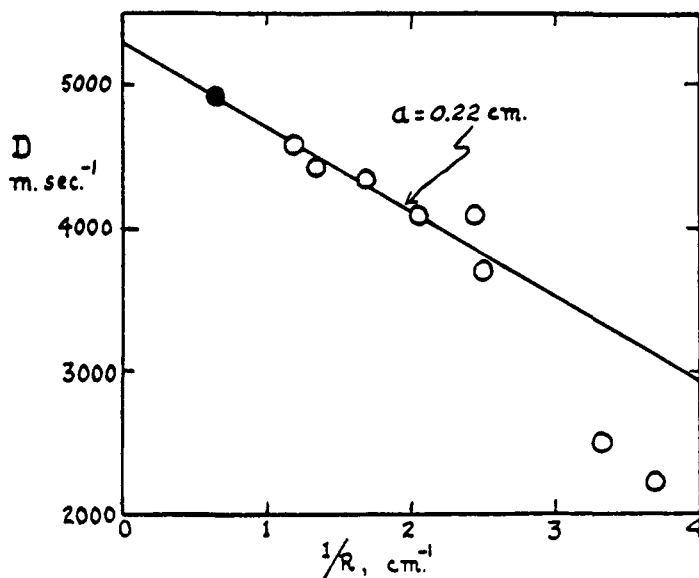

FIG. 23. Reaction zone curve for picric acid in glass. $V_0 = 1.11$ cm.³g.⁻¹ O, Parisot and Laffitte; ●, MacDougall.

lower than D_i. The former will be accomplished by initiating with a high-velocity booster charge, the latter with a low-velocity booster charge. As time goes on, the too high velocity will build down until it reaches the ideal value D_i; likewise, the too low velocity will build up until it reaches the ideal value D_i (unless it is so low that failure occurs).

The fact that any non-steady velocity will approach the steady value should be intuitively obvious. It can, however, be justified more rigorously: Suppose the wave to be initiated above its steady velocity. Then the energy liberated by the chemical reaction is less than sufficient to produce the pressure needed behind the wave front to maintain this high velocity. The velocity must therefore fall. The argument holds also for a wave initiated below its steady velocity, *mutatis mutandis*.
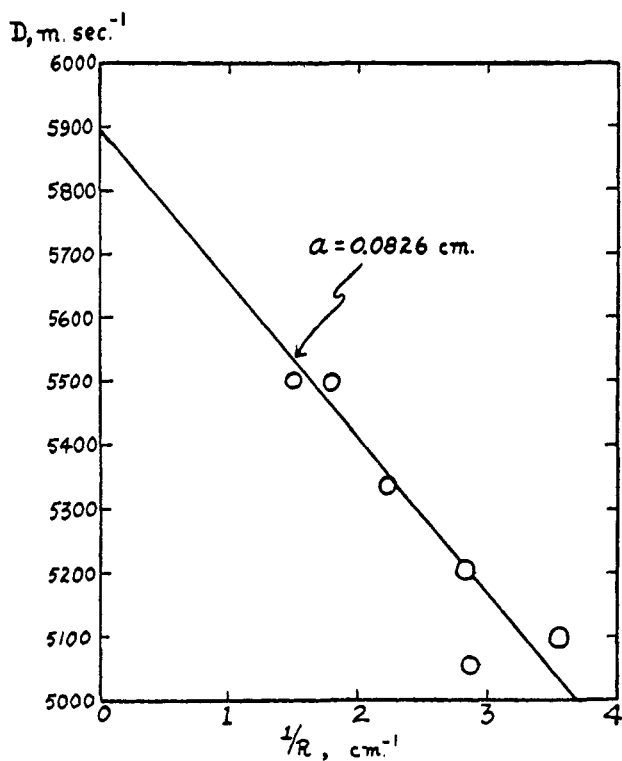
FIG. 24. Reaction zone curve for RDX; $V_0 = 1.11$ cm.^{3}g.$^{-1}$; O, Parisot and Laffitte
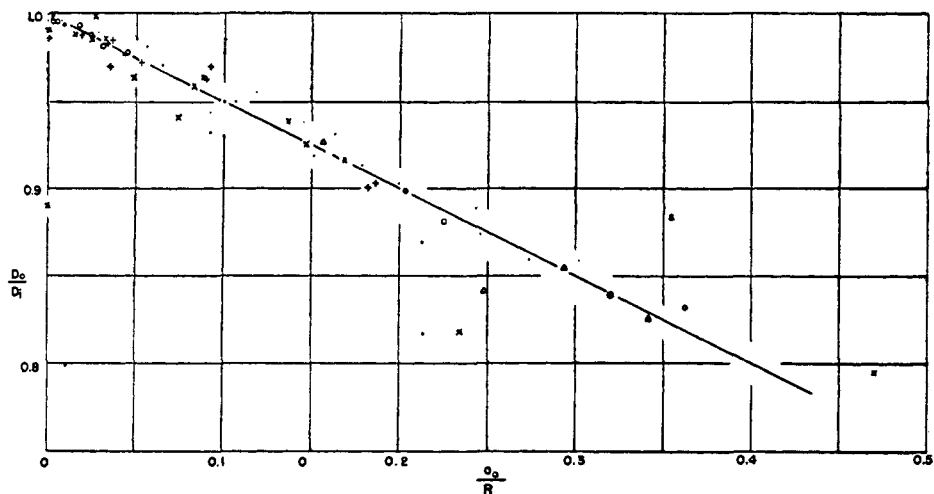

FIG. 25. Dimensionless chart for D vs. R. •, TNT; ×, PETN; +, Tetryl; O, nitroglycerin; ●, ammonium picrate; □, Minol 2; △, 60/40 Amatol; ▲, TNT + 5% Tetryl.
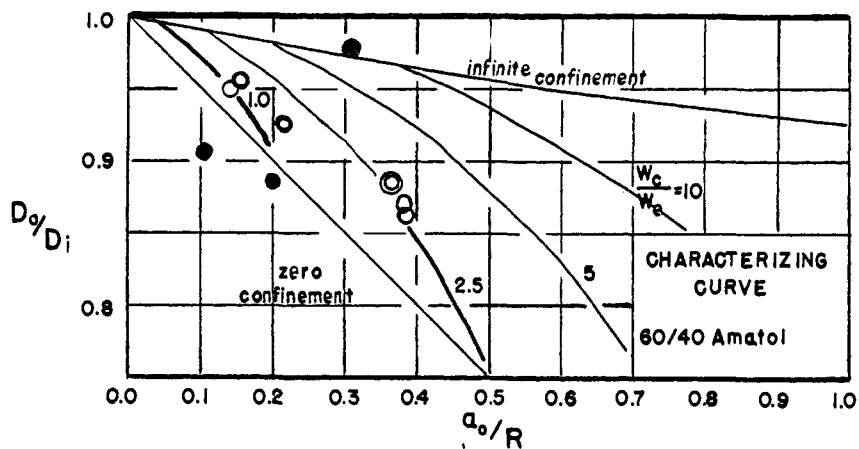
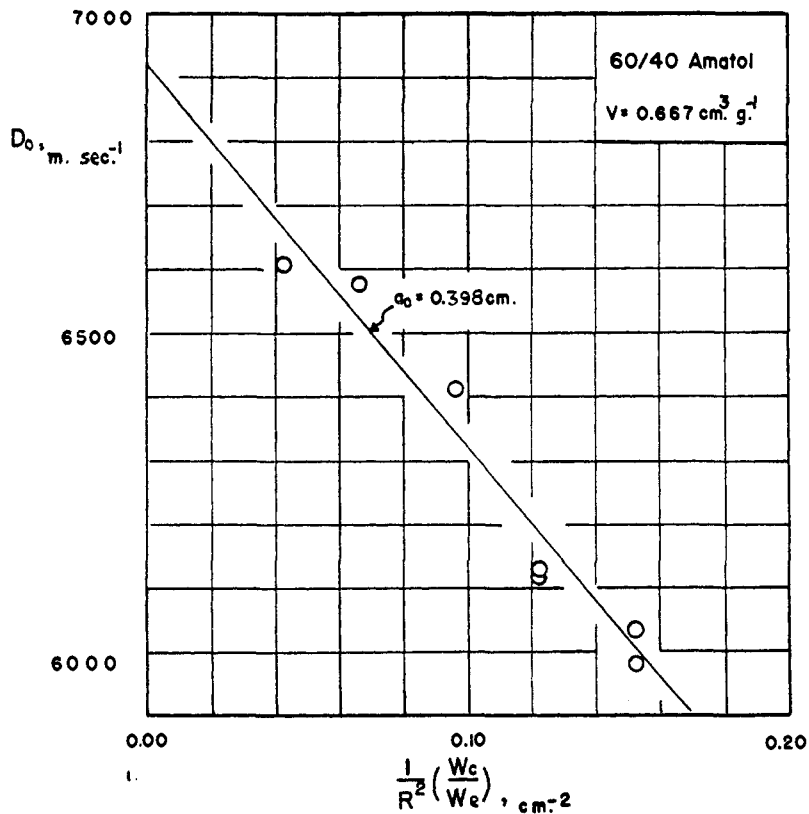FIG. 26. Characterizing curve for 60/40 Amatol

FIG. 27. Reaction zone curve for 60/40 Amatol

The following theory (admittedly somewhat heuristic) has been formulated to give the rate of build-up or build-down of such transient waves.

1. Details of theory

Consider a detonation wave propagating at a velocity not its steady velocity, yet close enough to the steady velocity so that the perturbation may be con-
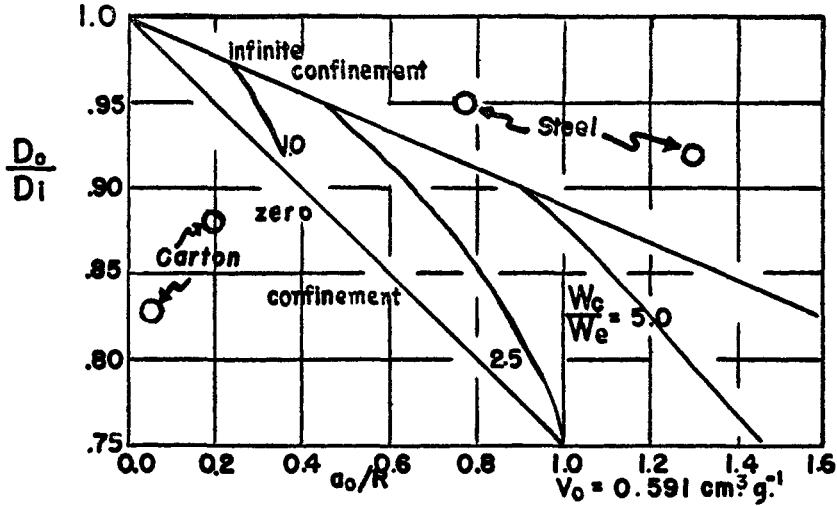

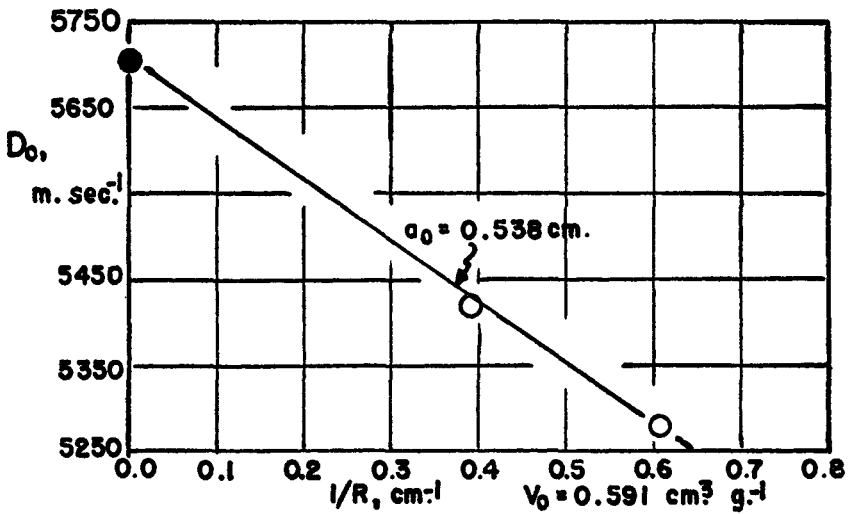FIG. 28. Characterizing curve for Minol 2 in lead

FIG. 29. Reaction zone curve for Minol 2 in lead

sidered small. If we denote the instantaneous velocity at the time of measurement by D, the velocity D_τ a short time τ later will be

$$D_\tau = D + \tau \frac{dD}{d\tau} \qquad (51)$$

Now it has been brought out in the discussion of the Chapman–Jouguet condition that the velocity of the detonation front is determined by the values of C and W at the rear of the reaction zone. But of course any changes which occur
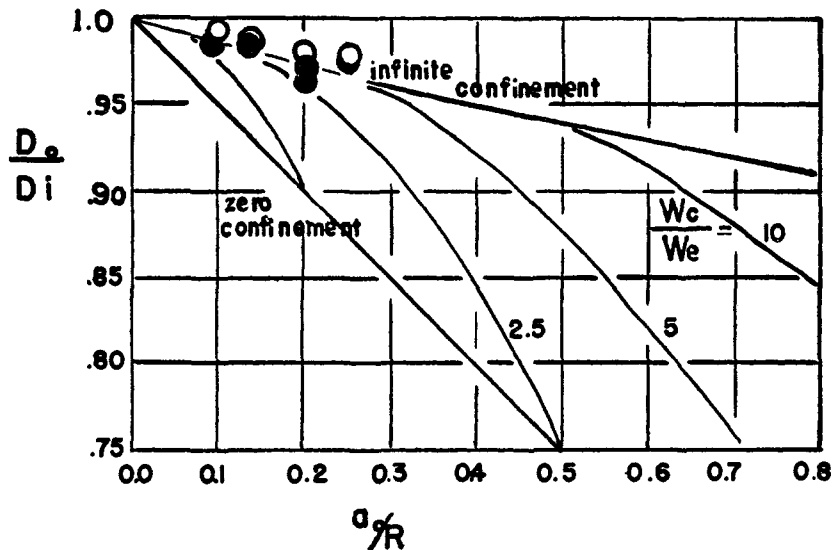
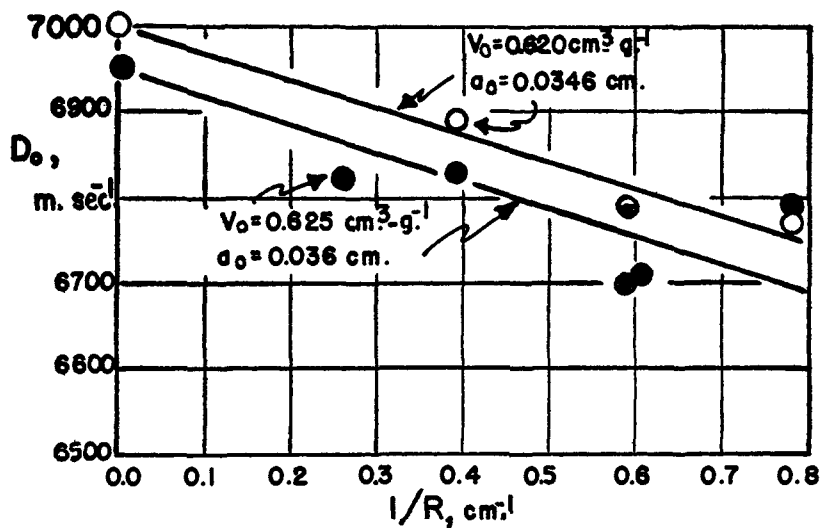FIG. 30. Characterizing curve for TNT in steel

FIG. 31. Reaction zone curve for TNT in steel

at the rear of the reaction zone will not at once make themselves felt at the front of the reaction zone; in fact, the value of C and W at the rear of the reaction zone at a particular instant will determine the velocity of propagation not at that

same instant, but at a time τ later where τ is the time required for a signal to traverse the reaction zone, or approximately the reaction time. Thus we write

$$C_1 + W_1 = D_r \tag{52}$$

Upon combining equations 51 and 52 we have

$$\tau \frac{dD}{d\tau} = -D + W_1 + C_1 = -U_1 + C_1 \tag{53}$$

It is necessary to evaluate U_1 and C_1. For this we may use two of the three hydrodynamic-thermodynamic equations (continuity, motion, energy), and we choose for this purpose the two which will be least perturbed by the transient state, so that we can take their steady-state values.

To the extent that the reaction zone length a remains unchanged, as much material flows into the reaction zone as flows out of it, so the continuity equation may be taken in its steady-state form. Since the compression ratio does not involve the heat of reaction, we may even use the same numerical value as for the steady state.

$$\frac{U_1}{D} = \frac{V_1}{V_0} = \frac{\gamma + \alpha/V_0}{\gamma + 1} \tag{54}$$

The differential equation for conservation of energy, $dE + PdV = dQ$, is quite independent of time. To a first approximation, this remains true of its integrated form, so we write as for the steady wave

$$\frac{1}{\gamma - 1} P_1(V_1 - \alpha) + P_1 V_1 + \tfrac{1}{2}U_1^2 = (\Delta Q + \bar{C}_v T_0) + \tfrac{1}{2}D^2 \tag{55}$$

If we now combine the three equations 53, 54, and 55, recalling the definition of C_1 and the value of D_i, and changing the time derivative to a space derivative

$$C_1^2 = \frac{P_1 V_1^2 \gamma}{V_1 - \alpha}$$

$$D_i^2 = 2(\Delta Q + \bar{C}_v T_0) \frac{\gamma^2 - 1}{(1 - \alpha/V_0)^2}$$

$$\tau \frac{dD}{dt} = a \frac{V_0}{V_1} \frac{dD}{dx}$$

we obtain as a final result after a little algebraic manipulation

$$a \frac{dD}{dx} = \left(\frac{V_1}{V_0}\right)^2 \left\{ \sqrt{D_i^2 - \frac{1}{2} \frac{(\gamma - 1)[2\gamma + (1 + \lambda)]}{\gamma^2 - \lambda} (D_i^2 - D^2)} - D \right\} \tag{56}$$

which has been presented graphically in figure 32. The calculated points of figure 32 are reproduced with some fidelity by the empirical equation:

$$a \frac{dD}{dx} = 0.333(D_i - D) \tag{57a}$$

Since it was found in Section II that the properties of a detonation wave in a finite stick are very closely the properties of an ideal wave with a smaller heat of

explosion, we can now without significant error extend the treatment to time-dependent waves in finite charges or of spherical shape. It is only necessary to replace the ideal velocity D_i by the steady velocity D_s appropriate to the particular finite charge.

$$a \frac{\mathrm{d}D}{\mathrm{d}x} = 0.333(D_s - D) \tag{57b}$$

Equation 57b will be used in application of the theory to experimental data.

2. Comparison with theory of pure shock waves: range of validity of the theory

In the derivation of equation 57b, for the transient velocity, it has been assumed (*i*) that the actual velocity D is not greatly different from the steady velocity D_s, and (*ii*) that the reaction zone length a remains constant. We may
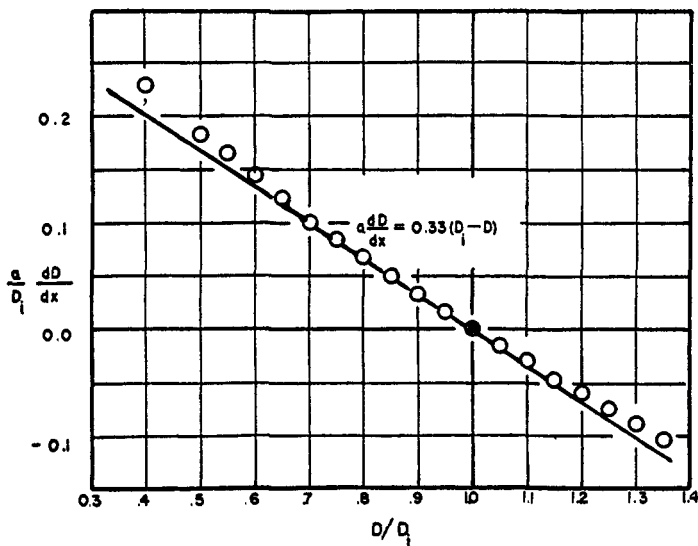

FIG. 32. Justification curve for approximation: building-up or building-down

sometime wish to use equation 57b for a more general transient wave in which D is not near D_s and a is not constant, so it will be useful to know whether the equation breaks down badly under extreme conditions.

To test this point, we may consider a pure shock wave of high intensity, in which no energy at all is supplied by chemical reaction, all the energy of the shock having been supplied at the origin of the wave. In such a wave the "steady" velocity to which it tends is zero (or at most a small sonic velocity); thus $D_s = 0$. Likewise the length of the "reaction zone," or distance to the energy source, is the distance traversed by the wave; thus $a = x$. If equation 57 be supposed valid even under these conditions, then the transient velocity will change with distance as follows:

$$\frac{\mathrm{d}D}{\mathrm{d}x} \cong - \text{const.} \times \frac{D}{x} \tag{58}$$

The numerical value of the constant in equation 58 would be about 0.33 by the approximate equation 57b, or somewhat smaller (0.12) if computed by equation 57a, for a typical solid explosive with $\gamma = 1.25$ and $\alpha/V_0 = 0.55$. If the explosive were a perfect gas with $\gamma = 1.4$ and $\alpha = 0$, the numerical value of this constant would be about 0.38.

We now compare the result proposed in equation 58 with the results obtained for the transient velocities of pure shock waves by investigators of such waves. One method of analysis of shock waves which vary with time and distance makes use of a rather tedious step-by-step graphical integration of the hydrodynamic equations, making use of the method of characteristics.[17] More convenient for the present purpose is the approximate result in closed form obtained by von Neumann for just the process considered (71). von Neumann finds for a wave of q-dimensional symmetry in a perfect gas

$$D = \frac{2}{q + 2} A^{-2/(q+2)} t^{-q/(q+2)} \tag{59}$$

$$t = A x^{(q+2)/2} \tag{60}$$

where A is a parameter inversely proportional to the square root of the energy supplied. For a shock wave obeying von Neumann's equations 59 and 60, the dependence of velocity on distance is seen to be

$$\frac{dD}{dx} = -\frac{q}{2} \frac{D}{x} \tag{61}$$

For a plane (one-dimensional) wave the numerical coefficient in equation 61 would be 0.5.

The close agreement between equations 58 and 61, extending even to the numerical coefficient, is quite unexpected and surely to some extent fortuitous. Nevertheless, it gives us confidence that equation 58 can be used without significant error over a range of conditions far wider than that for which it was expressly derived.

3. Application to experimental data

Bone and coworkers (11) have published some data on the transient building-down of a detonation in the medium $2CO + O_2$. From their data,

$$D = 2.62 \times 10^5 \text{ cm. sec.}^{-1}$$

$$D_s = 1.76 \times 10^5 \text{ cm. sec.}^{-1}$$

$$dD/dt = -0.427 \times 10^{10} \text{ cm. sec.}^{-2}$$

which with the assumption of a perfect gas of $\gamma = 1.4$ gives a reaction zone length of

$$a = 1.1 \text{ cm.}$$

a value which is reasonable for this gas reaction.

[17] Reference 3. An application of this method to the expansion of a finite layer of highly compressed gas will be found in the report by W. Döring (23).

Drum-camera photographs have been taken (at Explosives Research Laboratory, Bruceton, Pennsylvania) of a building-up detonation wave in TNT, and of building-down waves in nitroguanidine and in 80/20 Amatol.[18]

The simplest way of determining the reaction zone length from these data is to use the integrated form of equation 57b:

$$\ln (D_s - D) = -\frac{0.333}{a} x + \text{const.} \qquad (57c)$$

Thus we may plot graphically $(D_s - D)$ on a logarithmic scale against the distance x on a linear scale, and compute a from the slope of the graph. This has
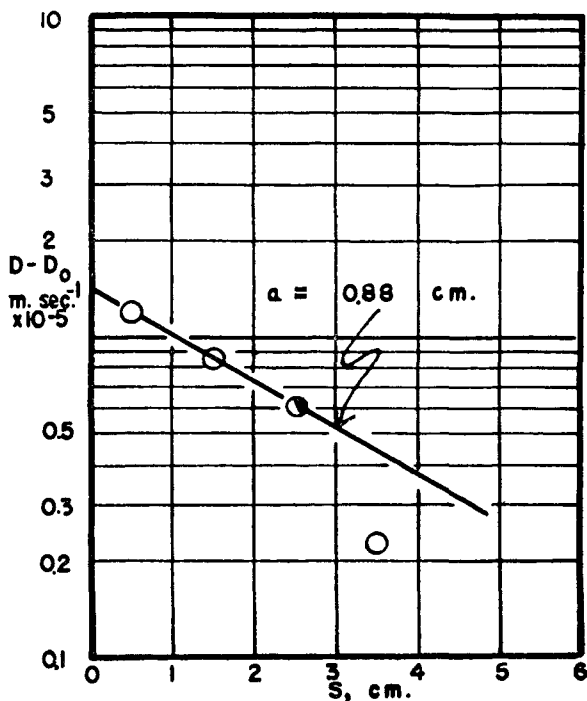

FIG. 33. Reaction zone curve for nitroguanidine. $V_0 = 1.89$ cm.^{3} g.$^{-1}$ Photograph No. 3141, Explosives Research Laboratory, Bruceton, Pennsylvania.

been carried through for the TNT, nitroguanidine, and Amatol data in figures 33, 34, and 35. On each diagram is recorded the reaction zone length for the particular explosive studied. These results will be discussed later (Section II E).

It is of some interest to point out that according to the present results, the detonation velocity approaches its steady value exponentially; and further, that the distance in which the difference from the steady value is cut to one-half is approximately two reaction zone lengths.

4. Calculation of transient spherical waves

The rate of change of the detonation velocity of a spherically propagating wave will depend both on its instantaneous velocity D and on its instantaneous

[18] Prints of the original photographs were kindly provided by Dr. G. H. Messerly.

radius of curvature, since $D_s = D_s(r_0/a)$. If it be assumed that the rate of change can be found from equation 57b, and that the appropriate steady velocity D_s can
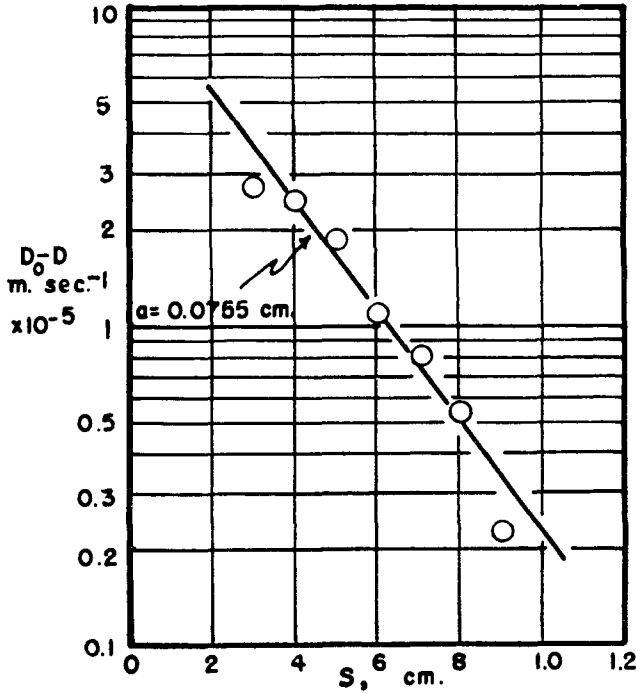
FIG. 34. Reaction zone curve for TNT. $V_0 = 1.0$ cm.^{3}g.$^{-1}$; $R = 1.27$ cm. Photograph No. 11, Explosives Research Laboratory, Bruceton, Pennsylvania.
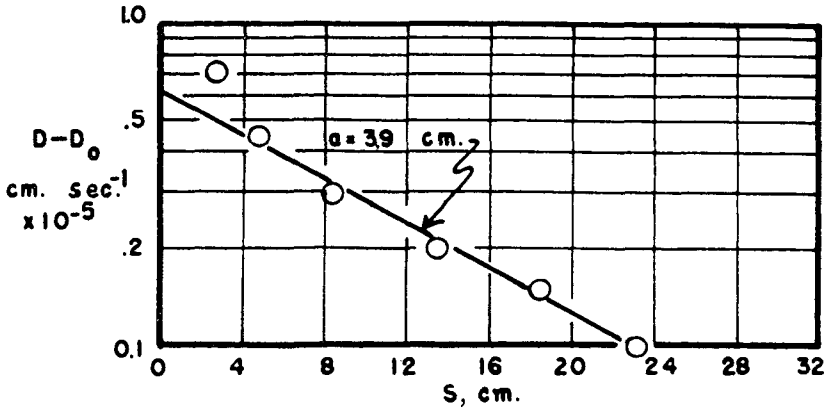
FIG. 35. Reaction zone curve for 80/20 Amatol. $V_0 = 0.61$ cm.^{3} g.$^{-1}$ Particle size: ammonium nitrate ~ 10 μ; TNT ~ 70 μ. Photograph No. 3737, Explosives Research Laboratory, Bruceton, Pennsylvania.

be read from the graph of figure 14, it is quite easy to follow by a step-by-step integration the behavior of the detonation velocity for any desired initial condition.

This calculation is presented in figure 36 for a spherical wave initiated (1) at its ideal velocity and (2) at a very low velocity (assuming, in the latter instance, that the reaction zone length remains constant so that failure does not occur).

Complications involved in the initiation process set difficulties in the way of the direct experimental study of transient spherical waves.

D. THE FAILURE OF DETONATION

The mere fact that a detonation wave has once been set up in an explosive charge is by no means a guarantee that the wave will continue to propagate. The wave may travel with a lower and lower velocity, until eventually it is moving so slowly that chemical decomposition is observed to cease and the wave subsequently travels as a sound wave. This behavior will be described as "failure of detonation." Under laboratory conditions, it is observed by the disappearance of the luminous trace on a high-speed photograph, by the lack of mechanical effect on a lead plate adjacent to the explosive, and by the recovery intact of the
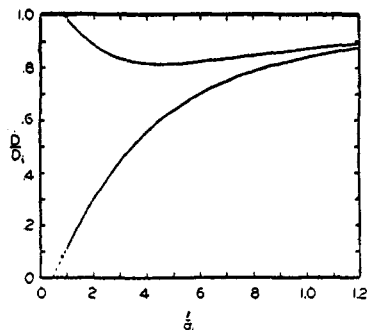
FIG. 36. Transient spherical waves

undetonated portion of the charge. Under conditions of service use, the failure phenomenon (also called "fading") in a high explosive leads to an only partial utilization of the chemical energy of the explosive, with a corresponding loss of mechanical effectiveness.

The discussion is here intentionally limited to the situation in which a detonation wave is once set up but subsequently fails. Specifically excluded is the more general problem in which the explosive is subjected to heating (either directly or by a mild blow) which initiates chemical decomposition, which then may or may not accelerate rapidly enough to build up a pressure shock leading to detonation. The greater physical complication of the process by which burning goes over into detonation adds tremendously to the mathematical difficulty of the problem. Some steps toward the solution of this more general initiation problem will be presented as a separate part of this paper.

In the program of experimental study of the sensitivity of military high explosives, a variety of measurements have been made of the conditions for failure of detonation. By combining the already developed theory of detonations with

lateral losses and the familiar theory of chemical reaction rates, we succeed in obtaining a theoretical criterion for failure. This theory permits a correlation of measurements already made and also suggests a direction for new measurements.

1. Theory of failure

In the theory developed in Section II B for the detonation velocity in a finite charge, it was supposed that the reaction zone length a remained constant. We shall now further assume that if we remove this restriction (thus let a depend upon D), the previous results remain applicable. Then the velocity in an uncased charge will be

$$\frac{D}{D_i} = 1 - 0.5\frac{a}{R} \tag{38}$$

where a can now depend on D. This assumption will surely be justifiable if a is only a slowly varying function of D.

Next, we investigate the dependence of the reaction zone length on detonation velocity. The reaction zone length is proportional to the reaction time τ:

$$a = \frac{V_1}{V_0} D \cdot \tau \tag{34}$$

The reaction time τ is the reciprocal of a specific rate constant for the chemical reaction, and is therefore dependent upon the temperature according to the law (34):

$$\frac{1}{\tau} = \frac{kT}{h} e^{\Delta S^{\ddagger}/R_0} e^{-\Delta H^{\ddagger}/R_0 T} \tag{62}$$

where k = Boltzmann's constant, 1.38×10^{-16} erg deg.$^{-1}$
   h = Planck's constant, 6.624×10^{-27} erg sec.
   R_0 = the gas constant, 1.986 cal. deg.$^{-1}$ mole^{-1}
   $\Delta S^{\ddagger}$ = the entropy of activation for the reaction, cal. deg.$^{-1}$ mole^{-1}, and
   $\Delta H^{\ddagger}$ = the heat of activation for the reaction, cal. mole^{-1}.

The reaction zone will therefore become longer as the temperature in the reaction zone falls lower.

Now the temperature T where the reaction is occurring will be throughout the reaction zone substantially the same as T_1 at the end of the reaction zone (see figure 2 in Section I of this report). So long as the detonation wave is traveling at its ideal velocity, the temperature T_1 is a constant independent of the initial density (see equation I:6c).

In particular, this rules out the possibility of finding the dependence of reaction zone length on temperature by using explosive charges of various initial densities. (The reaction zone length does in fact have some dependence on initial density, but this is for an entirely different reason which will be discussed later.)

However, a detonation wave with radial losses was seen to be equivalent to an ideal wave with a smaller heat of reaction (see discussion in Section II B).

For such a wave, the temperature is proportional to the heat of reaction, while the square of the detonation velocity is proportional to the heat of reaction, so that the temperature depends on the velocity according to the relation:

$$\frac{T}{T_i} = \frac{D^2}{D_i^2} \tag{63}$$
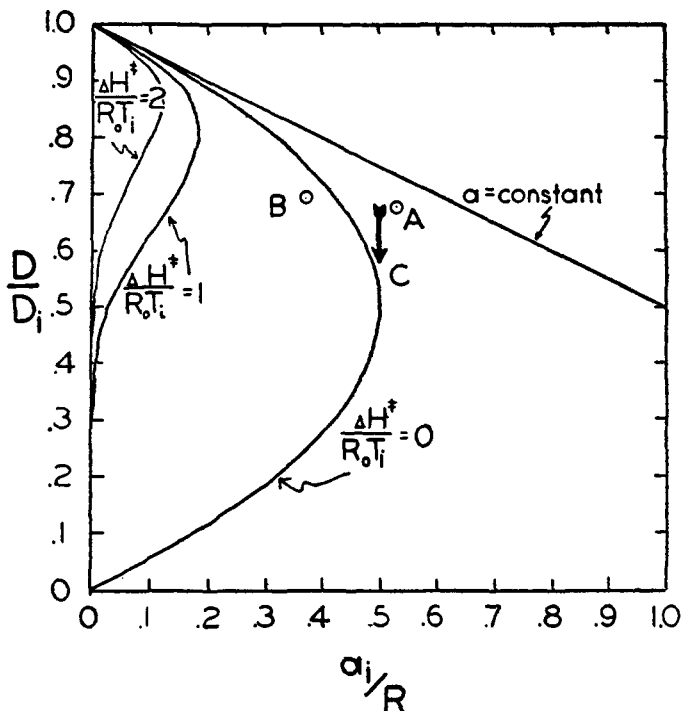
FIG. 37. Failure chart

Upon combining equations 34, 62, and 63, one obtains the desired dependence of reaction zone length on detonation velocity:

$$\frac{a}{a_i} = \frac{D_i}{D} e^{\frac{\Delta H^{\ddagger}}{R_0 T_i}\left[\frac{D_i^2}{D^2}-1\right]} \tag{64}$$

Here a_i is the reaction zone length when the velocity is the ideal velocity D_i.

With the aid of equations 38 and 64, it is now possible to prepare a graph of D/D_i against a_i/R for any desired value of the heat of activation parameter $\Delta H^{\ddagger}/R_0 T_i$. This has been done in figure 37 for $\Delta H^{\ddagger}/R_0 T_i$ equal to 0, 1, and 2.

The final results of the failure theory, as presented in figure 37, are important enough to deserve some additional comment. In the first place, there exists a minimum radius of the explosive charge below which no stable detonation will propagate; at however high a velocity such a charge be initiated, it will build downward until it eventually fails. The critical radius (in units of the ideal reac-

tion zone length) and the corresponding critical velocity (in units of the ideal velocity) depend only on the heat of activation parameter. Conversely, if the critical radius and velocity can be measured experimentally, the heat of activation can be computed.

For any charge radius greater than the critical radius, there can be *two* steady velocities corresponding to the two branches of the curve. The upper velocity is the stable velocity commonly measured; any initially imposed velocity above this should build down to it, while one below should build up to it. The lower velocity is a metastable velocity; any initially imposed velocity slightly above should build on up to the high velocity, while any initial velocity below should build down to failure. A lower limit for the lower branch of the curve is, naturally, the velocity of sound in the intact explosive.

For solid explosives, there do not seem to be examples of measured velocities which can unequivocally be assigned to the low-velocity branch of the curve. Some workers believe that they have set up a "low-order detonation" in a solid; but usually the possibility has not been excluded that such waves are transients, or are exhibiting a time lag or a directional effect at the point of initiation. It is quite reasonable that the lower curve be observed *only* as the limit above which build-up occurs and below which failure occurs.

For liquid explosives such as nitroglycerin, nitroglycol, methyl nitrate, and the gelatin dynamites, it has repeatedly been observed that two steady velocities are possible—one in the neighborhood of 8000 m. per second, the other in the neighborhood of 2000 m. per second (Lawrence and others (2, 22, 26, 28, 31, 33)). It is most tempting to assign the low-velocity detonation to the lower branch of the curve of figure 37. In this case, it is necessary to assume that although the velocity is too low to build up, it is in some way prevented from failing completely —possibly by the small but regular amount of reaction occurring in especially sensitive regions such as bubbles in the liquid. The following observations (references cited above) on the low-velocity detonation in liquid explosives are consistent with the proposed explanation:

(*i*) The velocities are near sonic. Thus the low-order detonation velocity in nitroglycerin is about 2000 m. per second; the velocity of sound in liquid glycerol is 1960 m. per second.

(*ii*) The low-velocity detonations are always initiated by weak priming charges. The low-velocity detonation can sometimes go over into a high-velocity detonation (as by propagating into a larger tube), but a high-velocity never goes over into a low-order detonation.

(*iii*) The rate of chemical reaction is so small that a large part of the explosive remains unreacted after the passage of the wave. Thus the mechanical effect of the low-velocity wave is very small. Also, unreacted nitroglycerin can be detected among the detonation products. And most striking of all, enough unreacted material is left for a second low-velocity detonation wave sometimes to be initiated (perhaps at a particularly reactive spot) at a distance behind the first, and then to be propagated following the first . . . and occasionally in the opposite direction as well.

(*iv*) The low-velocity detonation travels at a *lower* velocity the larger the

radius of the charge. This is a notable observation, quite contrary to the usual observation on high-velocity detonations and difficult to explain on any hypothesis other than that here offered.

2. Application to experimental data

The determination of the critical minimum charge radius below which failure always occurs is not easy in practice, since it requires the preparation of a number of casting molds of various diameters. This has been carried out in a few instances by, e. g., Ubbelohde, Cybulski, and coworkers. The data are tabulated in table 9.

TABLE 9

Cast TNT with 5 per cent Tetryl, density 1.6	
Critical radius..................................	1.27 cm.
Reaction zone length..........................	0.668 cm. (see figure 20)
Critical velocity..............................	4860 m.sec.$^{-1}$
Point A:	
Ideal velocity.................................	7140 m.sec.$^{-1}$
a_i/R...	0.525
D/D_i...	0.681
Cast 60/40 Amatol of density 1.5;	
nitrate 92 cm.^{2}g.$^{-1}$	
Critical radius..................................	1.588 cm.
Reaction zone length..........................	0.586 cm. (see figure 20)
Critical velocity..............................	4800 m.sec.$^{-1}$
Point B:	
Ideal velocity.................................	6920 m.sec.$^{-1}$
a_i/R...	0.37
D/D_i...	0.695
Clear cast TNT in conical charges.	
Critical radius..................................	1.0 cm. (see discussion in text)
Reaction zone length..........................	0.5 cm.
Point C:	
Critical velocity..............................	?
a_i/R...	0.5

The experimental method of Tranter and Ubbelohde is interesting. They used conical test charges of TNT, initiated at the base of the cone, and noted the diameter at which failure occurred. Their results are given as a full-scale drawing in figure 38. They found that the failure diameter depended upon the cone angle, being smaller for a greater angle; this is to be expected, since in a cone of large angle, the transient wave has some additional stability because it has recently come from a region of large radius. The value of 1.0 cm. taken for clear TNT in table 9 has been extrapolated so as to compensate roughly for this cone effect.

The effect of particle size (clear vs. cloudy vs. creamed TNT) is easily visible in figure 38.

The critical diameters and velocities computed in table 9 are plotted in figure 37. It appears from these results that the appropriate value of the heat of activation is zero, or at most a few kilocalories. We shall return in Section *II E* to discussion of the implications of this numerical result.
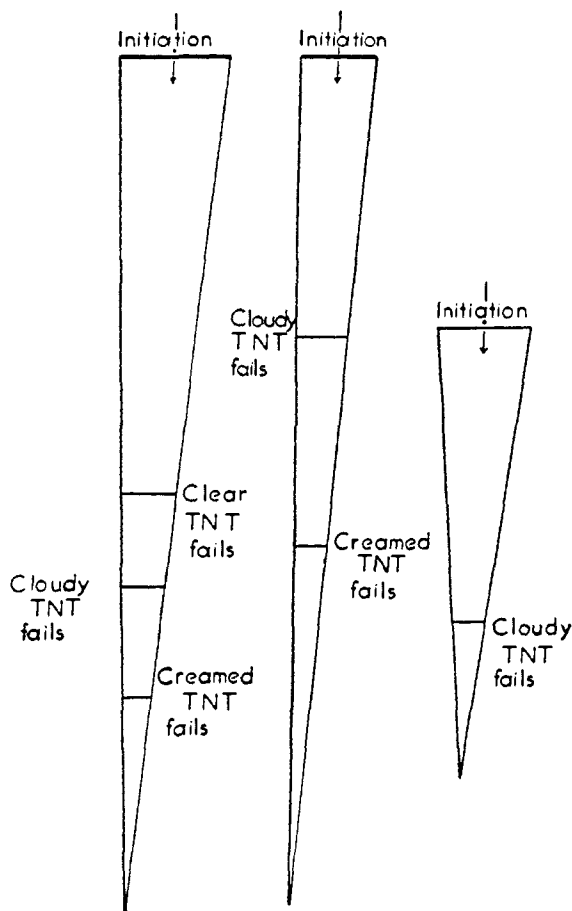

FIG. 38. Fading in conical charges

3. The failure diagram and the general measurement of sensitivity

The theory of failure as here developed rests upon two assumptions: of the effect of lateral loss on detonation velocity (equation 38), and of the effect of temperature on reaction rate (equation 64). While the particular shape and numerical values of the curves in figure 37 are decided by the particular forms and numerical parameters of equations 38 and 64, the existence and general shape of a curve similar to those in figure 37 are implied by the mere *existence* of the effect of lateral loss on detonation velocity and the effect of temperature on reaction rate. It is therefore legitimate to propose, independently of a particular

detailed theory, that a diagram like that of figure 37 could be prepared as a summary of the shock sensitivity of any explosive preparation. To prepare such a diagram, it would only be necessary for each of several charge diameters to run tests in which the samples had impressed on them shock waves of various velocities. Such a wave would be produced by hitting the sample with a calibrated shock wave.

The general principle of measuring sensitivity by means of a calibrated shock wave is by no means new; in fact, this is the guiding principle behind most of the familiar methods of testing sensitivity (exceptions being the drop test and the flame test). That this is so is evident when one lists the methods by which a calibrated shock wave can be set up.

(a) Gap tests

One method of controlling the intensity of a shock wave is to produce it with a standard "sender" charge, but then to allow it to attentuate over a controlled

TABLE 10

Data on gap test

Initiator, one No. 6 Electric Blasting Cap; gap, a number of sheets of paper of 0.080 mm. thickness; receiver charges, 5-g. pellets of 16 mm. diameter

EXPLOSIVE	MINIMUM NUMBER OF SHEETS PRODUCING AT LEAST ONE FAILURE	MAXIMUM NUMBER OF SHEETS FOR WHICH DETONATION OCCURRED
NENO, density 1.58–1.60	23	25
Tetryl, density 1.51	25	26
Tetryl, density 1.60	24	24
RDX-BWX 91-9, density 1.54	14.5	15.5
RDX-BWX 91-9, density 1.50	14	15
RDX-BWX 94-6, density 1.58	17	18.5
RDX-TNT 55-45, density 1.59	17	19
TNT, density 1.52–1.56	0	8–10 (?)

gap length of some inert material before striking the "receiver" or test sample charge. An air gap is commonly used (H. L. Porter), or a gap composed of layers of paper gives very good results (54); water gap tests find occasional use.

A minor disadvantage of the gap-test method is that in the present state of shock wave theory, and particularly with the matching problem introduced at the boundaries sender‖gap and gap‖receiver, it is difficult to obtain an absolute calibration. This difficulty might be obviated by photographic measurement of initial velocities in the receiver charges; or, for routine purposes, the gap distance itself may be used as a measure of sensitivity.

A definite advantage of the gap-test method is its high degree of reproducibility. For example, in the data by Herzberg and Walker listed in table 10, in which a gap of some twenty sheets of paper was used, with one (or at most two) more sheets of paper every shot failed; while with one (or at most two) less sheets of paper every shot went off. This excellent reproducibility of gap tests, which is to a great extent shared by the other shock wave tests, must be contrasted to the

poor reproducibility obtained in drop tests. In the latter, the statistical fluctuation in apparent sensitivity at a given height of fall is so pronounced that it is necessary to test many samples at each height, and then to report the sensitivity in terms of the height for which 50 per cent of the samples detonate.

(b) Minimum initiating charge tests

Another method of producing a shock wave of controlled intensity is to use an initiator charge of only finite size; then the rarefaction wave coming from the rear and the edges of the initiator charge will cut down the intensity of the shock wave set up in the test sample.

Of the sensitivity tests in which the amount of the initiating charge is varied, the simplest is the test for the standard size of electric blasting cap which will produce consistent detonation. Because of the limited number of sizes of such caps manufactured, this test is necessarily rough and not suitable for research purposes.

TABLE 11

Minimum priming charge test

Initiator, silver azide of density 2.98, amount as listed; receiver, explosive as listed

EXPLOSIVE	MINIMUM PRIMING CHARGE
	grams
Tetryl	0.02
Picric acid	0.035
TNT	0.07
Trinitroxylene	0.25
Trinitroanisole	0.26

An improved test of this sort is the minimum priming charge test, which measures the minimum amount of an initiating explosive needed to produce consistent detonation of the test samples. The minimum priming charge is widely used in practical testing of sensitivity. Table 11 gives a few representative results from the paper by Wohler and Martin (76). In minimum priming charge tests, typical initiators are metallic azides or fulminates. These are so effective that only a few centigrams of the initiator are needed. With such a small initiating charge, the shock wave in the receiver approximates a spherical wave.

A further improvement is the minimum boostering charge test, which measures the minimum length of booster (e.g., pressed Tetryl pellets) needed to produce consistent detonation of the test samples. The use of Tetryl (or a similar explosive) in place of azides or fulminates requires an initiator charge large enough so that the shock wave in the receiver is substantially a plane wave. Table 12 gives a few representative results from a report by Lawrence.

In all the types of minimum initiating charge tests, control over the intensity of the shock wave is achieved by causing a rarefaction wave to overtake the shock wave and to eat it away. Part of this rarefaction wave enters from the edges of the initiator, part from its rear: thus in the minimum boostering charge

experiments both the length and the diameter of the initiator charge must be taken into consideration.

Because the controlled shock wave is set up by a rarefaction superposed on a shock wave, the intensity of the shock wave in the test sample depends markedly on time and on distance. For so transient a wave, the theoretical solution of the hydrodynamic problem is almost prohibitively difficult and has not yet been carried through. The difficulty of the theoretical analysis is a serious disadvantage of all the minimum charge tests.

Since the test conditions in the minimum initiating charge tests resemble closely the conditions of actual use of explosives, the results of such tests can often be applied directly to full-scale design problems.

TABLE 12

Minimum boostering charge test

Initiator, pressed Tetryl pellet of density 1.56–1.60, diameter 1 in., length as listed; receiver, cast TNT, diameter $1\frac{3}{4}$ in., length $3\frac{1}{2}$ in., cooled as listed

EXPLOSIVE	LENGTH OF BOOSTERING CHARGE	RESULTS
	inches	
TNT cooled in 40 min.........	$\frac{3}{4}$	Five complete detonations
	$\frac{1}{2}$	One partial, one slight partial detonation
TNT cooled in 80–100 min.....	$1\frac{1}{4}$	Five complete detonations
	1	One complete, two partial detonations
	$\frac{3}{4}$	One complete, one partial, one failure
	$\frac{1}{2}$	One failure
TNT cooled in 10 hr..........	3*	Four complete, one partial detonation
	$2\frac{1}{2}$*	One partial detonation
	2*	Three complete, 1 partial detonation
	$1\frac{1}{2}$*	One complete, one partial detonation
	1*	One slight partial detonation

* Tetryl pellets of diameter $1\frac{1}{2}$ in.

(c) Initiator composition tests

Yet another method of producing a shock wave of controlled intensity is to control the chemical composition of the initiator. By starting with a high-velocity explosive (e.g., RDX) and progressively reducing its heat of explosion per gram —suitably by addition of an inert compound of similar physical properties— an explosive with any desired detonation velocity can be prepared. With a graduated series of such explosives from which to choose initiator charges, a shock wave of any desired intensity can be set up in any receiver charge.

So far as the authors are aware, the idea of a series of standard initiator explosives for sensitivity testing has not heretofore been applied or even suggested. From the point of view of mathematical analysis of experimental results, such a testing method would have two particular advantages: (*a*) Since the density of

the initiator could be made the same as that of the receiver (or as close to it as desired), and since the initiator and test explosive would be in direct contact, no problem would arise of matching pressures and velocities at interfaces, of reflected shocks or reflected rarefactions. (b) Since the dimensions of the initiator charge could be increased without limit, all effects due to rarefaction waves at the sides or rear of the initiator could be wiped out. The same holds for any effects for which a finite reaction zone length in the initiator is responsible.

The proposed test method would therefore be free of the one serious fault of gap tests, and of the one serious fault of minimum initiating charge tests. It may prove to be a useful supplement to existing tests.

To some extent, the shock wave set up in a receiver charge can be controlled by controlling the loading density of the initiator charge or the receiver charge
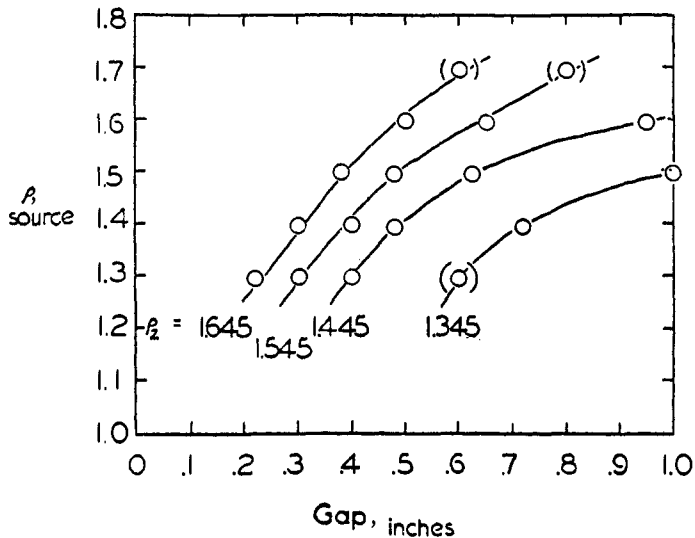

FIG. 39. Gap-test data (Porter)

To find exactly the behavior of a shock wave as it passes from a medium of one density into a medium of another density, it is necessary to match pressures and velocities at the boundary, and to take into account waves reflected from the boundary. A detailed discussion of this matching problem will be found in appendix F. For present qualitative purposes, it is enough to know that for a given initiator, a low-density receiver will experience a shock wave of higher velocity than a high-density receiver; also, for an initiator with a given heat of explosion, a high-density initiator will not only itself have a higher detonation velocity, but it will also set up shock waves of higher velocity than a low-density initiator. The direction and magnitude of these loading density effects is nicely illustrated by the experiment by Porter on Tetryl. Porter's data are plotted in figure 39, from which it can be seen that the more intense shock waves—longer gap jumped—are indeed found with high-density initiators and with low-density receivers.

The data by Porter do not lend themselves to quantitative mathematical analysis, because (a) the density variations were combined with a gap test, and (b) the Tetryl pellets were of such diameter that the ideal velocity was not reached, and of such length that not even the steady value was reached, as Porter has pointed out in his discussion of his results. In view of the serious radial losses and of the reflection phenomena at boundaries, a detailed theoretical analysis does not seem worthwhile.

The method of varying loading densities will always lead to reflected waves at the boundaries, and this detracts greatly from the value of the method as a tool for research. Moreover, the change of the density of the sample under test has some effect on the nature of its packing, which affects its reaction zone length; therefore, the density of the sample should not be changed if a study of reaction zone length is being made.

The effect of loading density on shock sensitivity, as illustrated in figure 39, is pronounced. It has repeatedly been observed under conditions of practical use that high-density explosives are much less sensitive than low-density explosives. For example, a gelatin dynamite which is detonated satisfactorily by a given cap at the earth's surface may fail when under the compression due to a few hundred feet of water. The same phenomenon is observable with some underwater bombs. We can now interpret all these density effects as due to the effect of density on the intensity of a shock wave entering the sample; and in any particular instance, we can solve the matching problem exactly to find the effect of density. On this interpretation, a low-density explosive is initiated by a shock while that same explosive at high density is not, for precisely the same reason that the low-density substance *air* is heated to incandescence by a shock wave from TNT while the high-density substance *steel* is heated a mere twenty degrees or so.

4. The failure distance

If an explosive charge is of radius less than a critical value, R_{crit}, it will surely fail no matter how strongly initiated. However, the failure does not take place at once; consequently the wave will travel some distance before the reaction ceases and it may be said to have failed.

The point of failure can be measured without difficulty on a moving-film or rotating-mirror photograph, or on a lead plate along which the explosive has been detonated. The distance traversed by the wave before failure has found some use as a routine measure of sensitivity.

A simple theory of the failure distance can be built upon the assumptions that the rate of building-down follows equation 57b, in which the steady velocity is given by equation 38 and the reaction zone length by equation 64.

$$a \frac{dD}{dx} = 0.333 \left[D_s - D\right] \tag{57b}$$

$$\frac{D_s}{D_i} = 1 - 0.5 \frac{a}{R} \tag{38}$$

$$\frac{a}{a_i} = \frac{D_i}{D} e^{\frac{\Delta H^{\ddagger}}{R_0 T_i}\left[\frac{D_i^2}{D^2} - 1\right]} \tag{64}$$

The integration of this set of equations can be accomplished graphically, for any choice of $\Delta H^{\ddagger}/R_0 T_i$ and initial velocity. This, has been done for a heat of activation assumed to be zero (as indicated in figure 37) and initial velocity D_i, and the results are presented graphically in figure 40.

It will be seen from figure 40 that for a radius somewhat smaller than the critical radius, the distance traveled before failure is some tens of reaction zone lengths.

Inspection of the experimental results on 80/20 Amatol shows that, on the average, detonation in failures traveled about 8 cm. If this distance is twenty reaction zone lengths, then one reaction zone length is for 80/20 Amatol about 0.4 cm. Because of the highly approximate nature of this theory of failure distance, the numerical value computed for the reaction zone length must not be taken too seriously.
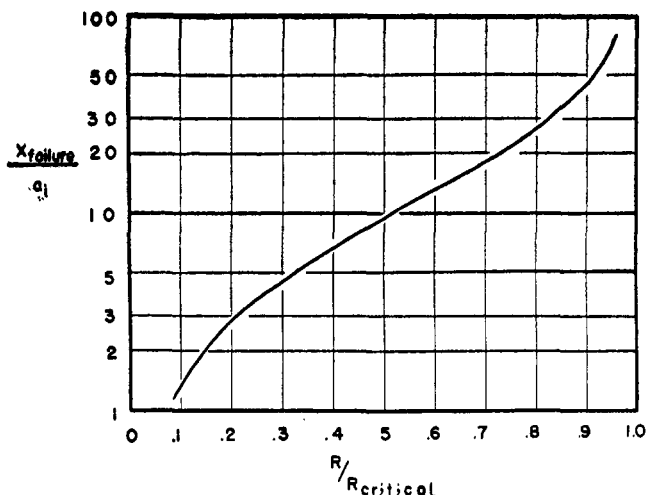

FIG. 40. Failure distance and charge radius for initiation at D_i, calculated for $\Delta H^{\ddagger}/R_0 T_i = 0$.

E. REACTION ZONE LENGTHS: SUMMARY

In the previous three sections (B, C, D) methods have been developed for computing the reaction zone length from experimental measurements on detonations in finite charges, on transient detonations, and on failure of detonations. We can now proceed to apply these methods to the available experimental data, in order to learn as much as possible about the chemical reaction in the reaction zone of a detonating explosive.

First we may point out the general result: *For typical high explosives, the reaction zone is about 1 mm. long.* The reaction zone ranges up to about ten times this length for the less sensitive explosives such as Amatol, and down to about one-tenth this length for the very sensitive explosives such as nitroglycerin.

The reaction zone lengths for the extremely sensitive primary explosives (azides, fulminates, DDNP, etc.) have not been determined. If, as seems likely,

their reaction zones are shorter than 0.1 mm., the experimental detection of any effects due to the finite reaction zone would be difficult.

It may also be pointed out that the three methods of computing reaction zone length, though they apply to different phenomena and are not essentially interdependent, agree in the numerical value which they assign to the reaction zone length. This circumstance gives us at least some degree of confidence in the results obtained.

1. The effect of grain radius

All solid explosives in actual use are composed of grains. These grains may range in size from a few microns upward to single crystals some centimeters across. The granular structure is sometimes produced intentionally by milling the explosive, but even cast explosives are granular polycrystalline materials, as may easily be seen under the microscope or inferred from the fact that the density of cast explosives is below the single-crystal density.

At first glance, it might be supposed that the granular nature of an explosive would be of no significance, that the high temperature in the detonation wave would first vaporize all the explosive, which would subsequently react according to the kinetic laws for homogeneous reactions. But this is not so. In the short time during which the explosive grain is exposed to the high temperature (a microsecond, more or less) the heat is unable to penetrate deeper than the surface layers. Consequently, each grain of explosive begins reacting at its hot surface, and the reaction progresses layer by layer until it reaches the center of the grain. The reaction for each grain within the reaction zone of a detonation is thus a sort of "cigarette burning," in which one layer of molecules is not ignited until the previous layer is consumed.

This *grain-burning theory* is supported by two kinds of arguments: the first from the impossibility of heat conduction through a grain, and the second from the experimentally observed effect of grain radius on the reaction time.

(a) Heat conduction into a grain

We wish to solve the following problem: If a cold spherical grain of substance (not reacting) is immersed in a heating bath, what is the temperature within the grain as a function of time and distance? Such a heating problem occurs frequently in engineering calculations, and graphs for its solution are available in several textbooks on heat flow or in engineer's handbooks (36). (This model is a reasonably good approximation to the actual problem of heat flow into a reacting sphere, for (*i*) the temperature outside a grain is substantially constant, and (*ii*) because of the endothermic nature of the first steps in a decomposition reaction, the chemical reaction at the immediate surface will not contribute to the heating in any important degree.) With the aid of these graphs, calculations have been made of the temperature distribution in a grain of 100 microns diameter, with an assumed thermal diffusivity $\kappa V/C_v$ of 0.018 cm.^{2} sec.$^{-1}$

The results (figure 41) show that even though the outside of a grain is at high temperature, the inside of the grain will remain cool for times of 1 microsec. or less. Chemical reaction must therefore proceed preferentially at the surface.

(b) Kinetics of a two-thirds-order reaction

If a sphere is ignited at its surface and reaction proceeds inward to the center, its rate law can be found as follows: The number of molecules reacting per second will be given by the product of the reaction rate for one molecule into the number of molecules on the surface:

$$\frac{\mathrm{d}n}{\mathrm{d}t} = k_r \frac{4\pi R^2}{s} \tag{65}$$

The number of molecules reacting per second will also be given as the time rate of change of the number of molecules in the sphere:

$$-\frac{\mathrm{d}n}{\mathrm{d}t} = \frac{\mathrm{d}}{\mathrm{d}t}\left[\frac{4/3\pi R^3}{v}\right] = \frac{4\pi R^2}{v}\frac{\mathrm{d}R}{\mathrm{d}t} \tag{66}$$
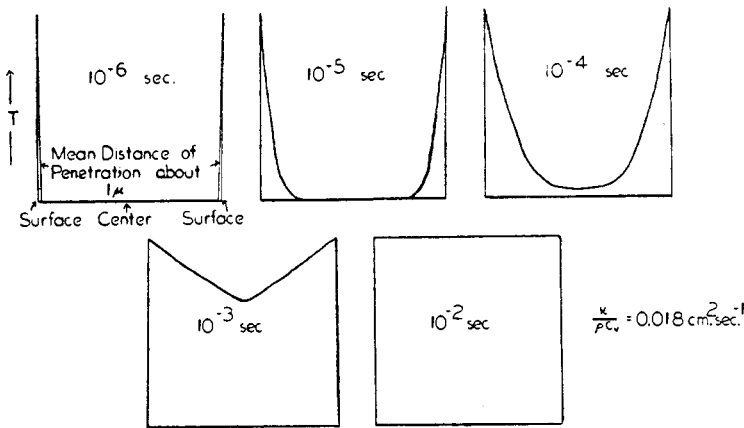

FIG. 41. Distribution of temperature in a sphere of diameter 100 μ, heated at the surface

Here n is the number of molecules unreacted; k_r is the specific reaction rate (reciprocal mean life) for one molecule, R is the grain radius at any time, s is the effective cross-sectional area of one molecule, and v is the volume per molecule.

Upon combining equations 65 and 66, we obtain the desired rate law for the grain-burning reaction:

$$\frac{\mathrm{d}R}{\mathrm{d}t} = k_r \frac{v}{s} \tag{67}$$

Thus the grain will burn at a rate which is radially constant. The ratio v/s is approximately the diameter λ of a molecule and will be so written. Then for every molecule reacting, the radius decreases by one molecular diameter. However, it must be pointed out that s is the *effective* cross-sectional area of a molecule and to the extent that a molecule fails to "shade" the molecule below it, heating can occur into more than the top layer; the effective area of a molecule will then be smaller and the ratio v/s larger than one molecular diameter.

The time τ required for complete reaction is merely the time required for the reaction to traverse the grain radius R_g:

$$\tau = \frac{1}{k_r} \frac{R_g}{\lambda} \tag{68}$$

Since the extent of reaction $N = 1 - (R/R_g)^3$, the rate law (equation 67) for grain-burning becomes:

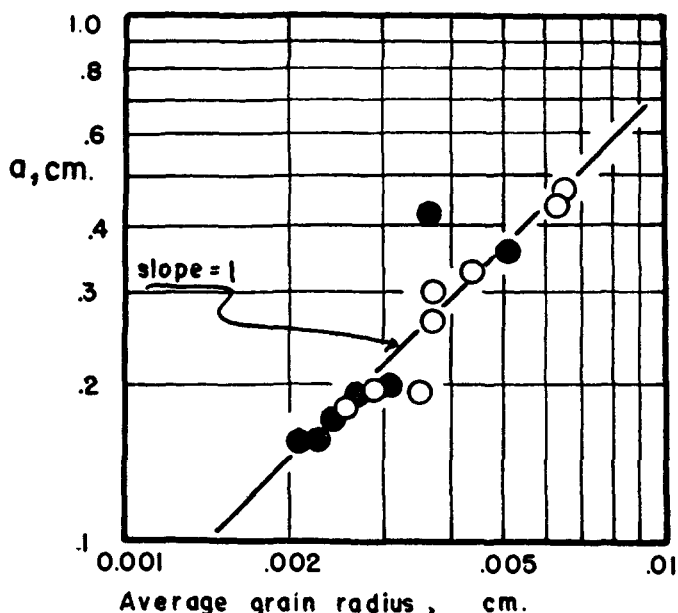$$\frac{dN}{dt} = \frac{3k_r\lambda}{R_g} (1 - N)^{2/3} \tag{69}$$

FIG. 42A. Reaction zone length and grain radius: $\bigcirc$, 60/40 Amatol; $\bullet$, 50/50 Amatol; $\square$, ammonium picrate, $V_0 = 1.0$; $\triangle$, TNT, $V_0 = 1.0$.

and the reaction is of two-thirds order. (For the integrated form of the two-thirds-order rate law, see appendix G.)

According to equation 68, if an explosive is undergoing grain-burning, its reaction time τ should be proportional to its grain diameter.

As a test of the grain-burning theory, we may now graph the reaction zone length (as determined by the theory of Section II B) as a function of grain radius. This has been done[19] in figures 42A and 42B for the available data (D. P. Mac-Dougall et al.) in which grain size was varied, for 60/40 and 50/50 Amatols, for

[19] In the analysis of these data the average grain radii were computed from the surface areas given by the authors. The ideal detonation velocity was taken to be 6500 m.sec.$^{-1}$ for 50/50 Amatol and 6150 m.sec.$^{-1}$ for 60/40 Amatol.

ammonium picrate[20] of density 1.0, and for TNT[21] of density 1.0. The data plotted in figure 42, particularly those for Amatol and ammonium picrate, fall nicely along a straight line of slope unity on logarithmic paper. This is confirmation of the grain-burning law for these particular explosives, and there is no reason to suppose that the grain-burning phenomenon is other than a general phenomenon to be observed in every solid explosive.

In view of the key role played by reaction zone length in the stability of propagation of detonation, the conclusion that solid explosives undergo grain-burning makes it a matter of first importance to know and to control the grain size of explosives. Thus a fine-grained explosive should always detonate stably, while in
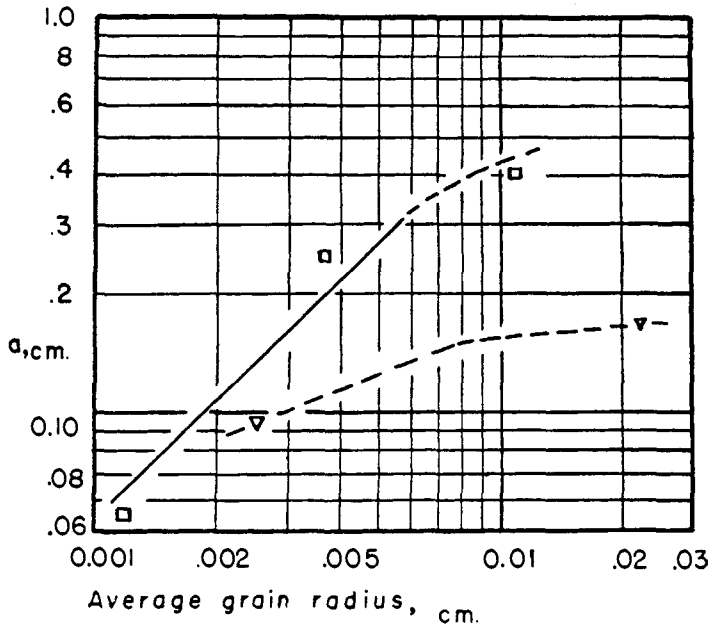
FIG. 42B. Reaction zone length and grain radius

a sufficiently coarse-grained explosive (say a large single crystal) it might well be impossible to maintain a stable detonation wave.

In some of the older measurements of shock sensitivity and of velocities in finite charges, the grain size was not known or controlled. Such measurements are not of much value. In recent investigations, the importance of grain size has been realized, and the observation has repeatedly been confirmed that coarse-grained explosives can only with difficulty be made to detonate. We may cite the experiments by Lawrence and by Woodhead and Wilson, already mentioned in this report in table 12 and figure 36, respectively.

Lawrence found that TNT cooled in 45 min. gave crystals of average size 50 x 50 x 500 microns: TNT cooled in 75 min. gave crystals of average size

[20] See figure 20 of this paper.
[21] See figure 23 of this paper.

100 x 100 x 700 microns; while with TNT cooled in 10 hr. very large crystals were obtained, some running the entire length of the charge (3.5 in.). With the normally cooled TNT, a 15-g. pellet of Tetryl was sufficient to produce five complete detonations; with the slowly cooled TNT, a 26-g. pellet of Tetryl was required to produce five consecutive shots; while with the very slowly cooled TNT, even 144 g. of Tetryl produced only four complete shots and one partial shot. "This illustrates the known fact that TNT cast clear (90°C.) and allowed to cool slowly is very insensitive."

Woodhead and Wilson found in their dying-out experiments using conical charges that cast TNT poured clear (large crystals) was considerably less sensitive than the poured cloudy (smaller crystals), which in turn was less sensitive than the same TNT creamed (still smaller crystals).

Tranter and Ubbelohde found that the addition of a eutectic proportion of such substances as RDX, PETN, hexanitrodiphenylamine, or dinitrobenzene produced TNT crystals which were markedly smaller. In such an explosive, "fading" in sticks of 1 in. diameter was completely or partly suppressed. Tranter and Ubbelohde also mention that "sensitization of cast TNT in shells, by creaming, improves fragmentation to about the same extent as the addition of 30% Tetryl."

Copp and Ubbelohde also note that "the addition of aluminum to 50/50 Amatol, to form Minol 2, has a marked effect in reducing the average cross-section of the TNT crystals in the casting."

With very large grains, there is some question as to what to take for the "grain size," for there is sure to be ignition at some of the crystal interfaces within the grain. Presumably this is the explanation for the behavior of TNT noted in figure 42B, in which a tenfold increase in grain size only gave a twofold increase in reaction zone length. Here the large grains were almost 0.5 mm. across, and apparently the explosive was polycrystalline with individual crystals smaller than this.

Liquid explosives propagate detonation in a manner not qualitatively different from solid explosives. They are initiated by shocks of about the same intensity as solids, and respond like solids to the effect of lack of confinement. Fragmentary data (34, 45, 55, 66, 70) suggest that liquids are if anything more sensitive than solids to initiation by shock, and that liquids have a reaction zone rather shorter than that of solids. Since a liquid is not composed of grains, another mechanism of initiation of liquid explosives must be found.

One may consider the following hypothesis for the initiation of liquid explosives: The decomposition of a liquid explosive is initiated at gas bubbles within the liquid. The detonation wave raises each bubble by compression to a temperature high enough to start decomposition, the temperature subsequently being maintained by the heat of decomposition. Reaction proceeds radially outward from each bubble. On this *bubble theory* the bubbles in liquids would play the same role as "hot spots" that hot grain surfaces play in solids. In fact, the linear rate of the surface reaction is the same whether reaction is proceeding inward toward or outward from a center. The time for complete reaction is just the time for the reaction to traverse half the interbubble distance. It does, therefore, have

some meaning to speak of a "grain" of liquid according to the bubble theory, where we mean by a "grain" that aliquot part of the liquid surrounding each bubble.

The bubble theory is susceptible to direct experimental investigation: Bubbles might be removed from a liquid explosive by protracted vacuum treatment, or forced to dissolve completely by high hydrostatic pressure. Or, additional bubbles might be introduced into a liquid explosive by mechanical or chemical means. In the first instance, the liquid explosive should become less sensitive to shock, in the second instance, more sensitive (34, 45, 55, 66, 70). The solution to this problem must wait upon further experimental evidence. There is some circumstantial evidence for the bubble theory:

(i) It is well known that ordinary liquids do contain a considerable number of "bubble nuclei" (small bubbles) entrapped, and that those small bubbles can only with difficulty be removed. For the organic nitrates which comprise most liquid explosives, bubbles would continually be produced by the slow room-temperature decomposition of the explosive.

(ii) Whenever a shock wave traverses a liquid containing bubbles, the mere fact that the bubbles are gaseous (i.e., of low density) guarantees that they will become far hotter than the main liquid. (It will be recalled that the air adjacent to TNT is heated to incandescence.) Such hot regions would be the logical site for reaction to begin.

(iii) Bubbles in the liquid would provide just the sort of specially sensitive regions needed to explain why the low-velocity detonation does not fail completely (see discussion in Section II E). The region around each bubble may be supposed to react to a small extent—not enough to lead to complete reaction of its own "grain," but barely enough to initiate the next bubble.

2. The mean lifetime of an explosive molecule

The time required for the completion of reaction in a detonation, the reaction time τ, we have seen to be about a microsecond. But this time is not itself the reciprocal of the rate of any *elementary* reaction, and so to consider it is fallacious. It is rather the time required to complete a sequence of elementary reactions—namely, the reaction of one molecule after another, from the surface of a grain to its center.

With the aid of the grain-burning equation

$$\tau = \frac{1}{k_r} \frac{R_g}{\lambda} \tag{68}$$

and data such as those in figure 42, we can compute the true specific reaction rate k_r for a single molecule. The reciprocal of k_r is the true mean lifetime of a single molecule at the detonation temperature.

The specific reaction rates computed for the explosives of figure 42 are listed in table 13. Here the effective molecular diameter was assumed to be 10^{-8} cm. Since the frequency factor kT/h in the absolute rate law

$$k_r = \frac{kT}{h} e^{-\Delta F^{\ddagger}/R_0 T}$$

is at 3000°K. equal to 60×10^{12} sec.$^{-1}$, it is clear that the decomposition of a single explosive molecule is proceeding at a rate which is quite normal for an ordinary chemical reaction at that temperature. Only a moderate factor of 1/250 remains to be explained, and such a factor has a variety of possible explanations.

The knowledge that the reaction proceeds at a "normal" rate is not so decisive as might be supposed, toward the elucidation of the nature of the rate-determining reaction. Among the possible rate-determining reactions are the following: (*i*) Simple unimolecular decomposition, with a small heat and/or entropy of activation against it. (*ii*) Bi- or multimolecular reaction, the extra reactants being present at moderately high concentration in the hot gases (this would be "pseudo-unimolecular"). No restriction as to the number of reactants, nor their nature (ions, free radicals, etc.). (*iii*) Diffusion of reactants to, or products away from, the site of reaction. Diffusion of heat may also be the slow step.

3. Heat of activation of the decomposition reaction

The only present analysis which yields direct information on the activation energy of the reaction in the detonating explosive is the analysis of detonation

TABLE 13

Specific reaction rates for explosives of figure 42

EXPLOSIVE	REACTION RATE, k_r
	sec.$^{-1}$
Amatol	0.2×10^{12}
TNT	0.3×10^{12}
Ammonium picrate	0.2×10^{12}

failure presented in Section II D. According to the result there found, the activation energy is zero or near zero—say within a half-dozen kilocalories.

This result is admittedly susceptible to further experimental testing. It is however not unreasonable, and if true is most suggestive.

Since the unimolecular decomposition would be expected to have a high activation energy, it would be ruled out. In any event, unimolecular decomposition as a rate-determining step does not seem particularly attractive from a chemical point of view; bimolecular (or multimolecular) reaction of free-radical (or ion) fragments with intact molecules seems more likely.

The same objection is to some extent applicable to bimolecular reactions, though here the case must be put less strongly, for free-radical reactions do sometimes occur with low activation energies.

Diffusion as a rate-controlling step is quite possible kinetically: If a reactant must diffuse to the site of the reaction, the specific rate k_d of its arrival at that site is

$$k_d = n_1 \frac{\lambda^2}{\Lambda^2} \frac{kT}{h} e^{-\Delta F\ddagger / R_0 T} \qquad (70)$$

where n_1 is the mole-fraction of such molecules in the solution, λ is the molecular diameter, Λ is the distance the diffusing molecule must traverse, and other symbols have their usual meaning. Since the activation energy for diffusion in condensed systems is only a few kilocalories, diffusion as a slow step would satisfy this requirement. Furthermore, if the concentration n_1 of diffusion reactants were not too large, or if the diffusing distance Λ were several interatomic distances, the absolute rate of the reaction would satisfy that requirement. It is perfectly plausible that at the high temperature involved, chemical reactions have become so fast that diffusion is the rate-determining step.

Another possibility is that the slow step is the diffusion of heat to the site of reaction. The rate of diffusion of heat obeys the same laws as the rate of diffusion of matter, except that the coefficients of diffusivity are somewhat different for the two processes:

$$\text{Diffusivity of matter} = \frac{kT}{h}\, e^{-\Delta F^{\ddagger}/R_0 T} \tag{53}$$

$$\text{Diffusivity of heat} = \lambda C_1 \tag{54}$$

For the reasonable numerical values of 3000°K. for temperature, 10^{-1} cm. for interatomic distance, 2×10^5 cm. sec.$^{-1}$ for the velocity of sound C_1, and zero activation energy for diffusion, those diffusivities become:

$$\text{Diffusivity of matter} = 0.60 \text{ cm.}^2 \text{ sec.}^{-1}$$
$$\text{Diffusivity of heat} = 0.02 \text{ cm.}^2 \text{ sec.}^{-1}$$

It is seen that the diffusivity of heat is the same as that of matter, to a factor of about 1/30. Therefore, the diffusion of heat would give even better numerical agreement with the absolute rate k_r found above than would the diffusion of matter. The two diffusion processes are alike in their slight dependence on temperature.

Remark concerning extrapolation of low-temperature measurements

It might be supposed that the heat of activation of the reaction in a detonation, as well as the specific rate itself, could be obtained by extrapolating to the detonation temperature measurements of the decomposition rate at room temperature or a few hundred degrees above. A considerable number of such measurements are available (1, 20, 30, 32, 33, 37, 48, 62, 63). In general, the rates measured upon heating at these low temperatures yield activation energies in the range 30–50 kilocal., and frequency factors in the range 10^{10}–10^{20} sec.$^{-1}$

Two remarks must be made concerning the extrapolation of those low-temperature data. The first remark is that even if the measurements are precise, any extrapolation of experimental data over an uncharted region four times as extensive as the region investigated, is of doubtful validity. As figure 43 shows, this is precisely the kind of extrapolation necessary to obtain reaction rates at detonation temperatures from reaction rates actually measured.

The second remark is that in different temperature regions, quite different re-

actions may be rate-controlling. In a sequence of consecutive reactions, the slowest reaction will always be rate-determining.

The full rate law for a sequence of reactions is, if a steady state is established:

$$\frac{1}{k_r} = \frac{1}{k_1} + \frac{1}{k_2} + \cdots \tag{73}$$

If two consecutive reactions have different activation energies, the reaction with higher activation energy will be rate-determining at low temperatures, and the reaction with lower activation energy will become rate-determining at high tem-
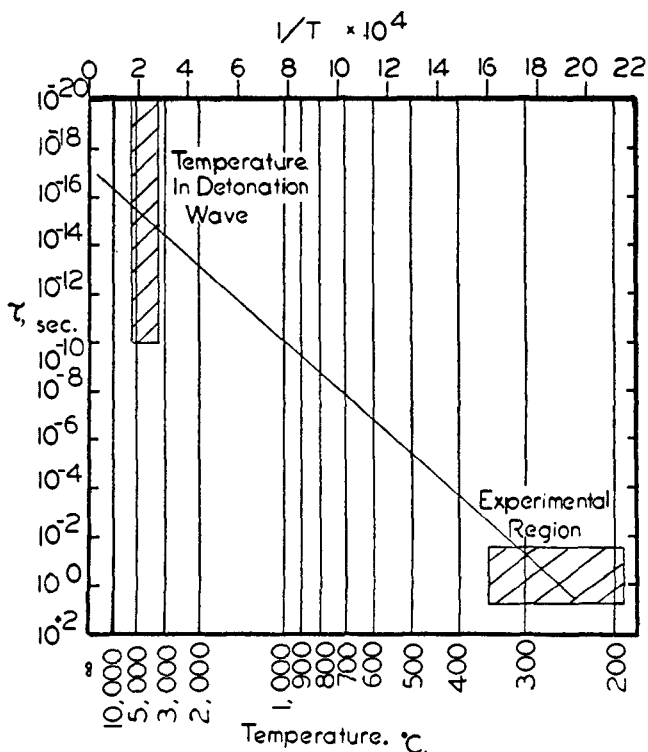
FIG. 43. Extrapolation of reaction time to detonation temperatures

peratures. It is evident that in the absence of a detailed knowledge of the reaction mechanism, one has no assurance that a complex reaction will even continue to be controlled by the same slow step as temperature is varied.

An interesting example of this phenomenon of change from one rate-controlling step to another in a set of consecutive reactions was found by Audubert (4) in the decomposition of metallic azides. Figure 44 gives his observations on the decomposition of sodium azide.

In view of these remarks, the extrapolation of low-temperature rate data to high temperatures does not appear to be acceptable.

4. The effect of packing

In an explosive composed of grains, the regions brought to the highest temperature upon impact of a shock wave will be the points of contact of grains. Such points are subject both to the greatest compressional heating and to greatest frictional heating. At such hot spots the chemical reaction will undoubtedly begin.
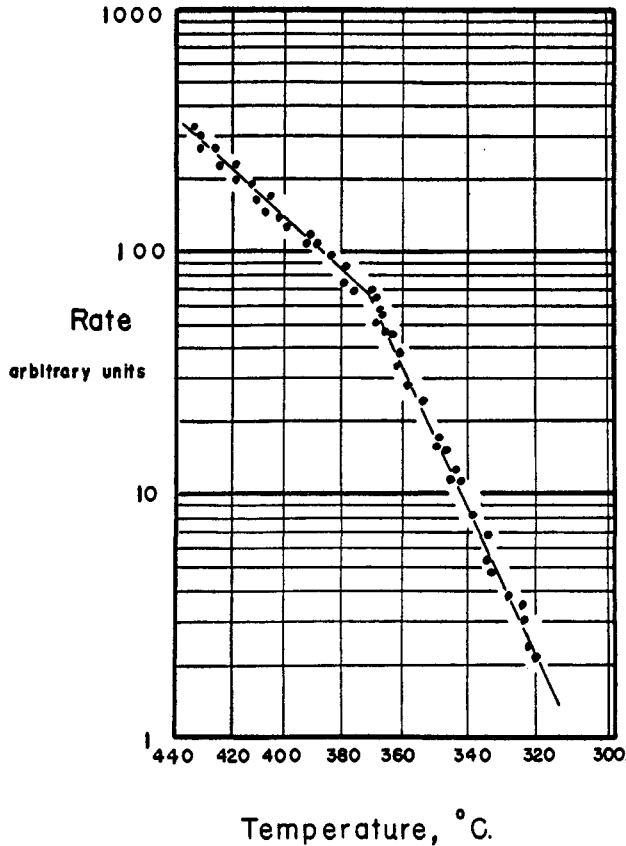

FIG. 44. Audubert's data on decomposition of sodium azide

So long as several such hot spots are present at the surface of each grain of explosive, the longest distance traversed by the decomposition will be the grain radius. The reaction zone length will then be substantially independent of the nature of the packing.

If, however, the number of load-bearing contact points is reduced to two, or one, or less than one per grain of explosive, the distance traversed by the decomposition will be much more than one grain radius. Under those conditions, the reaction zone length will be greatly increased, and the explosive will be correspondingly prone to fail. The reduction of the number of load-bearing contact

points can be accomplished in two ways: (1) the density can be decreased; (2) a mixture of small with large grains may be used. Both of these experiments have been tried on explosives.

(1) *Effect of low density:* In the close packing of spheres 74.5 per cent of the space is filled; in the simple cubic packing of spheres, 52.36 per cent of the space is filled (17, 18, 22). If, therefore, we take a typical high explosive of crystal density 1.65, each grain will not have twelve contact points below a density of about 1.2, and it will not have eight contact points below a density of about 0.9. The exact numerical values will depend on the shape of the crystals. Thus we
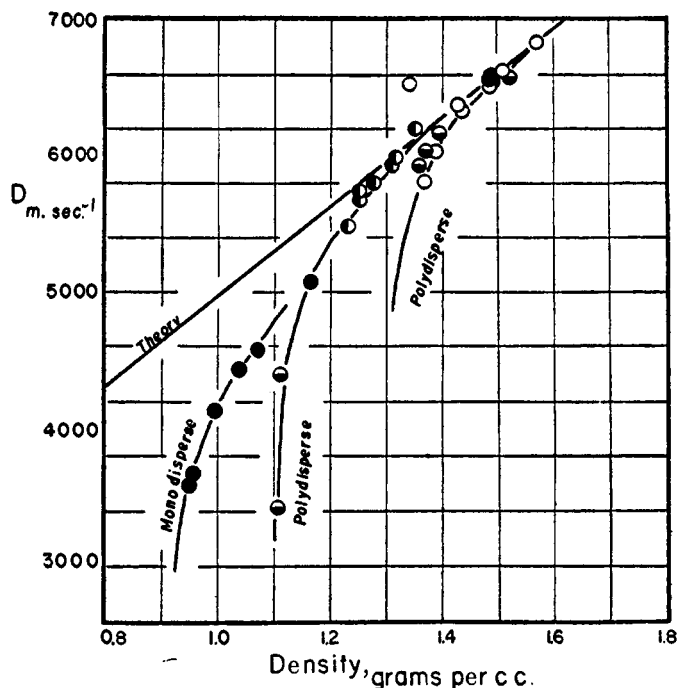

FIG. 45. Failure in Amatol due to mixed grain sizes. $\bigcirc$, 200 μ ball-milled; $\bullet$, 177–250 μ; $\circleddash$, 70 μ; $\ominus$, 30 μ.

might expect a perceptible lengthening of the reaction zone below density 1.2, and a marked lengthening below density 0.9. If the ratio of reaction zone length to charge radius is such that the effect on detonation stability is significant, any lengthening of the reaction zone will be fatal to the detonation wave.

Precisely this effect has been obtained by D. P. MacDougall and coworkers with ammonium picrate. The observed velocities for various densities are plotted in figure 45. It will be seen from figure 45 that below a certain density (which varies somewhat from preparation to preparation) the detonation velocity falls violently, and then detonation fails completely.

(2) *Effect of mixed grain sizes:* Suppose that a large number of spheres, all of the same diameter, be packed so as to have a particular percentage of voids.

Then the number of load-bearing contact points per grain will be independent of the actual diameter of the spheres: thus for 25.95 per cent voids the number of load-bearing contact points is twelve per sphere; for 47.65 per cent voids, the number of load-bearing contact points is six per sphere.

If now a collection of large spheres be packed so as to have any particular number of contact points per sphere, then small spheres can be put into the voids between the large spheres without changing the number of load-bearing contact points; for the small spheres can be so loosely packed as to bear little or no load. If the mixture of small and large spheres be then expanded to its original over-all density, the number of load-bearing contact points per sphere will have been decreased.

The more efficiently the small spheres pack into the voids of the large, the more effective will be the decrease in load-bearing contact points at constant over-all density. The efficiency of packing depends upon the per cent of large
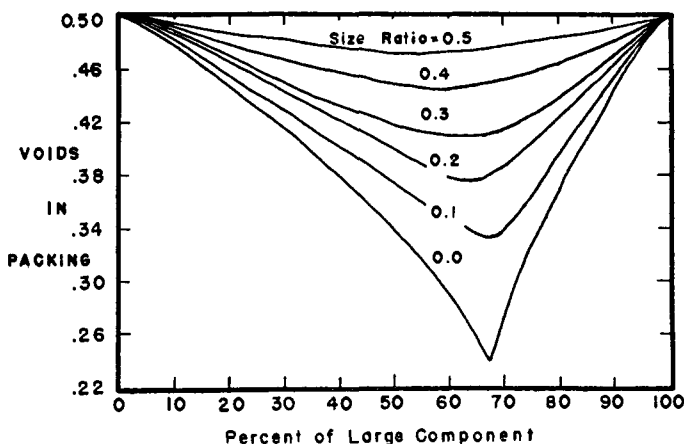

Fig. 46. Relation between voids and size composition in two-component systems of broken solids when the voids of single components are 0.5.

component in the mixture, and upon the size ratio of the spheres. This problem has been investigated by Furnas. As figure 46 shows, the packing is most efficient at about 65–70 per cent of the large component (31). Gamow has also shown by measurement of the electrical conductivity of packed ball-bearings of mixed sizes, that the number of load-bearing contact points (therefore conductivity) is a minimum at about 70 per cent of large ball-bearings.

It is now clear that if we mix explosive grains of two different sizes, the mixture will have many less load-bearing contact points than either of the monodisperse explosive preparations from which it has been prepared. The effect would be most pronounced at a composition of about 70 per cent large grains. If the reaction zone length is such that the effect on detonation stability is significant, then the lengthening of reaction zone produced by such mixing will be fatal to the detonation wave.

Precisely this effect has been obtained with ammonium picrate of densities 1.0

and 0.95, using fine grains of less than 44 μ diameter, and large grains of 177–250 μ diameter. Figure 47 shows the striking decrease in stability of detonation caused by mixing small grains with large grains.

It should be possible roughly to estimate the effect of packing by a simple counting of the average number of load-bearing contact points per grain, as determined by the geometry of the packing. In any such counting, grains which are separated in the direction of propagation of the wave by a narrow gap (say 1/20 their own diameter) should be counted as being in contact, for they will be brought into contact by the mass movement behind the detonation front.
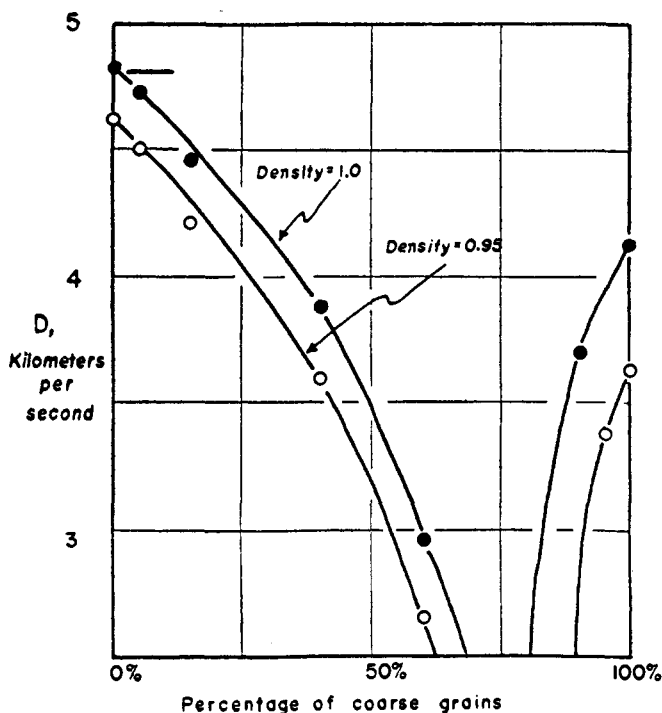

FIG. 47. Failure in D salt (ammonium picrate) due to mixed grain sizes

APPENDIX F. THE SHOCK WAVE AT MATERIAL BOUNDARIES

We wish to find the behavior of a shock wave as it crosses a boundary from one material into another. The general method of mathematical treatment of such a problem is well known (17, 18, 22). A shock wave will be sent into the second material, while a shock or a rarefaction wave will be reflected back into the first material, depending on whether the first material is less dense or more dense than the second. The amplitude of each of these waves is readily found by making use of the condition that the pressure P and the fluid velocity W must match at the boundary, together with the known P,W relations for shocks and for rarefactions.

The actual computation can of course be carried out numerically. An alterna-

tive method of great simplicity is to plot on a P,W diagram (*1*) the curve representing all possible shocks in the second material, and (*2*) the curve representing all possible reflection rarefactions (or shocks) in the first material; the crossing point of the two curves gives the desired matching conditions.

1. P,W relation in a shock

All the required relations for shock waves and detonation waves have already been derived in Section I of this report. From equations I: 4d and I: 6e, the relation between P and W is for a detonation wave:

$$\frac{P - P_0}{(W - W_0)^2} = \frac{\gamma + 1}{V_0 - \alpha} \tag{F1}$$

For a pure shock wave the relation between P and W is slightly different, being

$$\frac{P - P_0}{(W - W_0)^2} = \frac{1}{2} \frac{\gamma + 1}{V_0 - \alpha} \tag{F2}$$

Equation F1 or F2 permits us to plot the P,W relation for any intense shock or detonation wave. Here it has been assumed that the Abel equation of state holds, but an analogous equation is readily found for any desired equation of state.

For shock waves of low intensity (near sonic), it is more convenient to evaluate the P,W relation from equation 4e, which reads:

$$(P - P_0)V_0 = (W - W_0)D \tag{F3}$$

For near sonic velocities this becomes

$$\frac{P - P_0}{W - W_0} = \frac{C}{V_0} \tag{F4}$$

These equations (F1 or F2, and F4) are to be used for both the transmitted and the reflected shock wave.

2. P,W relation in a rarefaction

The following is a very simple derivation of the relations which hold in a rarefaction wave: It will be assumed that a steady state exists, so the equation of continuity is

$$\frac{dW}{D - W} = -\frac{dV}{V} \tag{F5}$$

The velocity of a rarefaction wave is equal to the local velocity of sound,

$$D = C + W \tag{F6}$$

where the velocity of sound is as usual defined by the relations for the Abel equation of state

$$C = V \sqrt{-\gamma \left(\frac{\partial P}{\partial V}\right)_T} \tag{F7}$$

and

$$C = V \sqrt{\frac{\gamma P}{V - \alpha}} \qquad C_0 = V_0 \sqrt{\frac{\gamma P_0}{V_0 - \alpha}} \qquad \text{(F7a, b)}$$

The expansion is assumed to be adiabatic (i.e., isentropic) so that for the Abel equation of state

$$P(V - \alpha)^\gamma = P_0(V_0 - \alpha)^\gamma \qquad \text{(F8)}$$

If equations F5 and F6 are combined, they give

$$W - W_0 = \int_V^{V_0} \frac{C}{V} \, dV \qquad \text{(F9)}$$

which is the basic equation for a rarefaction wave. This may be integrated when the appropriate value of C is inserted: with the value of C given by equation F7 with equation F6, this becomes

$$W - W_0 = \frac{2C_p}{\gamma - 1} \frac{V_0 - \alpha}{V_0} \left[1 - \left(\frac{P}{P_0} \right)^{(\gamma - 1)/2\gamma} \right] \qquad \text{(F10)}$$

Equation F10 permits us to plot the P,W relation for any rarefaction wave in a substance obeying the Abel equation of state.

When the pressure and velocity have been found by the intersection of the two lines on the P,W plane, the shock velocity D can be obtained at once by the relation:

$$(P - P_0)V_0 = (W - W_0)D \qquad \text{(F11)}$$

The actual details of the matching technique can be illustrated most easily by a few worked-out examples:

Example: Shock wave produced in air by a normally incident detonation wave in TNT

Figure 48 gives the curves for a rarefaction wave sent into the detonation products of TNT and for a shock wave sent into air. Their intersection gives the pressure and velocity of the initial wave sent from TNT into air.

The rarefaction curve was computed according to equation F10 with

$$P_0 = 109{,}000 \text{ atm.}$$
$$W_0 = 1.02 \text{ km. sec.}^{-1}$$
$$C_0 = 5.83 \text{ km. sec.}^{-1}$$
$$\gamma = 1.24$$
$$V_0 = 0.540 \text{ cm.}^3 \text{ g.}^{-1}$$
$$\alpha = 0.4225 \text{ cm.}^3 \text{ g.}^{-1}$$

The shock curve was computed according to equation F2 with $\gamma = 1.4$, $V_0 = 0.845$ cm.^{3} g.$^{-1}$, and $P_0 = 0$.

The pressure and velocity of the air shock given by figure 48 are 2500 atm. and 52 km. sec.$^{-1}$, respectively. Those values are far higher than the values observed experimentally (about 600 atm. and 7.65 km. sec.$^{-1}$). This is partly the

fault of too simple an equation of state for air, but primarily the fault of using the Abel equation of state for the adiabatic expansion of TNT. Over such a large pressure range as here covered, the use of the Abel adiabatic introduces a large error. Investigations by Boggs and coworkers, G. I. Taylor, H. Jones, Strickland, Dasgupta, and Penney, in which the primary aim was the determination of accurate numerical values in these shock problems have used more elaborate equations of state, and have succeeded in obtaining excellent agreement between theory and experiment.
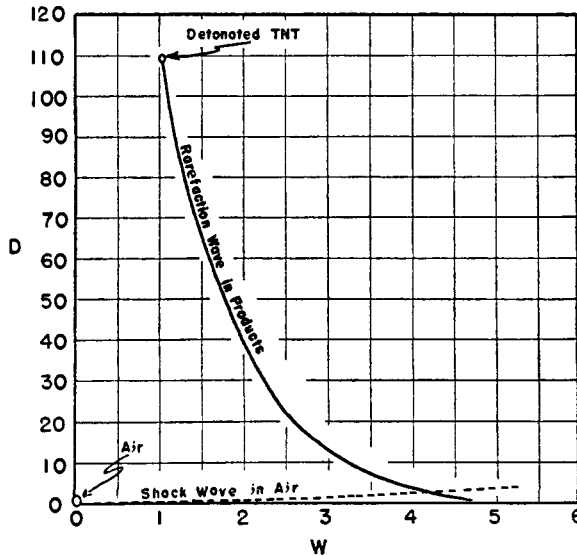

FIG. 48. P,W plot; TNT matched to air

*Example: Reflected shock produced by a detonation
wave in TNT normally incident to a rigid wall*

Figure 49 gives the curve for a shock wave sent into the detonation products of TNT, and the curve for a rigid wall. Their intersection gives the shock pressure produced when a detonation wave in TNT meets a wall.

The shock wave in the TNT products was computed according to equation F2 with the same numerical parameters needed for the previous example.

The P,W relation in the wall is very simple: The velocity of the wall is zero for any pressure.

At the intersection of the two curves, the pressure is 165,000 atm. It is interesting to point out that while a pure shock wave reflected at a wall always more than doubles its pressure, the same cannot be said for a detonation. This is because the P,W relations F1 and F2 are different for a shock and a detonation.

Example: Shock wave set up by a moving projectile

If the wall is moving rather than fixed, it is only necessary to displace the vertical line of figure 49 to the appropriate velocity. This has been done sche-

matically in figure 50, which represents the shock set up in a medium by a moving wall. Essentially this matching method was used by Taylor and Maccoll (67) to find the pressure at a moving wedge.

The equation of the shock curve in figure 50 is equation F1 or F2, depending on the magnitude of the velocity of the wall.
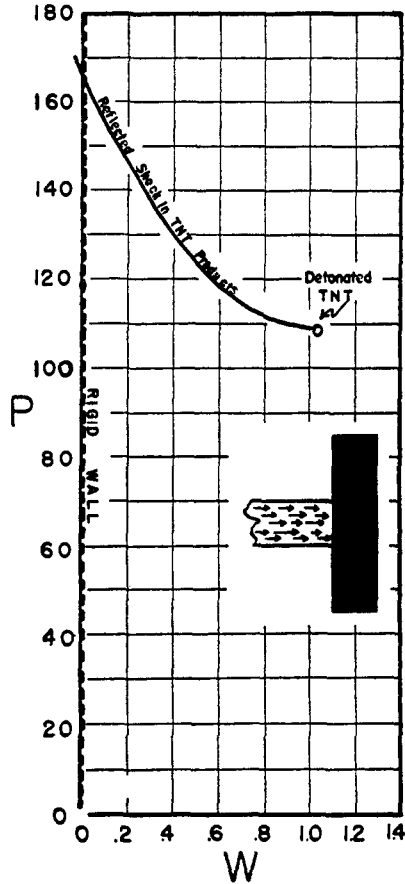

FIG. 49. *P,W* plot; TNT matched to rigid wall

The velocity W of the wall must be the component of its velocity normal to the shock front. Thus for a wedge moving with forward velocity W if the half angle of the wedge is β, the wall velocity is

$$W = W' \sin \beta \sec \left[\sin^{-1} \left(\frac{D}{W'} \right) - \beta \right] \tag{F12}$$

Example: Asymmetric initiation

Following the observation by Herzberg and Walker that a detonation wave does not spread as a perfectly spherical wave from its point of initiation (the

phenomenon gives rise to a "hook" in rotating-mirror photographs), Boggs and Strecker have made a series of experiments which demonstrate that the initiation process is indeed asymmetric. Each new portion of explosive is found to be initiated at its highest velocity in the direction of propagation of the initiating wave, and the wave will only with difficulty propagate around a corner. We shall return in a moment to a discussion of the numerical results obtained by Boggs and Strecker.

If it be supposed that the velocity measured in these experiments is merely the initial velocity of the shock wave set up in the receiver charge, the results can be explained beautifully in terms of the matching theory. We idealize the experimental situation slightly: Suppose a spherical portion of detonated explosive, with all fluid velocities in the same direction, to be embedded in a large
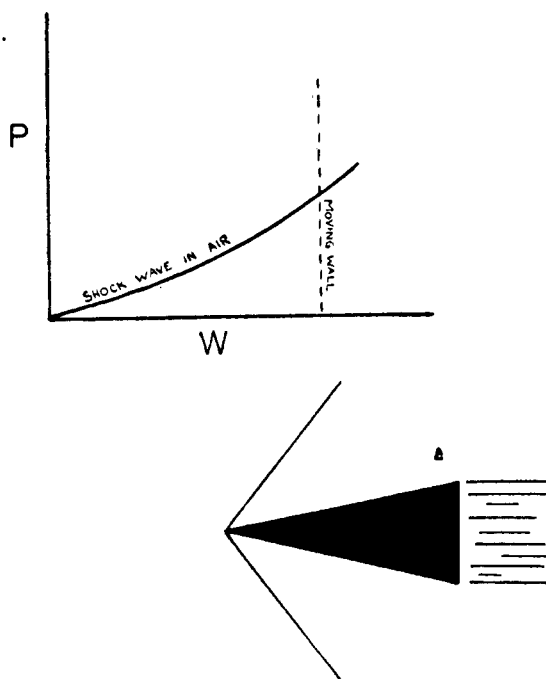

FIG. 50. Shock wave due to moving wall

intact portion of the same explosive. What then will be each point of the sphere?

The model for this problem, and the P,W graphs for its solution, are given in figure 51.

For the detonation wave in the intact explosive, assumed to be TNT of density 1.67, the curve is calculated by equation F1 with the numerical values:

$$P_0 = W_0 = 0$$
$$V_0 = 0.600 \text{ cm.}^3 \text{ g.}^{-1}$$
$$\alpha = 0.4225 \text{ cm.}^3 \text{ g.}^{-1}$$
$$\gamma = 1.24$$

For the rarefaction wave in the initiating explosive, assumed to be detonated TNT, the curve is calculated by equation F10 with the values $W_0 = 1.02 \cos \theta$ km. sec.$^{-1}$ and other numerical parameters as in previous examples.

From the points of intersection obtained in figure 51, a velocity is obtained for propagation at any angle to the direction of propagation of the initiator. The resulting velocities are presented graphically in figure 52, as percentages of the forward velocity. Also included in figure 52 are the experimental data by Boggs and Strecker listed in table F1, for pressed TNT of density 1.48, initiated by a train of the same TNT.
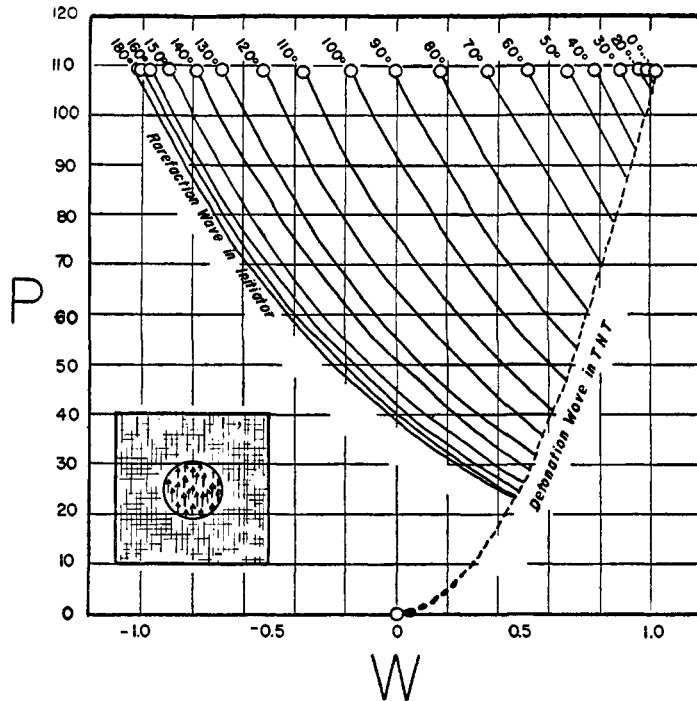

FIG. 51. P,W plot; initiator matched to TNT

The agreement between theory and experiment is quite striking, and leaves little doubt that the observed phenomena are due to asymmetric initiation of the kind discussed.

As figure 52 shows, the resulting wave does resemble a spherical wave sent out from a center of initiation projected somewhat ahead of the true center of initiation. Herzberg and Walker were led by this resemblance to propose that the wave propagated as a "low-order detonation" to this point, where it went over into a high-order detonation which then was propagated spherically.

The theory here developed lends strong support to the former of the two explanations.
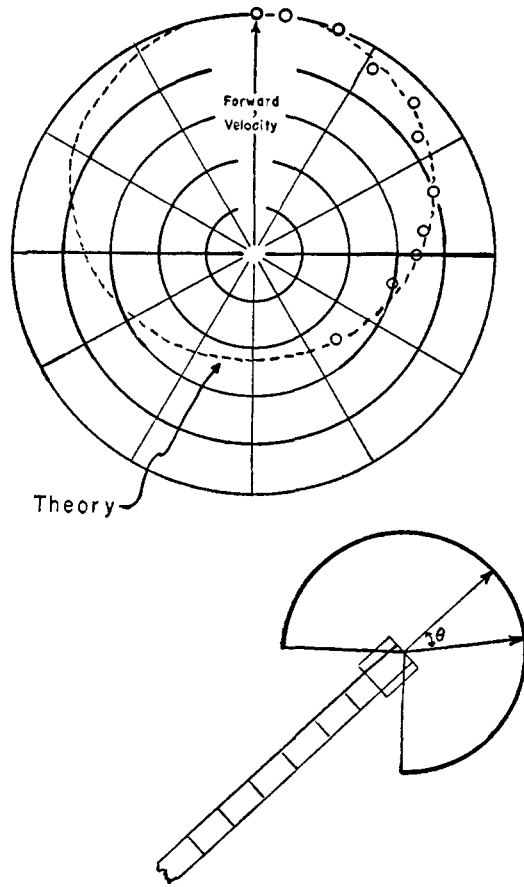
FIG. 52. Asymmetric initiation

TABLE F1

Data for pressed TNT of density 1.48

TYPE OF CHARGE	ANGLE	VELOCITY
		$m. \ sec.^{-1}$
Hemi-cylinder...............................	0°	6300
	7	6300
	32	5800
	54	5300
	82	4500
	90	4300
Three-quarter-cylinder......................	0°	6300
	20	6300
	46	5800
	70	5000
	102	3850*
	135	3150*

* Computed from time lag given by the authors.

APPENDIX G. RATE LAWS OF SURFACE-BURNING REACTIONS

It is of some interest to find the dependence of extent of reaction on time, for topochemical reactions of the surface-burning type, in which the *linear* rate of burning is constant.

Example 1: Sphere uniformly ignited over its surface

Here the boundary between burned and unburned material is given by

$$\frac{R}{R_g} = 1 - \frac{t}{\tau} \tag{G1}$$

and the fraction of material reacted is obviously

$$N = 1 - \left(\frac{R}{R_g}\right)^3 \tag{G2}$$

Therefore the rate law in its integrated form is

$$N = 1 - \left(1 - \frac{t}{\tau}\right)^3 \tag{G3}$$

Example 2: Sphere ignited at its center

Here the boundary between burned and unburned material is given by

$$\frac{R}{R_g} = \frac{t}{\tau} \tag{G4}$$

and the fraction of material reacted is obviously

$$N = \left(\frac{R}{R_g}\right)^3 \tag{G5}$$

Therefore, the rate law is

$$N = \left(\frac{t}{\tau}\right)^3 \tag{G6}$$

Example 3: Sphere ignited at one point on its surface

Here the boundary between burned and unburned material is given by

$$\frac{R}{R_g} = 2\frac{t}{\tau} \tag{G7}$$

The fraction of material reacted is found by a simple integration to be

$$N = \frac{1}{2}\left(\frac{R}{R_g}\right)^3 - \frac{3}{16}\left(\frac{R}{R_g}\right)^4 \tag{G8}$$

Therefore, the rate law is

$$N = \left(\frac{t}{\tau}\right)^3 \cdot \left[4 - 3\frac{t}{\tau}\right] \tag{G9}$$

The dependence of N on t has been plotted in figure 53 for these three examples.

III. DETONATION INITIATED BY A MILD BLOW

A. FORMULATION OF PROBLEM: THE "INTERNAL BURNING" MODEL

If a small fragment of explosive is placed on an anvil and struck a smart enough blow with a hammer, it will explode with a sharp report. When this same experiment is carried out in a machine under quantitatively controlled condi-
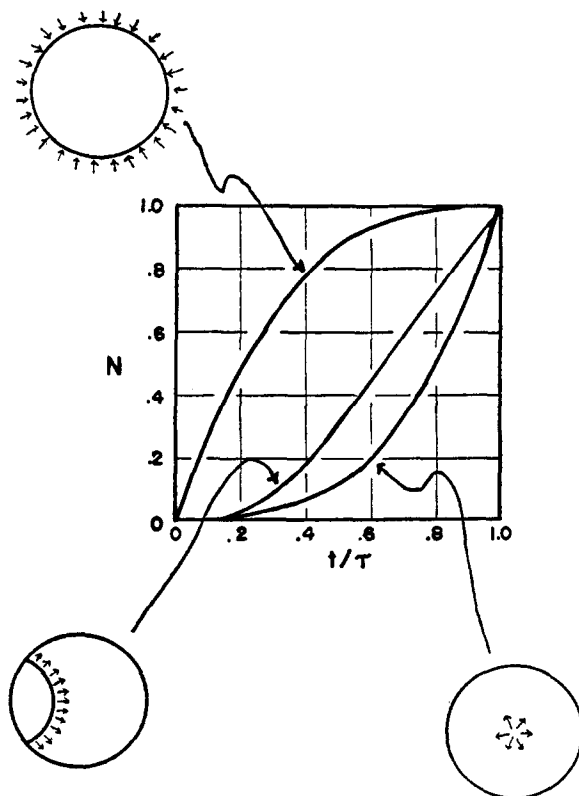

FIG. 53. Burning rate for various models

tions (thus a known weight of explosive, under controlled confinement, on a large rigid anvil, struck by a hammer of known weight falling from a measured height), it becomes the *drop test*. The drop test is universally used and is of first importance as a routine test for characterizing the sensitivity of explosives.

Two difficulties (of a primarily experimental nature) in drop testing have not yet been completely resolved.

In the first place, what is the criterion for "detonation" in a drop test? It is often remarked that the unaided human ear cannot distinguish between the noise of a true detonation and the noise of a very rapid partial burning. Certain

it is that an explosive under the hammer can give a loud report while (a) a good fraction of it remains undecomposed and (b) it is unable to initiate an adjacent portion of the same explosive not under the hammer. A more accurate statement of the situation is that there is no true boundary line between "rapid burning" and "detonation". Any rapid local chemical reaction will send out a sound wave of finite amplitude (generally a shock wave), and the intensity of this wave will be greater, the greater the amount of reaction and the shorter the time required for reaction. Further, even a shock wave of low intensity will in general be able to cause initiation at a few sensitive points before it has attenuated too much, a shock of greater intensity will merely remain able to cause initiation over a larger region.

Thus any rapid burning will in principle lead to a detonation—albeit a failing detonation. (If one chooses to restrict the term "detonation" to a *stable detonation*, one which will continue to propagate, then the dimensions and confinement of the charge through which propagation is to be measured must be specified; see discussion in Section II D.) It seems natural to measure the results of a drop test not as "detonates" or "does not detonate" but in terms of some variable which assumes a continuous range of values. One step in this direction is the measurement of the fraction of explosive decomposed under the hammer (by means of the volume of gas evolved: the Rotter Test Machine). Another is the use of a microphone arrangement to replace auditory observation (developed at the Explosives Research Laboratory, Bruceton).

In the second place, if the drop test on a particular explosive be repeated under identical conditions, it will sometimes give detonation and sometimes not. It becomes necessary to carry out at each height of fall enough experiments so that the results have statistical meaning. Suitably, from a graph of the data on probability paper, it is then possible to report the height of fall producing 10 per cent shots, 50 per cent shots, and 90 per cent shots (or any desired percentage of shots). The fact that sensitivity tests exist which do not show this large statistical scattering of data (namely, shock sensitivity tests such as cardboard gap tests) leads one to suppose that the fluctuations in drop tests are fluctuations in the operation of the machine, not fluctuations in the explosive preparation.

Yet even granting that drop testing involves some difficulties on the experimental side, one key fact is inescapable: A detonation can be started in an explosive by a hammer blow.

In comparison with the blow delivered by another detonating explosive, any blow delivered by a falling hammer is a mild blow. For the material velocity of an explosive is of the order of 1 km. per second, and an explosive will not be initiated by a shock wave whose material velocity is less than a fraction (say one-third to one-half) of that, while a hammer falling from a typical height of 1 m. will have a velocity of only 4.4 m. per second, or far less than sonic velocity in the explosive. So slow is the motion of the falling hammer that we can for practical purposes assume that stresses produced by the hammer are macroscopically uniform through the sample. The problem is thereby simplified to one involving the application of static stresses.

It is perfectly possible to carry out an impact test with a striking hammer whose velocity is 1 km. per second by dropping a bomb from an airplane onto a hard surface, or by mounting explosive in the nose of a rocket projectile and firing it against a concrete target, or by using as striker a high-velocity rifle bullet (R. J. Finkelstein). Such impact tests are better considered as true shock tests than as hammer-blow tests.

As a preliminary to a quantitative theory of initiation by a mild blow, it is first necessary to know the site of action of the mechanical stress. Experimental evidence, cited in detail below, indicates that the stress is concentrated at load-bearing contact points distributed uniformly through the bulk of the explosive.

1. Mass vs. energy relation

It was first proposed by Taylor and Weale (68) that the kinetic energy of the drop hammer required to produce a detonation was proportional to the mass of the explosive sample. Figure 54 presents Taylor and Weale's data for
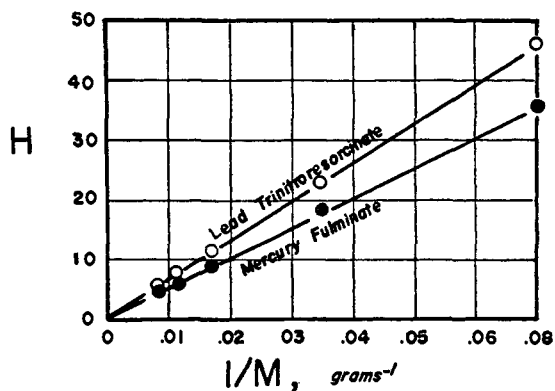

FIG. 54. Drop heights (H, fall in centimeters) for 50 per cent shots (Taylor and Weale (68))

the 50 per cent heights necessary to ignite a fixed amount of (a) mercury fulminate and (b) lead trinitroresorcinate with hammers of varying masses; the results indicate that the product MH (thus the kinetic energy of the falling hammer), rather than either mass or height alone, is critical in determining ignition. Figure 55 presents Taylor and Weale's data for the energies necessary to ignite varying amounts of an explosive consisting of mercury fulminate, potassium chloride, and antimony sulfide; here the amount of explosive was varied by changing the area of the end of the striking pin.

The proportionality of energy to mass in laboratory ignition tests has been confirmed for a large number of explosives by Lawrence (see figure 57 and discussion below).

The proportionality holds over a range of explosive mass from a few centigrams to 100 g., as shown by measurements on the 17 per cent energy for TPX (figure 56.) It can be observed from figure 56 that the proportionality of energy to mass is not rigid, the requisite energy density being somewhat less with the large charges. This is probably best interpreted as a time effect: The total time

of impact is longer for the heavier impacts, and it is reasonable to suppose that somewhat less energy is required for detonation if the explosive be maintained under stress for a longer time.
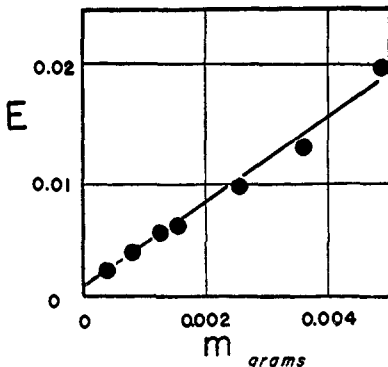

FIG. 55. Drop-weight energy for 50 per cent shots (E in calories)
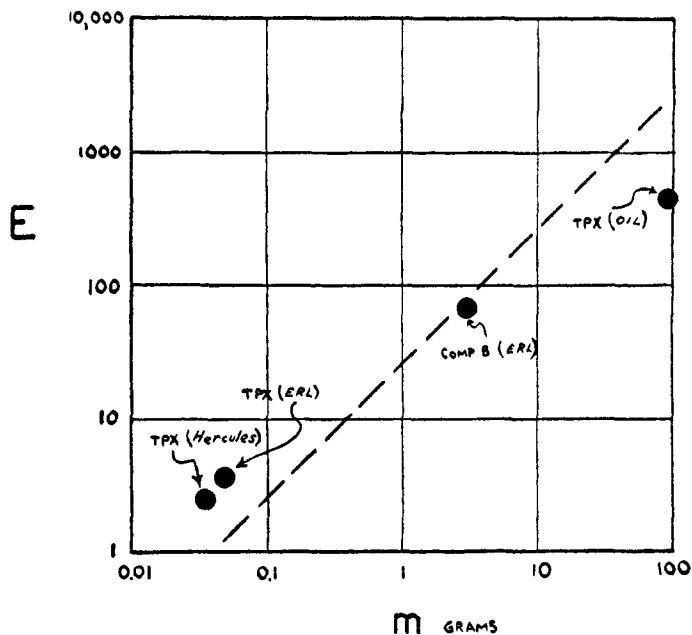

FIG. 56. Energy *vs.* mass for drop tests (E in calories for 17 per cent shots)

The statement that the energy necessary to cause initiation is proportional to mass must be qualified in two minor respects: (*a*) Since some portion of the energy of the hammer will always be lost into the anvil, and by rebound of the hammer, and perhaps by heating of a portion of the explosive which does not lead to reaction, the energy *vs.* mass relation plot remains linear but will have

an intercept corresponding to a finite energy requirement even for zero mass of explosive. Figure 57 presents data by Lawrence to illustrate this effect. (b) It has been assumed that the machine itself does not produce any concentration of stress. The casing of an actual bomb may, by acting as a compound beam, produce highly concentrated local stresses when subjected to impact. This possibility may have a bearing on the few instances in which accidental bomb drops of a few feet have led to explosions.

The proportionality of energy of the falling hammer to mass of explosive must be interpreted to mean that the initiating effect of the stress is exerted throughout the *bulk* of the explosive. Initiation is not a surface effect. Neither
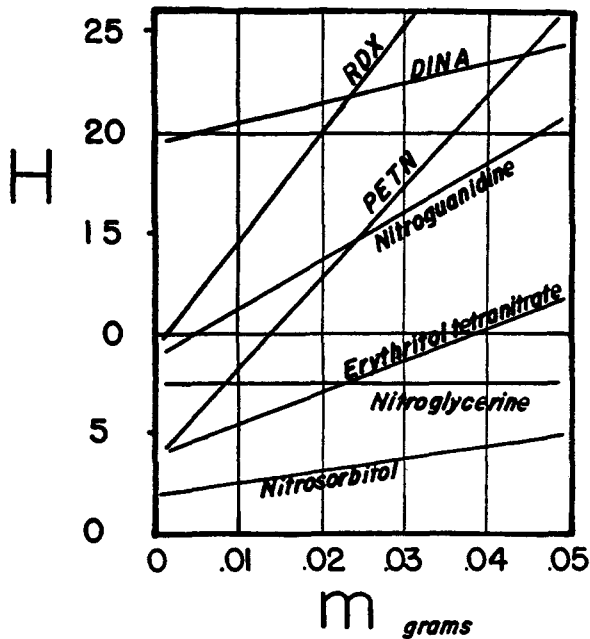

Fig. 57. Height *vs.* mass for shots (H, fall in centimeters of 2-kg. hammer for 50 per cent shots).

is it an accident which occurs at only a single point in the explosive; for if this were so, at a constant energy density a sample of explosive of twice the size would have twice as great a chance of initiation.

2. Absolute energy density for initiation

The numerical value of the energy density necessary to cause 50 per cent detonations varies from explosive to explosive, but it is of the order of 25 cal. per gram for typical organic nitro compounds. Therefore, if the explosive were to be heated uniformly throughout by the energy of the blow, its temperature would rise by only some 70°C. Since such a temperature rise would have no effect on the explosive, it is clear that the stress must be so concentrated as to

produce local high temperatures at a number of highly favored spots. These "hot spots" will undoubtedly be the load-bearing contact points between grains, or the corresponding interfaces in the interior of polycrystalline materials.

As additional circumstantial evidence for the hot-spot hypothesis, it is to be noted that the addition of sharp, angular, stress-concentrating materials (powdered glass) makes explosives more sensitive to impact, while the addition of lubricants (waxes; water) makes explosives less sensitive to impact.

We may now summarize the theory of the site of action of the mechanical stress, developed (at least in its broad outlines) by Taylor and Weale, and now generally accepted by investigators in the field:

Mechanical stress is concentrated at spots distributed uniformly through the bulk of the sample, so that these spots become hot. At each hot spot chemical reaction begins, so that the entire bulk of explosive is subject to a sort of internal burning. If the chemical reaction then becomes fast enough, the internal burning goes over into a detonation.

This is the "internal burning" model for initiation in a drop test. Bowden and coworkers (12, 13) have actually observed that when liquid nitroglycerin is ignited by impact, the initiation begins as a tiny flame which only after a period of about 100 microsec. goes over into detonation.

It appears likely that when an explosive is ignited by a flame at its surface, losses will be so great that no pressure can be built up, and the explosive will burn quietly without detonating. Only if the burning is able to penetrate to the interior of the substantially intact explosive, thus producing internal burning, will conditions be right for a detonation.

In particularizing the site of initiation, mention has been made neither of the exact mode of heating nor of the kinetics of the chemical reaction in the presence of thermal and dynamical losses. It is these omitted details which really make up the kernel of the theoretical problem, which we may now attempt to solve.

B. APPROXIMATE SOLUTION OF THE PROBLEM

It is easy enough to write down the differential equations for the problem of a spreading exothermic chemical reaction with thermal conduction and with dynamical gains and losses (they are in fact the equations given in the footnote to equation I: 1b of this report). But the complete equations are so difficult as to be hopelessly insoluble.

Now the application of the mechanical stress requires some tens of microseconds in a typical drop test; there is then a time lag of some 100–1000 microsec. during which the burning is going on,[22] and finally the detonation wave itself traverses the sample in about a microsecond. It is therefore possible to visualize the process as occurring in three separate steps, and for purposes of computation to neglect the overlapping of one step by another. In the first step, the mechanical stress gives rise to a temperature distribution at each load-bearing contact point. In the second step, the chemical reaction spreads at a rate determined

[22] Oscillographic measurements of the time delay between impact and detonation.

by its rate–temperature law and the temperature distribution given by heat evolution and conduction. In the third step, the pressure produced by the products of burning gives rise to a detonation wave. The replacement of the actual process by these three successive processes simplifies the mathematical treatment to the extent that at least an approximate solution can be obtained for each process.

Step 1. Initial temperature distribution due to mechanical stress

To find the temperature pattern at a hot spot or contact point, it is necessary to know (1) the number of contact points and thus the total stress at any one contact point; (2) the stress pattern around a contact point; (3) whether the material under such a stress will behave elastically or will flow; (4a) if it behaves elastically, what temperature is produced by elastic compression at each region of the stress pattern; and (4b) if it flows, what will be the frictional heating.

Unfortunately, not one of the items in the list above is known. The number of hot spots might be estimated roughly from the geometry of the packing. But does the number change with the applied stress, or not? The finding of the stress pattern is a straightforward problem in stress analysis, once the geometry of the contact regions is known. Since these first two are essentially problems in static stresses, the methods of photoelastic analysis at once suggest themselves. The last three items require a knowledge of the stress-strain and viscous behavior of the substance, which is not excessively difficult to obtain by direct measurement (preferably on a non-explosive analog!).

In the complete absence of necessary data, about all that can be done is to assume arbitrarily a size and a temperature of the initial hot spot.

Step 2. The spreading exothermic finite chemical reaction with thermal conduction

In the above definition of the problem, "spreading" indicates that intact explosive substance is progressively heated and consumed; "exothermic" that the chemical reaction evolves heat (but the dynamical effect of any pressure change is neglected); "finite" that the amount of explosive in any one region is not limitless, so it does not keep evolving heat forever; "thermal conduction" that heat is conducted away from the zone of reaction into the cooler intact explosive.

The integro-differential equation governing this process is, for spherical symmetry,

$$\frac{\partial(rT)}{\partial t} = \frac{\kappa V}{C_v}\frac{\partial^2(rT)}{\partial x^2} + \frac{Z\Delta Q}{rC_v}e^{-\Delta H^{\ddagger}/R_0T}\,e^{-\int_0^t Ze^{-\Delta H^{\ddagger}/R_0T}\,dt} \qquad (1)$$

where the reaction rate has been assumed to obey the law

$$\frac{dN}{dt} = (1 - N)Ze^{-\Delta H^{\ddagger}/R_0T} \qquad (1a)$$

In equation 1 the first term on the right gives the conduction of heat, while the second term gives the heat produced by reaction; the first exponential

factor contains the dependence of reaction rate on temperature, and the second exponential factor takes into account the finite amount of the reacting substance.

We have attempted to solve equation 1 by a point-by-point graphical integration, in order to obtain a general idea of the behavior of the process. But this integration is so excessively tedious that it has been abandoned. The results of a particular computation are given in figure 58, from which it will be seen that the reaction is beginning to progress in the originally intact explosive.
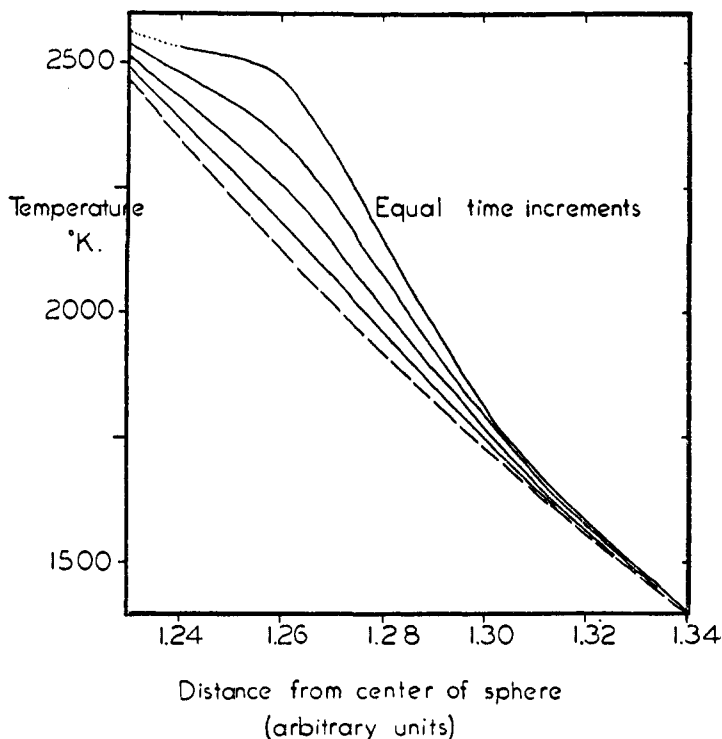

FIG. 58. Numerical integration of initiation problem

The numerical parameters used in this integration were as follows: Initial temperature as given by a dashed line; this is the temperature distribution appropriate to heat spreading from an instantaneous point source.

$$\frac{\kappa V}{C_v} = 0.003 \text{ cal. cm.}^{-1} \text{ sec.}^{-1}$$

$$V = 0.667 \text{ cm.}^3 \text{ g.}^{-1}$$

$$C_v = 0.5 \text{ cal. g.}^{-1}$$

$$\Delta Q = 600 \text{ cal. g.}^{-1}$$

$$Z = 10^{13} \text{ sec.}^{-1}$$

$$\Delta H^{\ddagger}/R_0 = 17{,}000 \text{ deg.}$$

Since the complete equation for the process cannot practicably be solved, the next move is to drop one or more requirements of the original problem, in the hope that the simpler problem will be soluble.

(*2a*) *The exothermic chemical reaction with thermal conduction:* Here the requirements have been relaxed that the chemical reaction spread and that it be finite. The model is of a small hot sphere of uniform internal temperature; reaction proceeds only within this sphere; heat is conducted away by the surrounding medium. This problem has been attacked by Rideal and Robertson, who find that the appropriate sizes and temperatures of hot spots such that the rate of heat production shall just balance the rate of heat conduction are as given in table 14.

As will be seen from table 14, the calculated critical hot-spot temperature is very sensitive to the assumed hot-spot radius.

(*2b*) *The spreading finite chemical reaction with thermal conduction:* Here the requirement that the reaction be exothermic has been relaxed. Because of the absence of sources, the problem is easy to solve. The temperature as a function of time and distance can be found by the classical methods for heat conduction

TABLE 14

Critical hot-spot temperature for hot-spot radius as listed

EXPLOSIVE	$r = 10^{-3}$	10^{-4}	10^{-5}	10^{-6} CM.
	°C.	°C.	°C.	°C.
PETN	310	385	495	640
RDX	380	485	615	815
HMX	410	510	645	825
Tetryl	425	570	815	1250
Ammonium nitrate	590	825	1230	2180

problems. Then the amount of reaction at any point must be found by numerical integration of the rate law, as is customary in reaction-rate problems with varying temperature.

Figure 59 presents the calculated extent of reaction for this model, the heat spreading from an instantaneous point source of 10^{-10} cal. strength. It will be noted that the reaction proceeds at about the rate at which the heat spreads, then ceases abruptly when the temperature becomes too low to initiate reaction. Numerical parameters for computation of figure 59 were the same as those for figure 58.

(*2c*) *The finite exothermal chemical reaction:* Here the requirements that the reaction spread and that heat is conducted away have been relaxed. This is just the problem of an exothermic reaction proceeding adiabatically (27).

If the rate law for the reaction is

$$\frac{dN}{dt} = (1 - N)Ze^{-\Delta H^{\ddagger}/R_0 T} \tag{2}$$

and the extent of reaction N is given by

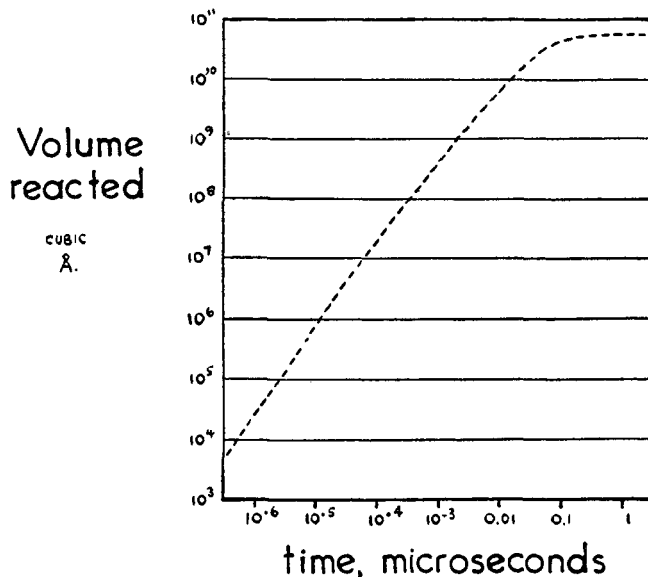$$N = \frac{T - T_0}{T_1 - T_0} \tag{3}$$

FIG. 59. Athermic spreading reaction rate

Then the rate law becomes

$$\frac{dT}{dt} = (T_1 - T)Ze^{-\Delta H^{\ddagger}/R_0 T} \tag{4}$$

This may be integrated without difficulty to give

$$Zt = Ei\left(\frac{\Delta H^{\ddagger}}{R_0 T}\right) - Ei\left(\frac{\Delta H^{\ddagger}}{R_0 T_0}\right) + e^{-\Delta H^{\ddagger}/R_0 T_1}\left\{Ei\left(\frac{\Delta H^{\ddagger}}{R_0 T_0} - \frac{\Delta H^{\ddagger}}{R_0 T_1}\right)\right.$$
$$\left. - Ei\left(\frac{\Delta H^{\ddagger}}{R_0 T} - \frac{\Delta H^{\ddagger}}{R_0 T_1}\right)\right\} \tag{5}$$

where

$$Ei(x) = \int_{-\infty}^{x} \frac{e^y\, dy}{y} \tag{5a}$$

for which tabulated values are available. For all values of T except those in the immediate neighborhood of T_1, the exponential integral may be replaced by its approximate value

$$Ei(x) \approx \frac{e^x}{x}$$

giving as a final result

$$t = \frac{R_0}{Z\Delta H^{\ddagger}}\left\{\frac{T_0^2}{T_1 - T_0}e^{-\Delta H^{\ddagger}/R_0 T_0} - \frac{T^2}{T_1 - T_0}e^{-\Delta H^{\ddagger}/R_0 T}\right\} \tag{6}$$

Figure 60 presents the extent of reaction as a function of time for the adiabatic exothermal reaction, as computed from equation 6, for the same reaction rate used in computing figures 58 and 59. The general course of the reaction resembles a long inhibition period followed by a rapid completion of the reaction.
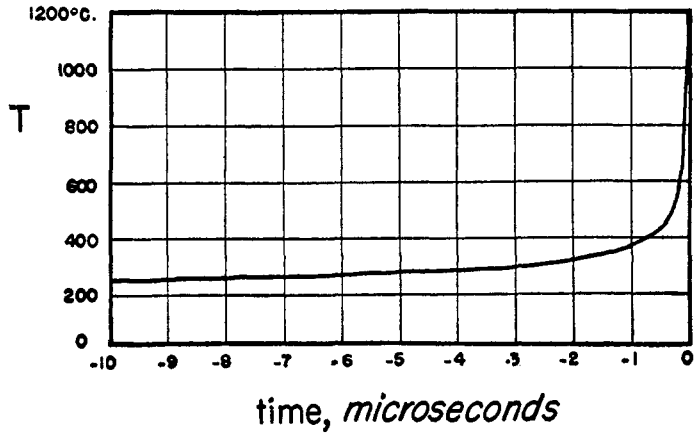
time, *microseconds*
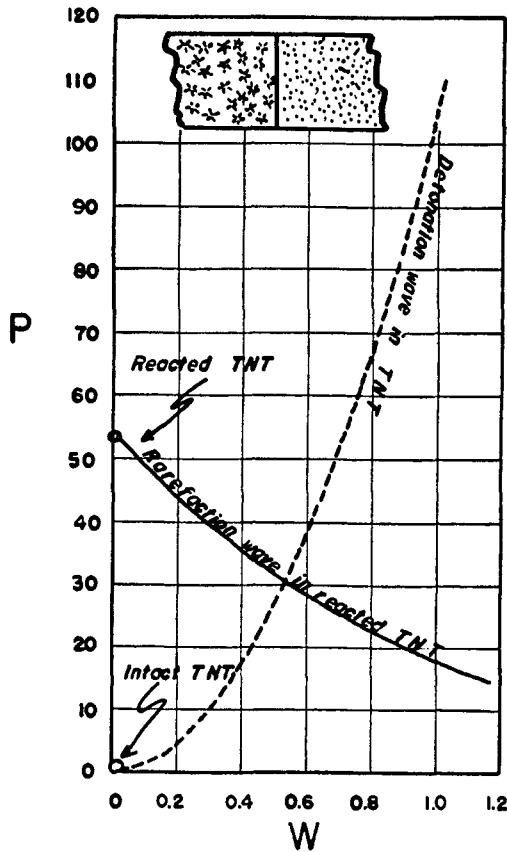
Fig. 60. Exothermic adiabatic reaction rate

Fig. 61. TNT matched to TNT; D,W plot

The various approximate calculations listed above do not give a very satisfactory picture of the course of a spreading reaction of the type described.

This is a sufficiently fundamental problem in reaction kinetics so that a thorough investigation of it would be useful. From the theoretical side, such a study has not yet been made. From the experimental side, it may be possible to study the kinetics of the spreading reaction by a technique such as quenching the reaction after various elapsed times. In such an experimental investigation, it would of course be necessary to control the initial temperature pattern at each hot spot.

Step 3. The detonation wave set up by pressure

The exact solution of the hydrodynamic equations for the process by which internal burning goes over into detonation is very difficult. We propose, instead, an heuristic approach to the problem.

In the first place, consider a quantity of explosive undergoing static reaction— burning. Let another quantity of intact explosive be placed adjacent to it. Under what conditions will the burning substance *most effectively* set up a shock wave in the intact substance? Clearly, these conditions are (1) the burning substance is of infinite dimensions, (2) the intact substance is of infinite dimensions, and (3) the entire burning process is completed instantaneously. For under any other conditions, losses will supervene to cut down the intensity of the shock wave.

The mathematical tools are at hand to find precisely this most effective shock (see appendix F of this report). Figure 61 presents the details of the solution, for reacted TNT against intact TNT.

The shock curve in intact TNT was computed according to equation F1 with

$$P_0 = W_0 = 0$$

$$\gamma = 1.24$$

$$V_0 = 0.600 \text{ cm.}^3 \text{ g.}^{-1}$$

$$\alpha = 0.4225 \text{ cm.}^3 \text{ g.}^{-1}$$

The rarefaction curve in reacted TNT at rest was computed according to equation F10 with

$$W_0 = 0$$

$$P_0 = 54,500 \text{ atm.; this}$$
$$\text{is one-half the detonation}$$
$$\text{pressure, as pointed out}$$
$$\text{in Section I}$$

$$C_0 = 3.58 \text{ km. sec.}^{-1}$$

$$\gamma = 1.24$$

$$V_0 = 0.600 \text{ cm.}^3 \text{ g.}^{-1} \text{ (reaction at}$$
$$\text{constant volume)}$$

$$\alpha = 0.4225 \text{ cm.}^3 \text{ g.}^{-1}$$

From the point of intersection of the two curves, the detonation velocity is computed to be 53 per cent of the ideal detonation velocity for TNT.

A velocity of 53 per cent of the ideal velocity is therefore the best that can be done if burned TNT at rest is initiating intact TNT. A similar computation can be made for any explosive.

Is now a shock velocity of 53 per cent D_i sufficient to initiate a stable detonation in TNT? By referring to the discussion of failure (Section II D) we see that such a velocity is able to produce stable detonation if the radius of the receiver charge is no less than two reaction zone lengths (of the receiver substance). However, the wave of this velocity is on the verge of being too weak to initiate a stable detonation; if the velocity should fall to, say, one-half this velocity, it would almost certainly fail to initiate detonation. We may say that the initiation is precarious.

For some explosives, the maximum shock producible by static burning might be less than the minimum shock which would produce stable detonation. Such an explosive could not be detonated at all in a drop test. Ammonium nitrate is perhaps such an explosive.

We can proceed to remove, one by one, the restrictions under which the most effective wave was computed.

(1) *Length and width of receiver charge:* If the length of the receiver charge is not at least several of its own ideal reaction zone lengths, it will not be possible to observe whether the wave is building up; but this restriction is somewhat trivial. Likewise, if the receiver charge is of less than the critical radius, it will of course not propagate stably. The receiver charge must therefore be of radius at least two of its own ideal reaction zone lengths, preferably more.

(2) *Width and length of initiator charge:* If the burned material is of either finite width or length, a rarefaction wave will be superimposed on the shock wave and eat it away. To produce initiation, it is necessary to maintain the shock intensity in the receiver for a distance not less than the reaction zone length of the receiver substance. This will only be possible if the dimensions of the initiator charge are of this same order of magnitude.

Since what we have called the "initiator charge" is in reality the burned products arising from a collection of hot spots, or "super-hot-spot", we can write: *The minimum size of "super-hot-spot" which will initiate detonation is approximately the ideal reaction zone length of the substance to be detonated.*

It is particularly to be noted that a single hot spot, of less than 1 micron diameter, may (if its reaction is fast enough) outrun temperature losses and continue to burn. But only a much larger hot spot, say a "super-hot-spot" 1 mm. in diameter, will be able to outrun dynamical losses enough to initiate detonation in a typical organic nitro explosive.

(3) *Time of reaction:* Assuming that the super-hot-spot which acts as initiator is a sphere of the dimensions of the reaction zone length, any shock wave sent out by it into a non-reacting substance will fall to half its velocity within a distance of about that same magnitude. The time required to build up the pressure must therefore be not more than the time for the wave to traverse this

distance, which is the reaction time τ of the receiver charge. For typical organic nitro explosives, this is about 1 microsec. We can write: *Of the pressure increase produced by burning, only the increment of pressure over about one reaction time of the substance to be detonated can be utilized for initiation.* Any pressure which is produced more gradually simply appears as hydrostatic pressure, which is not useful for initiation.

This result indicates that it is undesirable for any appreciable amount of the explosive in the super-hot-spot to have burned in the long time-lag preceding detonation, for such burned explosive cannot contribute pressure to the initiation. On the other hand, it is very desirable for the explosive in the super-hot-spot to show a long induction period and then to decompose all at once. One way in which this could arise would be for the reaction to spread over the internal surface throughout the region originally heated by mechanical stress; for this would lead to burning ignited over a large region before any appreciable amount of explosive had been consumed. (The possibility is suggested of *chemical* sensitizing and desensitizing of the surface of explosives, as a means of controlling their impact sensitivity. This experiment is to be distinguished from *mechanical* sensitizing and desensitizing, as by sharp grains or by lubricants, respectively.)

It is interesting to point out that the familiar technical design for initiation of explosives—namely, primer‖booster‖explosive—is beautifully designed to circumvent difficulties in initiation. The primer is a substance of very short reaction zone, and usually of well-defined sharp-edged crystals (often metallic or metal-organic salts), so that it is easily detonated by a mild hammer blow. The booster is an explosive whose reaction zone length is of the same order as the dimensions of the primer, so it is readily detonated by the primer. The dimensions of the primer are, in turn, of the order of the reaction zone length of the substance which comprises the main explosive charge, so the latter is readily detonated.

In summary, we may outline the procedure to be followed in the proposed theoretical analysis of sensitivity toward impact, for a particular experimental situation:

(*1*) The macroscopic stress pattern due to the falling weight must be determined. For an ordinary drop test the stress is uniform, but in a more general experiment it might not be uniform. From the macroscopic stress pattern, the microscopic stress pattern is then found for each load-bearing contact point. From the microscopic stress and the time of its application, the amount of heating at each contact point is determined. It seems likely that most of the heating will turn out to be due to flow and frictional heating, rather than to reversible compressive heating, but this point must be checked for each individual case.

(*2*) From the initial temperatures and the kinetics of the burning reaction, the rate of reaction must be found as a function of time. As pointed out above, the kinetics of such reactions are not now satisfactorily known, so they will have to be determined. It is to be noted that the burning process will not only come to a stop if thermal conduction outruns it, but will also largely stop when the pressure is released by the removal of the hammer.

(*3*) The maximum increment of pressure produced by the burning over any 1-microsec. time interval is found. If the magnitude of this pressure increment is enough to produce a minimum initiating shock, while also the size of the spot producing it is as great as a reaction zone length in the explosive to be detonated, than a stable detonation will be produced.

At the present time, our knowledge of the internal stresses in a polycrystalline material under load is very slight. The theoretical treatment of heating by an applied stress (thus of the dissipation of energy) has not been developed to a degree that it could immediately be applied to our problem. The theory of the kinetics of spreading exothermic reactions is in a completely unsatisfactory state. The present theory of reaction zone lengths and the matching of shock waves at boundaries does seem to be in a satisfactory state, but even here our numerical knowledge is limited to the examples given in Section II of the present report.

It is evident from the foregoing remarks that the complete theory of initiation by impact must wait upon a thorough theoretical and experimental program of study of stress heating, burning reactions, and reaction zone lengths in high explosives.

IV. References

(1) ANDREEV, K. K.: Physik. Z. Sowjetunion **5**, 174 (1934).

(2) ANDREEV, K. K.: Z. ges. Schiess- u. Sprengstoffw. **29**, 95 (1935).

(3) Applied Mathematics Panel, National Defense Research Committee, August, 1944.

(4) AUDUBERT, R.: Trans. Faraday Soc. **35**, 197 (1939).

(5) BATEMAN, H.: Bull. Natl. Research Council No. **84** (1931).

(6) BECKER, R.: Z. Physik **8**, 321 (1922).

(7) BECKER, R.: Z. Physik **8**, 321-62 (1922).

(8) BERTHELOT, M., AND VIEILLE, P.: Compt. rend. **93**, 18-22 (1881).

(9) BERTHELOT, M., AND VIEILLE, P.: Compt. rend. **94**, 149-52 (1882).

(10) BOLLE, E.: In Auerbach-Hort's *Handbuch der physikalischen technischen Mechanik* **6**, 310-401 (1928).

(11) BONE, W. A., FRAZER, R. P., AND WHEELER, W. H.: Phil. Trans. **235**, 29-68 (1935).

(12) BOWDEN, F. P., EIRICH, F., FERGUSON, A. E., AND YOFFE, A.: Council of Scientific and Industrial Research, Australia, 1943, Bull. **167**, 44 pp.

(13) BOWDEN, F. P., EIRICH, F., FERGUSON, A. E., AND YOFFE, A.: Council of Scientific and Industrial Research, Australia, 1943, Bull. **173**, 75 pp.

(14) BRIDGMAN, P. W.: J. Chem. Phys. **15**, 311-13 (1947). Hydrostatic pressures up to 50,000 atm. on solid explosives.

(15) CHAPMAN, D. L.: Phil. Mag. **47**, 90-104 (1899).

(16) CHAPMAN, S., AND COWLING, T. G.: *Mathematical Theory of Non-Uniform Gases*, pp. 96-9. University Press, Cambridge (1939).

(17) COURANT, R., AND coworkers: AMP Report No. 38.2R, August, 1944.

(18) COURANT, R., AND FRIEDRICHS, K.: OSRD Report No. 1567, July, 1943.

(19) DALLA VALLE, J. M.: *Micromeritics*, p. 102. Pitman Publishing Corporation, New York (1943).

(20) DEVONSHIRE, A. F.: Theoretical Research Report No. 3/43.

(21) DIXON, H. B.: Phil. Trans. **184**, 97 (1893).

(22) DÖRING, W.: *Beiträge zur Theorie der Detonation*, Part VII. Unpublished German report.

(23) DÖRING, W.: *Beiträge zur Theorie der Detonation*, Part VIII.

(24) DUFFEY, G. H.: Thesis submitted to the Chemistry Department of Princeton Uni-

versity in partial fulfillment of the requirements for the degree of Doctor of Philosophy, 1945.

(25) EARNSHAW, S.: Proc. Roy. Soc. (London) **9**, 590-1 (1859); Phil. Trans. **150**, 133-48 (1860).

(26) EYRING, H.: J. Chem. Phys. **4**, 283 (1936).

(27) EYRING, H., POWELL, R. E., DUFFEY, G. H., AND PARLIN, R. B.: OSRD Report No. 2026.

(28) EYRING, H., POWELL, R. E., DUFFEY, G. H., AND PARLIN, R. B.: OSRD Report No. 3794.

(29) EYRING, H., POWELL, R. E., DUFFEY, G. H., AND PARLIN, R. B.: OSRD Report No. 3796, June 17, 1944.

(30) FARMER, R. C.: J. Chem. Soc. **117**, 1432, 1603 (1920); **121**, 174 (1922).

(31) FURNAS, C. C.: Ind. Eng. Chem. **23**, 1052-8 (1931); quoted in reference 19, p. 111.

(32) GARNER, W. E., AND GOMM, A. S.: J. Chem. Soc. **1931**, 2123.

(33) GARNER, W. E., AND HAILES, H. R.: Proc. Roy. Soc. (London) **A139**, 576 (1933).

(34) GLASSTONE, S., LAIDLER, K. J., AND EYRING, H.: *The Theory of Rate Processes.* McGraw-Hill Book Company, Inc., New York (1941).

(35) GOLDSTEIN, S.: *Modern Developments in Fluid Mechanics*, Vol. I, p. 95. University Press, Oxford (1938).

(36) GURNEY, H. P., AND LURIE, J.: Ind. Eng. Chem. **15**, 1170 (1923).

(37) HAILES, H. R.: Trans. Faraday Soc. **29**, 544 (1933).

(38) HINSHELWOOD, C. N.: J. Chem. Soc. **119**, 721 (1921).

(39) HUGONIOT, J.: J. math. [4] **3**, 477 (1887); J. école polytech. (Paris) **57**, 3-97 (1887); **58**, 1-125 (1889).

(40) JONES, H.: Proc. Roy. Soc. (London) **A189**, 415-26 (1947); also the work of G. I. Taylor and J. H. Wilkinson.

(41) JOST, W.: *Explosions- und Verbrennungsvorgänge in Gasen*, pp. 161-71, 199-207. J. Springer, Berlin (1939).

(42) JOUGUET, E.: J. math. **1905**, 347-425; **1906**, 6-86.

(43) JOUGUET, E.: *Mécanique des explosifs.* O. Doin et fils, Paris (1917).

(44) KENNARD, E. H.: *Kinetic Theory of Gases*, p. 177. McGraw-Hill Book Company, Inc., New York (1938).

(45) KHARITON, YA. B., AND RATNER, S. B.: Doklady Akad. Nauk. S.S.S.R. **41**, 293-5 (1943).

(46) KINCAID, J. F., AND EYRING, H.: J. Chem. Phys. **6**, 620 (1938).

(47) KISTIAKOWSKY, G. B., AND WILSON, E. B.: NDRC Report, 1941.

(48) LAFFITTE, P., AND PATRY, M.: Compt. rend. **193**, 171 (1933).

(49) LAMB, H.: *Hydrodynamics*, 6th edition, p. 576. University Press, Cambridge (1932).

(50) LEWIS, B., AND FRIAUF, J. B.: J. Am. Chem. Soc. **52**, 3905 (1930).

(51) LEWIS, B., AND VON ELBE, G.: *Combustion, Flames and Explosions of Gases*, pp. 237-49. University Press, Cambridge (1938).

(52) MALLARD, E., AND LE CHATELIER, H. L.: Compt. rend. **93**, 145-8 (1881).

(53) MILNE-THOMSON, L. M.: *Theoretical Hydrodynamics*, p. 509. The Macmillan Company, New York (1938).

(54) MURAOUR, H.: Chimie & industrie **47**, 477 (1942).

(55) NAUCKHOFF, S.: Z. ges. Schiess- u. Sprengstoffw. **26**, 45-7 (1931).

(56) PARISOT, A., AND LAFFITTE, P.: Congr. chim. ind., Compt. rend. 18me congr., Nancy **1938**, 930-6. Picric acid, RDX.

(57) PAYMAN, W., AND WALLS, N. S.: J. Chem. Soc. **123**, 420 (1923).

(58) PRANDTL, L., AND TIETJENS, J.: *Fundamentals of Hydro- and Aeromechanics*, p. 258. McGraw-Hill Book Company, Inc., New York (1934).

(59) RANKINE, W. J. M.: Phil. Trans. **160**, 277-88 (1870).

(60) RATNER, S. B.: Doklady Akad. Nauk. S.S.S.R. **42**, 276-8 (1944).

(61) RIEMANN, B.: Göttinger Nachr. **8**, 156 (1860).

(62) ROBERTSON, R.: J. Chem. Soc. **119**, 1 (1921).

(63) ROGINSKY, S.: Physik. Z. Sowjetunion **1**, 640 (1932).

(64) SCHMIDT, A.: Z. ges. Schiess- u. Sprengstoffw. **24**, 41, 90 (1929); **25**, 97, 144 (1930); **26**, 253, 293 (1931); **27**, 1, 45, 82, 145, 184, 225, 264, 299 (1932); **28**, 259, 299 (1934); **30**, 33, 75, 101, 145, 230 (1935); **31**, 8, 37, 80, 114, 149, 183, 218, 248, 284, 322 (1936); **33**, 230, 312 (1938); **34**, 38 (1939).

(65) SCORAH, R. L.: J. Chem. Phys. **3**, 425–30 (1935).

(66) SELLE, H.: Z. ges. Schiess- u. Sprengstoffw. **24**, 469–74 (1929).

(67) TAYLOR, G. I., AND MACCOLL, J. W.: In Durand's *Aerodynamic Theory*, Vol. 3, pp. 209–50. Julius Springer, Berlin (1935).

(68) TAYLOR, W., AND WEALE, A.: Proc. Roy. Soc. (London) **A138**, 92–116 (1932).

(69) THOMAS, L. H.: J. Chem. Phys. **12**, 449–53 (1934).

(70) TRAUTZL, K.: Z. ges. Schiess- u. Sprengstoffw. **37**, 1946–8 (1942).

(71) VON NEUMANN, J.: NDRC Report, June 30, 1941.

(72) VON NEUMANN, J.: OSRD Report No. 549, May, 1942.

(73) VON NEUMANN, J.: AMP Report No. 38.3R.

(74) WEATHERBURN, C. E.: *Advanced Vector Analysis*, p. 152. Bell, London (1937).

(75) WENDLANDT, R.: Z. physik. Chem. **A116**, 227–60 (1925).

(76) WOHLER, L., AND MARTIN, F.: Z. ges. Schiess- u. Sprengstoffw. **12**, 1–3, 18–21, 39–42, 54–7, 74–6 (1917).